Universidade de Aveiro

2015/2016

Departamento de Química

Eduarda Serra Morais

Desenvolvimento de novos biomateriais com propriedades anti-inflamatórias e antioxidantes para aplicação tópica

Development of new biomaterials with anti-inflammatory and antioxidant properties for topical application

Universidade de Aveiro

2015/2016

Departamento de Química

Eduarda Serra Morais

Desenvolvimento de novos biomateriais com propriedades anti-inflamatórias e antioxidantes para aplicação tópica

Development of new biomaterials with anti-inflammatory and antioxidant properties for topical application

Tese apresentada à Universidade de Aveiro para cumprimento dos requisitos necessários à obtenção do grau de Mestre em Biotecnologia, ramo de Biotecnologia Industrial, realizada sob a orientação científica da Doutora Mara Guadalupe Freire Martins, Investigadora Coordenadora do Departamento de Química da Universidade de Aveiro e da Doutora Carmen Sofia da Rocha Freire Barros, Investigadora Principal do Departamento de Química da Universidade de Aveiro

O júri

presidente

Prof. Ana Maria Rebelo Barreto Xavier
Professora Assistente do Departamento de Química da Universidade de Aveiro

Dr. Fernando Octávio de Queirós Dourado
Investigador Pós-Doutoramento do Centro de Engenharia Biológica da Universidade do Minho

Dra. Carmen Sofia da Rocha Freire Martins
Investigadora Principal do CICECO/Departamento de Química

agradecimentos

Á Doutora Mara Freire e à Doutora Carmen Freire pela orientação, ajuda, transmissão de conhecimentos e disponibildiade durante a realização deste trabalho.

Ao Nuno Silva e Tânia Sintra pela ajuda, apoio e paciência e por estarem sempre disponíveis para me ouvir e esclarecer dúvidas.

Ao Professor Bruno Neves, por toda a disponibilidade e ajuda durante os testes biológicos.

Aos meus colegas de laboratório pelo companheirismo e boa disposição no local de trabalho, disponibilidade e espírito de entre-ajuda.

A todos os meus colegas dos grupos Path e Lignomacro pelo companheirismo e ajuda.

A todos os meus amigos pelo suporte, amizade, compreensão, paciência e aconselhamento durante este ano de trabalho.

Aos meus pais por me terem conseguido proporcionar 5 anos de universidade, por todo o apoio e compreensão e por terem tornado a elaboração deste trabalho possível.

Por fim, ao departamento de Química da Universidade de Aveiro e CICECO pelas condições e equipamento disponibilizado na realização deste trabalho.

Palavras-chave Biomateriais, celulose bacteriana, líquidos iónicos, catião colínio, ácidos fenólicos, propriedades antioxidante e anti-inflamatória, aplicações tópicas

Resumo

A demanda por cosméticos com propriedades anti-envelhecimento e para proteção da pele contra as radiações ultra violeta (UV) tem aumentado consideravelmente nos últimos anos. Preferencialmente, estes devem ter na sua composição produtos naturais ou derivados com propriedades biológicas reconhecidas. Entre estas propriedades, destacam-se as propriedades antioxidante e anti-inflamatória. Dentro dos antioxidantes naturais, os compostos fenólicos têm recebido um destaque especial, visto que se encontram naturalmente em grande quantidade numa ampla variedade de plantas. No entanto, para que a sua utilização e biodisponibilidade sejam eficazes, é necessários que estes compostos apresentem uma elevada solubilidade em soluções aquosas. Uma das formas de tornar estes compostos mais solúveis passa pela alteração da sua estrutura química, sendo que por exemplo se podem converter em sais e/ou líquidos iónicos.

Com base no exposto, neste trabalho, pretendeu-se produzir novos biomateriais para aplicação tópica com propriedades antioxidantes e anti-inflamatórias. Neste sentido, sintetizaram-se líquidos iónicos com estas propriedades, com o catião colínio em comum, combinados com aniões derivados de ácidos fenólicos, que posteriormente foram incorporados em membranas de celulose bacteriana (BC). Todos os materiais foram caracterizados por espectroscopia de infravermelho com transformada de Fourier com reflexão total atenuada (FTIR-ATR), ressonância magnética nuclear (RMN) de estado sólido, difração de Raios-X, microscopia eletrónica de varrimento (SEM), termogravimetria (TGA) e testes mecânicos (ensaios de tração). Posteriormente, realizaram-se ensaios de libertação controlada destes compostos, ensaios para determinar a atividade anti-oxidante e por fim, realizaram-se estudos biológicos de modo a avaliar a sua citotoxicidade e atividade anti-inflamatória.

Através da caracterização física e química das membranas preparadas foi possível concluir que os LIs foram incorporados na estrutura da BC, não afetando a sua estrutura cristalina mas tendo originado um pequeno decréscimo nas propriedades mecânicas e temperatura de decomposição. Nos ensaios de absorção de água, os valores obtidos para as membranas BC-LI estão de acordo com a solubilidade dos LIs. A dissolução dos LIs com membranas húmidas atingiu valores máximos de 100% para [Chol][Gal]. Os valores máximos para capacidade antioxidante foram 80% para [Chol][Caf] e [Chol][Gal]. As membranas de BC-ILs não afectam a viabilidade dos queratinócitos e macrófagos e apresentaram atividade anti-inflamatória.

keywords Biomaterials, bacterial cellulose, ionic liquids, cholinium cation, phenolic acids, antioxidant and anti-inflamatory properties, topical applications

abstract In the past few years, the demand for cosmetics with anti-aging and ultraviolet (UV) protection properties has increased considerably. Preferentially, these must have in their composition natural compounds with recognized biologic properties. Among these properties, antioxidant and anti-inflammatory activities stand out as the most important. Amongst natural antioxidant compounds, phenolic compounds have gained special attention since they are naturally found in an ample diversity of plants. However, for their effective use and bioavailability, these compounds should present a high solubility in aqueous solutions. One way of improving their solubility is through the modification of their chemical structure, by their conversion into salts and/or ionic liquids (ILs).

This work aimed at producing new biomaterials for topic applications incorporating antioxidant and anti-inflammatory compounds. To this end, the cholinium cation was conjugated with anions derived from phenolic acids and afterwards were incorporated into bacterial cellulose (BC) membranes. All materials were characterized through Fourier transform infrared spectroscopy with attenuated total reflection (FTIR-ATR), solid nuclear magnetic ressonance (NMR), X-ray diffraction, scanning electron microscopy (SEM), thermogravimetry (TGA) and mechanical tests. Then, controlled release assays were carried out, and antioxidant assays, followed by biological assays to evaluate their citotoxicity and anti-inflammatory properties.

The chemical and physical characterization of the obtained membranes it was possible to conclude that the ILs were incorporated into the BC network while maintaining its crystalline structure with only a slight decrease in its mechanical performance and decomposition temperature. The swelling ability of the BC-IL membranes swelling was in agreement with each of the ILs solubility.

The dissolution assays for wet membranes reached maximum values of 100% for BC-[Chol][Gal]. The maximum antioxidant values of BC with the incorporated ILs reached were 80% for [Chol][Caf] and [Chol][Gal. The BC-ILs membranes did not affect the macrophage and keratinocytes viability and presented anti-inflammatory activity.

INDEX

LIST OF FIGURES

LIST OF TABLES

ABREVIATIONS

[Chol][Caf] – Cholinium caffeate

[Chol][Gal] – Cholinium gallate

[Chol][Sal] – Cholinium salycilate

[Chol][Syr] – Cholinium syringate

[Chol][Van] – Cholinium vanillate

$[Chol]_2[Ell]$ – Dicholinium ellagate

API - Active pharmaceutical ingredients

BC – Bacterial cellulose

BHA – Buthylated hydroxyanisole

BHT - Buthylated hydroxytoluene

BLM - Bulk liquid membranes

COSMO-RS - Conductor like screening model for real solvents

D_2O – Deuterated water

DNA – Deoxyribonucleic acid

DMSO – Dimethyl sulfoxide

ELM - Emulsion liquid membranes

FTIR-ATR - Fourier transform infrared spectroscopy with attenuated total reflection

ILs – Ionic liquids

LPS - Lipopolysaccharide

NO – Nitric oxide

NMR – Nuclear magnetic resonance

PILs – Protic ionic liquids

ROS – Reactive oxidant species

SEM - Scanning electron microscopy

SLM - Supported liquid membranes

UV – Ultraviolet

VOCs - Volatile organic compounds

TMS – Tetramethylsilane

TSP – Trimethylsilyl propanoic acid

XRD – X-ray diffraction

1 Scope and objectives

An increase in the consumption of skin care products, such as anti-aging creams, creams to restore the fullness of the skin and mostly products to protect skin from adverse effects of sun, has been observed in the past few years. In fact, the human excessive exposure to sun and to endogenous and environmental pro-oxidant agents are the main factors that contribute to premature skin aging, skin damage, and skin cancer. Studies have shown that UV-induced skin damage is in part caused by the formation of noxious reactive oxidant species (ROS), leading to a wide variety of pathological effects, such as DNA (deoxyribonucleic acid) modification, lipid peroxidation, as well as to the activation of inflammatory pathways (1,2). Although mammalian skin cells have natural antioxidant defense mechanisms, these systems may not be enough to ensure the skin barrier integrity (3).

Cosmetic and skin care products based on natural compounds have shown a strong growth in the past decades. Cosmeceuticals are an emerging concept in this field, which is related to cosmetic products with biologically active ingredients with medicinal or drug-like benefits (4). These products comprise ingredients with biological features in their formulation, such as vitamin C and E, which display antioxidant activity, panthenol, that is essential for normal cellular metabolism, allantoin, which promotes cell proliferation, or hydroxy acids, that make the skin look smoother and uniform, reducing the signs of aging (4).

Natural antioxidants, as phenolic compounds, are present in many plants. Due to their instability, since they are susceptible to hydrolysis and photodegradation in the presence of oxygen, keeping constant the activities of antioxidants in formulations during their claimed shelf life is often problematic. In fact, natural antioxidants are quite unstable and have low solubility in water, as well as a low bioavailability. For this reason, their chemical stability and content should be controlled to ensure that consumers get a product with the desired properties. Thus, their chemical modification aiming at increasing their stability and solubility in aqueous media, while not raising their citotoxicity, can be seen as a promising approach for their safe and effective use in topical formulations (3). The combination of active pharmaceutical ingredients (APIs) with ionic liquids (ILs)

constitutes a solution since it can synergistically enhance the antioxidant activity as well as their solubility and bioavailability (5).

Cholinium-based ILs with anions derived from phenolic acids constitute an interesting alternative to conventional phenolic compounds since they have higher water-solubility, higher antioxidant activity, and anti-inflammatory properties and toxicity in the same levels (6). Due to their outstanding properties, these compounds can be incorporated into biopolymeric materials, like bacterial cellulose (BC) or chitosan, for topical applications and controlled release.

The principal aim of this work, was to produce new biomaterials with antioxidant and anti-inflammatory properties by incorporating cholinium-based ILs with these features, such as dicholinium ellagate ($[Chol]_2[Ell]$, di((2-hydroxyethyl)trimethylammonium) 3,8-dihydroxy- 5,10-dioxo-5,10-dihydrochromeno[5,4,3-*cde*]chromene-2,7-bis(olate)), cholinium gallate ([Chol][Gal], (2-hydroxyethyl)trimethylammonium 3,4,5-trihydroxybenzoate), cholinium caffeate ([Chol][Caf], (2-hydroxyethyl)trimethylammonium (E)-3-(3,4- dihydroxyphenyl)acrylate) (6) into nanocellulose (bacterial cellulose) membranes. These biomaterials were optimized in order to be used in topical applications while allowing a controlled release of the bioactive compounds for the treatment of skin ageing and some skin diseases.

The aforementioned cholinium-based ILs were synthesized according to procedures described in the literature (6), and further analyzed for their purity, and incorporated into BC membranes. Then, the different BC-ILs membranes were characterized in what concerns their morphology, thermal stability and mechanical properties (using Fourier transform infrared spectroscopy with attenuated total reflection (FTIR-ATR), solid state nuclear magnetic resonance (NMR), X-ray diffraction (XRD), scanning electron microscopy (SEM), and thermogravimetry (TGA) and mechanical (tensile) tests). Then, the absorption process of ILs into the BC membranes and their controlled release was investigated and optimized. Finally, the evaluation of their biological properties and cytotoxicity was carried out.

2 Antioxidants in cosmetic applications

Nowadays, we are facing a growing apprehension on skin care and health. One of the major concerns is the exposure that our skin has to endogenous and environmental pro-oxidant agents, such as high concentrations of exogenous oxygen, environmental oxidants, and especially UV light. This exposure leads to the formation of noxious reactive oxidant species (ROS). In Figure 1, it is shown the natural ROS formation process during cellular respiration. This term covers molecules that are known as free radicals and those who behave in a similar way. These molecules are characterized by their high reactivity and capacity to easily oxidize other molecules (1), which means that they can extract electrons. ROS-mediated oxidative damage includes a wide variety of pathological effects, such as DNA modification, like base modification, covalent binding of bases within DNA or DNA-protein cross-links, abasic sites and strand breaks (7), lipid peroxidation, as well as the activation of inflammatory pathways (8). Free radicals are responsible for a large array of diseases, such as cancer (9), cardiovascular diseases (10), neural disorders (11), Alzheimer's disease (12), mild cognitive impairment (13), Parkinson's disease (14), among many others (15).

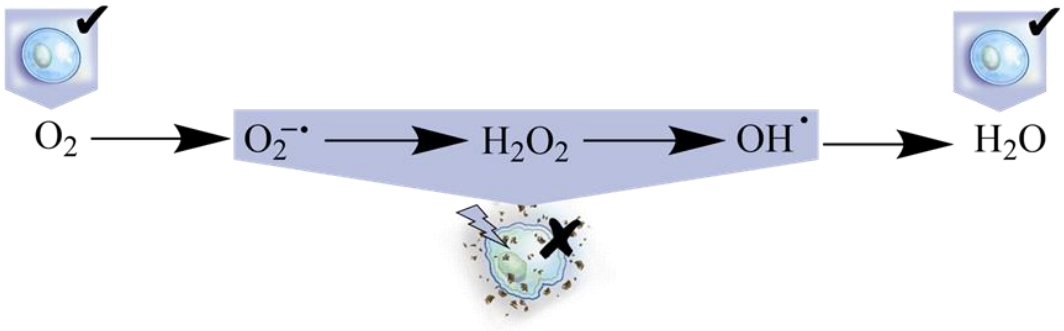

Figure 1 - ROS formed during mitochondrial transport. Superoxide anions (O_2-•), hydrogen peroxide (H_2O_2), and hydroxyl (HO•) radicals are formed as a result of the successive transfer of single electrons (1).

Defense systems against ROS damage can be exogenous or endogenous. Endogenous antioxidants originate from melanin and enzymes, while exogenous antioxidants derive from antioxidants that are administrated orally through food and topically, like vitamins A, C and E (3,16). Mammalian skin cells have endogenous defense

systems comprising enzymatic and non-enzymatic antioxidant systems. The human body produces molecules with antioxidant effects, such as ubiquinone (coenzyme Q), tripeptide glutathione, polypeptide thioredoxin or lipoic acid (1). Nevertheless, these systems are not enough to protect the skin and to ensure its integrity. Because of that, the interest in the intake of antioxidants has grown considerably throughout the years. Antioxidants are substances capable of prevent or significantly delay the oxidation of a substrate, when present in lower concentrations than the substrate itself (17). Their mechanism of action is represented in Figure 2. Some evidences have shown that a large uptake of antioxidant-rich foods is of major importance to prevent these diseases (15).

Figure 2 – Representation of the antioxidant reaction with ROS. Phen stands for phenolic compound. Adapted from (2)**.**

Another way of using antioxidant compounds, maximizing their potential, is by using them in cosmetic products, like dermatological pharmaceutical formulations and skin care products (1). Cosmetics are used for cleansing, protecting, and moisturizing the skin. Nowadays, consumers prefer cosmetics that are safer to their skin and, if possible, based on natural compounds. These cosmetics, based on natural compounds with drug-like benefits, are called “cosmeceutical” products and are now being developed by many pharmaceutical industries (4).

Antioxidants can be divided into natural and synthetic. The natural antioxidants class usually comprises mineral compounds, such as selenium, copper, iron or zinc, antioxidant vitamins (C and E), and phytochemicals that are neither vitamins nor minerals, and include compounds like flavonoids, which are phenolic compounds present in vegetable fruits, grains, seeds, among others. Natural antioxidants react with lipid and peroxy radicals and convert them into more stable products (18). They act as singlet and triplet oxygen quenchers, free radical scavengers, peroxide decomposers, and enzyme inhibitors (19). The functions of synthetic antioxidants consist on the capture of free radicals and in closing the chain reaction. Some examples are buthylated hydroxyanisole (BHA), buthylated hydroxytoluene (BHT), propyl gallate and metal chelating agents, among others (18,20).

In cosmetic products, it is very difficult to get a good formulation containing antioxidants. In general, antioxidants from natural sources are unstable, deeply colored, and susceptible to hydrolysis and photodegradation in the presence of oxygen. Chemical modification of these antioxidants to form the respective esters (e.g., tocopheryl acetate, ascorbyl palmitate), have shown to improve their compatibility/stability in formulations, yet it reduces their activity (3). Antioxidants act not only as the active ingredients themselves but also as protectors of other ingredients against oxidation/degradation. However, in order to obtain the desired activities, antioxidants must not be transformed into their radical forms, i.e., they cannot react with other ingredients and must be protected from oxygen radicals until they are applied on the skin. The antioxidants selection also depends on their lipophilic or hydrophobic characteristics. Most of them display a low water-solubility and are only present at low contents in aqueous-rich topic formulations (3). Based on these drawbacks, the chemical modification of antioxidants into ionic liquids can be seen as a promising approach in order to increase their solubility in water, and to as well enhance properties as their antioxidant and anti-inflammatory activities (6).

2.1 **Phenolic compounds**

Phenolic compounds are abundant in nature since they are ubiquitous in all plants and are therefore an integral part of the human diet. These compounds have proven antioxidant properties and can prevent some diseases related to oxidative stress (21). Phenolic compounds have one or more aromatic rings with one or more hydroxyl groups directly bonded. In plants, they are involved in the defense role against UV light and aggression by pathogens, as well as in the organoleptic properties of plant foods. They contribute to the bitterness and astringency of fruits because of their interaction with glycoproteins in saliva (2).

Phenolic compounds are divided into several classes according to the number of aromatic rings with hydroxyls group and to the structural elements that bind these rings. The main groups of phenolic compounds are: flavonoids, phenolic acids, phenolic alcohols, stilbenes and lignans (Figure 3) (22). Phenolic acids can be divided into two classes: benzoic acid derivatives, such as gallic acid, and cinnamic acid derivatives, such as coumaric, caffeic and ferulic acids. Caffeic acid is the most abundant phenolic acid in

many fruits and vegetables, most often esterified with quinic acid as in chlorogenic acid, which is the major phenolic compound in coffee (22).

Phenolic compounds have been considered powerful antioxidants *in vitro* and proved to be more potent antioxidants than Vitamin C and E and carotenoids (23). In fact, these compounds have been recognized as one of the key factors to the inverse relationship between fruit/vegetable intake and the risk for oxidative stress-associated diseases, such as cardiovascular diseases, cancer or osteoporosis (2).

Phenolic extracts or isolated phenolic compounds from different plant foods have also been studied in a number of cancer cell lines representing different evolutionary stages of cancer. Several studies, where solutions of phenolic compounds inhibit the growth of human oral (KB, CAL-27), breast (MCF-7), colon (HT-29, HCT-116) and prostate (LNCaP, DU-145) tumor cell lines, in a dose-dependent manner with different sensitivity between cell lines, have been reported (24,25). Some *in vivo* tests have also been carried out in animals with good results, showing that phenolic compounds can reduce the size of tumors and inhibit the cancer proliferation (2).

It has been proposed that phenolic compounds can act as antioxidants using one of the three following mechanisms: (1) by scavenging radical species, such as ROS; (2) by suppressing ROS formation through the inhibition of some enzymes or chelating trace metals involved in free radicals production; and (3) by up-regulating or protecting the antioxidant defense (2). Moreover, it has been shown that natural phenolic compounds can inhibit carcinogen/toxin-induced cellular oxidative damage. For example, in nicotine-treated rat peripheral blood lymphocytes, ellagic acid effectively restored the antioxidant status and reduced DNA damage, as well as lipid peroxidation (26). A phenolic apple juice extract, as well as its reconstituted phenolic compound mixture, composed of rutin, phloridzin, chlorogenic acid, caffeic acid and epicatechin, were shown to effectively reduce menadione-induced oxidative DNA damage and reduced the cellular ROS level (27). Purified phenolic compounds, such as anthocyanins, proanthocyanidin and epigallocatechin gallate (EGCG) have demonstrated to inhibit the UV-radiation-induced oxidative stress and cell damage in human keratinocytes (2).

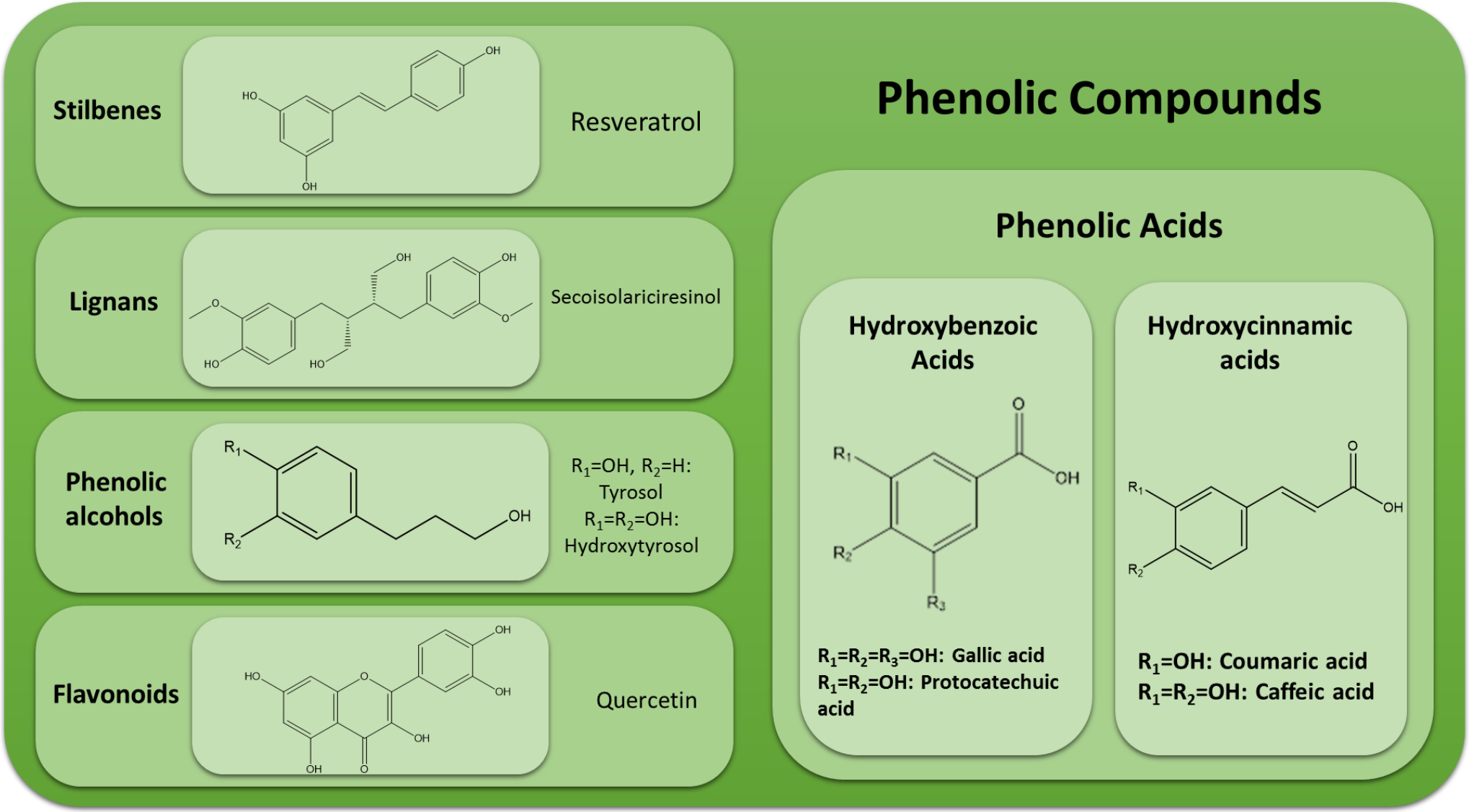

Figure 3 - Chemical structures of some phenolic compounds.

3 Ionic liquids

3.1 Characteristics and applications

Ionic liquids (ILs) are salts, usually composed of large organic cations and organic or inorganic anions, with a melting point lower than 100 °C, since they do not present an ordered crystalline structure (28,29). The increasing attention around ILs is largely justified by their unique properties, such as a negligible vapor pressure (30), non-flammability, high heat capacity, high chemical and thermal stabilities (31) and high solvation ability (32). Furthermore, these ionic compounds can be designed for a specific purpose by the selection of adequate cation/anion combinations, which contributes for their classification as ‘‘*designer solvents*’’ (33,34). In fact, their physicochemical properties can be tailored by a judicious choice of the cation, anion and alkyl chain type, length and functionalization. The main structural factors of the cation that have an effect on their properties are symmetry, charge density, alkyl chain length and its flexibility, rotational symmetry of the head ring, cyclic and branched structures and functionalized tails. Regarding the anions, they are usually quite different in nature, although they display similar structural factors, including a large charge delocalization (35). Figure 4 depicts the chemical structure of some ILs. The most common ILs investigated are composed of imidazolium, pyridinium, quaternary ammonium, quaternary phosphonium and pyrrolidinium cations and chloride, bromide and hexafluorophosphate anions (36,37).

The possibility of modifying the properties of ILs is one of their main advantages since it allows the optimization of their solvation properties, viscosity, conductivity and thermal and chemical stabilities, making them tailor-made for a wide range of applications (34). Recent reviews have highlighted the industrial applications of ILs as an innovative approach to Green Chemistry and Sustainability concepts (38–40).

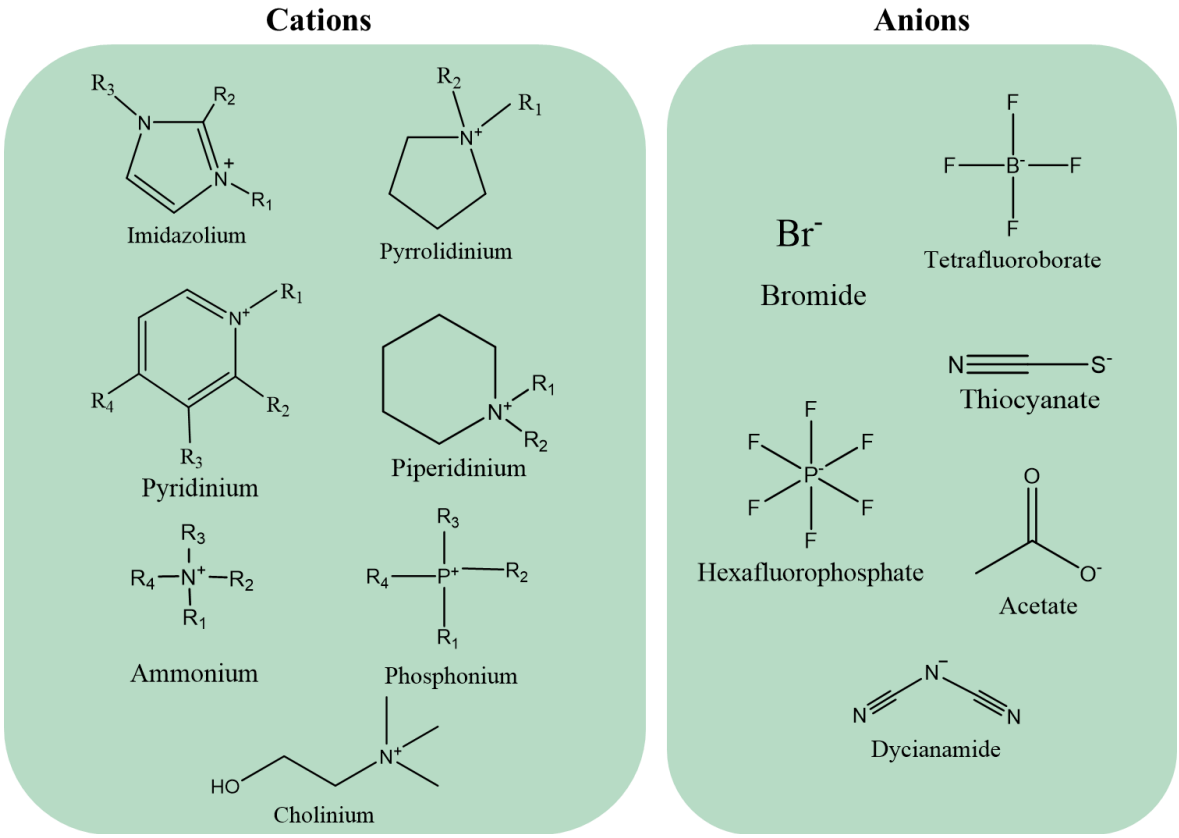

Figure 4 – Some examples of typical cations and anions in ILs.

Due to their insignificant vapor pressure at ambient conditions, ILs have been considered as promising "greener" solvents over volatile organic solvents (VOCs). However, the fact that they normally have a negligible vapor pressure is not enough to assure that these compounds can be considered as real "green" solvents, and where some of the most investigated ILs are far from a green solvent designation (37,41–43). In this context, the synthesis of ILs from renewable raw materials through a green chemistry procedure is strictly required to fulfill the "green solvents" categorization. Aiming at finding more benign and biocompatible ILs, cholinium-based ILs, based on the *N*,*N*,*N*-trimethylethanolammonium cation, an essential nutrient, have been receiving considerable attention (34,44). This cation is biocompatible, has a "nontoxic" nature and is also completely degradable under aerobic conditions (43,45). This family of ILs is derived from quaternary ammonium salts that are described as important structures in living processes, used as precursors for the synthesis of vitamins (e.g. vitamin B complexes and thiamine) and enzymes that participate in the carbohydrate metabolism (46). Additionally, ILs

containing quaternary ammonium and alicyclic cations (morpholium, piperidinium and pyrrolidinium) generally display a significantly lower toxicity than those with aromatic cations, such as imidazolium and pyridinium (47).

3.2 **Ionic liquids with therapeutic properties**

Amongst the many applications of ILs, their use in the pharmaceutical and cosmetic industries stands out since these industries are constantly demanding for innovation and new products. However, the deficient information surrounding the toxicological impact of ILs is a major barrier to their widespread industrial application and international registration as solvents. Nevertheless, ILs as pharmaceutical salts have been reported for long (34). Some examples include ranitidine hydrochloride (Zantac^{TM}), an anti-ulcer drug with problems derived from its polymorphic forms and purity, that was transformed into an IL through reaction with sodium docusate, a common emollient, to form ranitidine docusate (48). Bretylium is a antifibrillatory and antiarrhythmic compound synthetized by the quaternization of *o*-bromo-*N*,*N*-dimethylbenzylamine with ethyl-*p*-toluenesulfonate (49). Cetylpyridinium chloride is produced by the alkylation of pyridine with cetyl chloride and it is used as antiseptic and disinfectant (50). The exchange of the inert counter-ion of a drug with a pharmaceutically active counter-ion should be chosen in order to synergistically enhance the desired effects or to neutralize unwanted side effects of the active drug. When dissolved, the drug combination (ions) will dissociate and the cationic and anionic components will follow their independent kinetic and metabolic pathways (34,51). On the other hand, microemulsions based on ILs allow an increase in the solubilization of pharmaceutical ingredients and have also been reported (52). Most of these works have the goal of eliminating problems related to polymorphism transitions between crystalline forms and one of the biggest problems of solid drugs, to increase the solubility of the drug and also its bioavailability (53). The pharmaceutical industry currently has a large portfolio of active pharmaceutical ingredients (APIs), yet most of them with limited aqueous solubility. Therefore, the conversion of APIs into ILs is also a suitable way of overcoming these compounds low solubility in aqueous media (5). Finally, ILs can also be combined with APIs (by their solubilization in IL media), producing new

drugs with enhanced water solubility and able to overcome the problem of polymorphism (Figure 5).

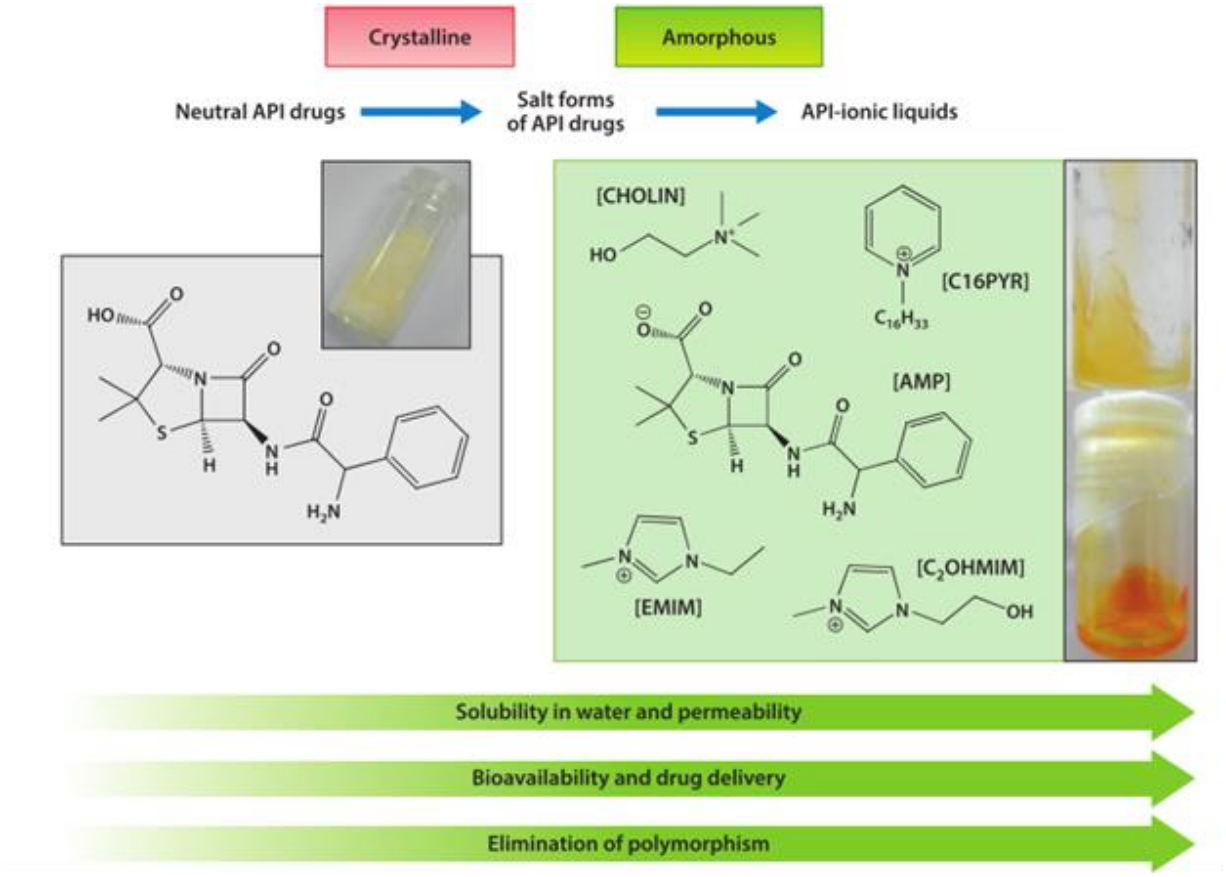

Figure 5 – Future perspectives on active pharmaceutical ingredients (APIs), in this case ampicillin – ionic liquids mixtures (5)**.**

ILs can also be used to improve the shelf life of certain active compounds. For example, choline dihydrogen phosphate aqueous solutions can dramatically improve the shelf life of cytochrome c, without modifying its structure and activity (54). This is of extreme importance for therapeutic applications since the protein efficacy is determined by its proper folded structure (54).

A final important advantage of using ILs in pharmaceutical formulations and as excipients is that some of them were already approved by the Food and Health Administration (FDA). That is the case, for example, of cholinium phosphate salts (55). Moreover, cholinium salicylate ([Chol][Sal]) is already being used as an active pharmaceutical component, namely in drugs like Bonjela, Trilisate, Arthropan and

Bucagel. [Chol][Sal] is preferred to salicylic acid since it presents higher solubility in aqueous media while still being biocompatible. [Chol][Sal] is currently used as an analgesic, antipyretic and anti-inflammatory drug (56).

As stated before, the cholinium cation, an essential nutrient, has been receiving considerable attention as a promising candidate to produce biocompatible ILs when combined with an appropriate anion. A huge number of cholinium salts, conjugated with a wide range of anions, such as amino acids (57,58), carboxylic acids (59) and good's-buffer-based anions (60), has been reported. The anion selection has been carried out according to the target application, while distinct applications have been suggested, such as in catalysis (57), as co-substrates for microorganisms in the degradation of dyes (61), in photodynamic therapy (62), as cross-linking agents for collagen-based materials (44), as self-buffering compounds for the extraction and purification of biologically active molecules (60) and also as major solvents in the pretreatment and dissolution of biomass (63).

Recently, Sintra *et al.* (6) reported the synthesis and characterization of antioxidant cholinium-based ILs with high water-solubility and anti-inflammatory activities. For that, cholinium hydroxide was neutralized with the respective acid, with well-known antioxidant/anti-inflammatory character, namely gallic, caffeic, vanillic, syringic, and ellagic acids. [Chol][Sal] was also synthetized in order to compare with the antioxidant performance of the new cholinium-based salts. In this work, it was concluded that all cholinium-based salts studied presented not only similar but even higher antioxidant and anti-inflammatory activities (6). Moreover, it was observed that they have a solubility three orders of magnitude (in average) higher than the respective acidic precursors, representing a significant advantage with respect to the incorporation of these antioxidants into topic formulations. In what concerns their ecotoxicity, it was shown that all cholinium-based salts synthesized are less toxic than their precursors. The less ecotoxic salts and with higher antioxidant activity, namely $[Chol]_2[Ell]$, [Chol][Caf] and [Chol][Gal], were also tested for anti-inflammatory properties with all of them displaying a good performance. Finally, regarding their cytotoxicity, all cholinium-based salts showed results similar to their acidic precursors which means they can be safely used in products for human healthcare (6). Thus, these cholinium-based salts, with significant antioxidant and anti-inflammatory properties, are valuable candidates in the formulation of

pharmaceutical/cosmetic products. Since they are based on the cholinium cation, an essential nutrient for cells, they are also of great interest in topical or oral formulations. Because of these features, in this work, the incorporation of this class of cholinium-based ILs in bacterial cellulose membranes for cosmetic applications was investigated.

4 Bioactive films based on polysaccharides

4.1 Types and applications

One of the main solutions for the environmental problems arising from the excessive use of non-biodegradable materials from fossil resources is the development of materials based on biopolymers, namely polysaccharides, proteins or even lignin (Figure 6). These biopolymers have been receiving a large attention over the last years in several areas, like biomedical products and devices, functional packaging, coatings and films, electronic devices, structural materials, among others (64). Due to their abundance, polysaccharides, including cellulose, chitin (and its derivative chitosan), starch and pullulan, are one of the most explored families of biopolymers (64,65).

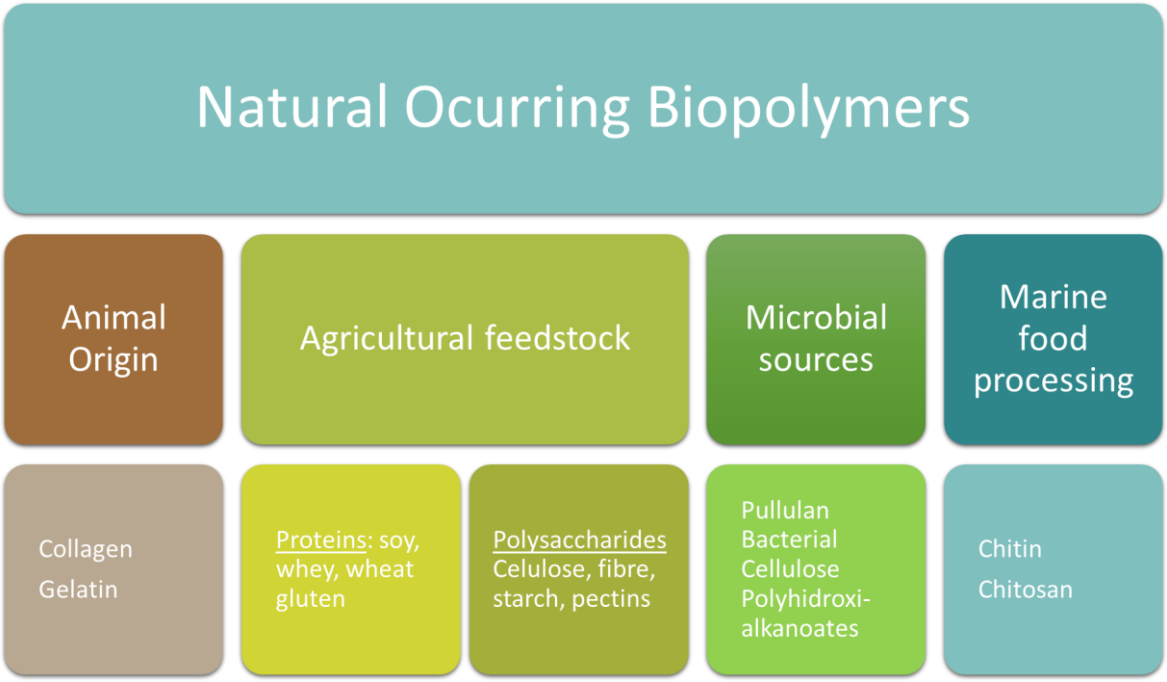

Figure 6 - Naturally occurring biopolymers, adapted from (65)**.**

Cellulose $(C_6H_{10}O_5)n$ is the most abundant biopolymer on Earth. It is a homopolymer of β-D-glucopyranose units covalently linked through β(1→4) glycosidic bonds, i.e. acetal functions between the equatorial OH group of C4 and the C1 carbon atom (β(1→4)glucan). It is a linear polymer with a large number of hydroxyl groups (66). In plants, cellulose is organized in the form of fibers that are composed of fibrils with

diameters that can vary between 1.5 to 100 nm. Cellulose is the most used natural resource to produce paper and cardboard, clothing and other derivatives with various industrial applications, such as optical films, additives in building materials, and in the pharmaceutical, cosmetic and food industries (66,67). More recently, new applications for cellulose were related to its biocompatibility and capacity to immobilize proteins and antibodies (68,69), to separate enantiomers (70), and to produce sustainable composites with good biodegradability and improved mechanical properties (71).

4.2 **Bacterial cellulose**

4.2.1 **Production, properties and applications**

Bacterial cellulose is a type of cellulose produced by bacteria and was initially reported by Brown (1886) (72). It is characterized by a 3-D structure which consists of an ultrafine network of cellulose nanofibers (3-8 nm) highly uniaxially oriented (73). BC fibrils are known to be about 100 times thinner than plant cellulose ones, as can be seen in Figure 7 (74).

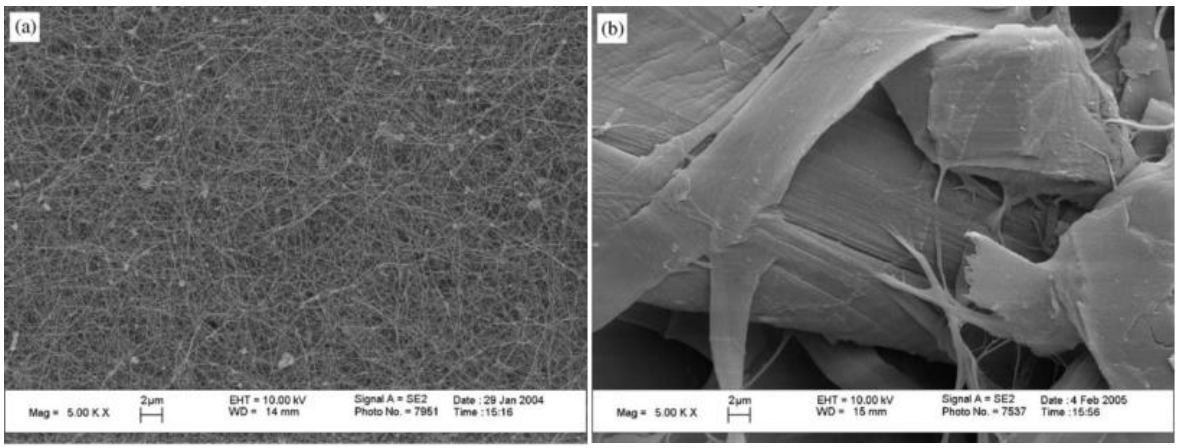

Figure 7 – Scanning electron microscope (SEM) images of bacterial cellulose (a) and wood pulp cellulose (b) (both at 5000x) (73)**.**

BC can be produced by many Gram-negative bacteria, like those from the genus *Acetobacter*, *Agrobacterium*, *Achromobacter*, *Aerobacter*, *Sarcina*, *Azotobacter*, *Rhizobium*, *Pseudomonas*, *Salmonella* and *Alcaligenes* (75). The most effective producers of cellulose are *G. xylinum* (76), *G. hansenii* (77) and *G. pasteurianus* (78), with maximum

yield of 15.30, 2.5 and 0.54 g/L, respectively (75,78). Bacteria from the *Gluconacetobacter* genus produce an extremely pure variety of BC, in the form of a highly swollen membrane, with around 99% water, on the culture medium surface (73,79). *Gluconacetobacter sacchari* is also used for BC production with yields on the same level or even better than the most used *Gluconacetobacter* species (80). Bacterial cellulose is also synthesized by the Gram-positive bacterium *Sarcina ventriculi*, accounting for about 15 % of the total dry cell mass (75).

In general, the strain most used is *Glucanocetobacter xylinum*. This is an aerobic Gram-negative bacterium with the ability to synthetize a large quantity of high-quality cellulose through acetic acid fermentation (73,74). These aerobic gram-negative bacteria actively grow at pH 3-7 and at temperatures between 25 and 30˚C, having good fermentation yields using saccharides as the carbon source. It was reported that almost 30% of the cost of bacterial fermentation is due to the fermentation medium constituents (74,81); nevertheless, in the biomedical and pharmaceutical field this factor is not a main problem due to the high value of the current biomedical devices and pharmaceuticals. There has been many attempts for using economical carbon sources, such as waster beer yeast, dry oil mill residue (82), thin stillage (83) and grape skin (84). In these studies, the addition of nitrogen and phosphorus sources normally increases BC production (75). Although glucose is still the carbon source most commonly used due to its good fermentation yield, it causes the formation of gluconic acid and the decrease of pH, which affects the bacterial metabolism and consequently the production of BC. The presence of polyphenolic compounds and antioxidant manages to inhibit this by-product (74).

Gluconacetobacter xylinum bacteria use various carbon compounds present in the nutrition media to produce cellulose, as single linear β(1→4) glucan chains, and then secrete them outside the cells through a linear row of pores located in the outer membrane. The following steps, which occur outside the cell, are organized in a hierarchical process:

1) Formation of subfibrils, that consist of 10 to 15 glucan chains;
2) Formation of microfibrils;
3) Formation of bundles of microfibrils in a shape of a loosely wound ribbon comprised of about 100 individual glucan chains (73).

The biochemical pathways involved in cellulose synthesis by *G. xylinum* are extensively documented (74,75,85). It is a precisely and specifically regulated multi-step

process, including a large number of individual enzymes and proteins. The respective metabolic pathway is shown in Figure 8. The process includes the formation of UDPGlc, which is the precursor of cellulose, followed by glucose polymerization into the β(1→4) glucan chains with the formation of ribbon like structures that are extruded from the cell and assemble in fibrils as described before (75).

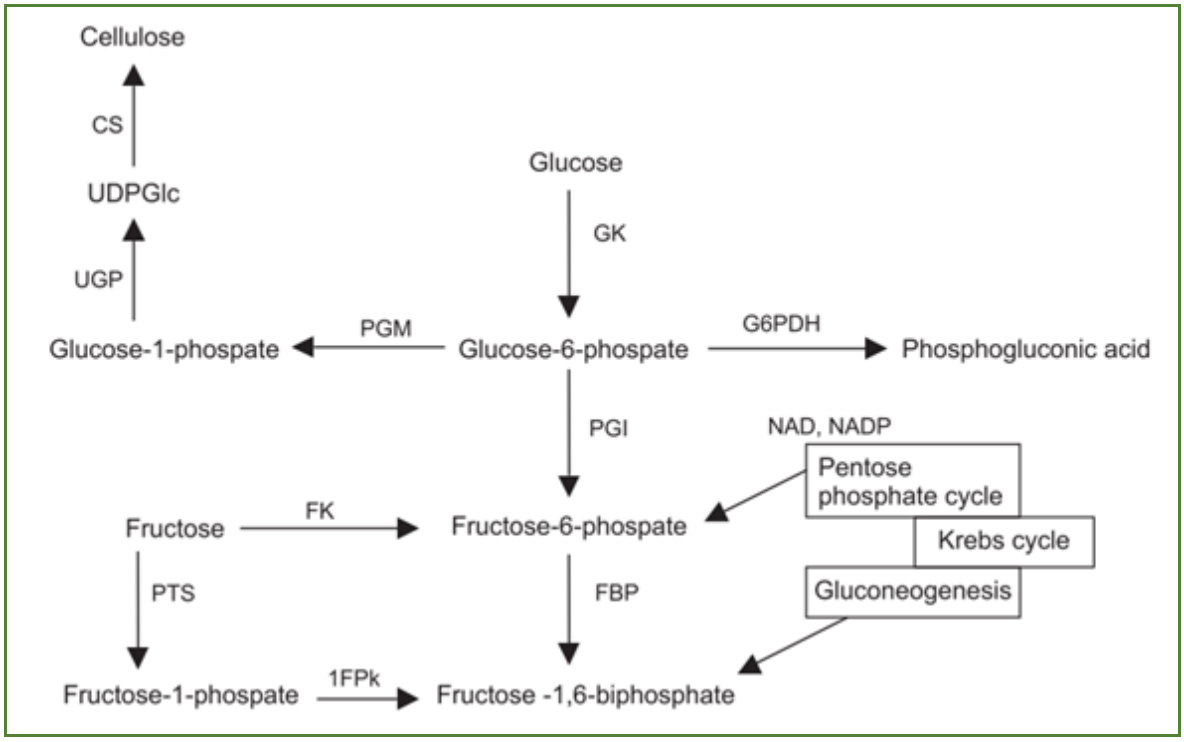

Figure 8- Biochemical pathway for cellulose synthesis by *G. xylinum* (75).

BC production can be done in static and agitated (or stirred) conditions (74). In static medium, a pellicle is formed while under agitated and stirred conditions, irregular shape sphere-like cellulose particles (SCP) are produced. In static conditions, the process is regulated by the air supply at the medium surface and the carbon source concentration. The production stops when the pellicle grows downward and entraps all bacteria that become inactive due to insufficient oxygen supply (74). Because of that, on an industrial scale, a semi-continuous process is recommended for static conditions since it allows to increase BC productivity in comparison with the continuous process, since the product BC is removed from time to time allowing the cells to have always access to oxygen (86).

BC has different characteristics from plant cellulose, since it can be obtained with higher purity and has a higher degree of polymerization and crystallinity index, porosity,

tensile strength and water holding capacity. Its high crystallinity is due to the glucan chains interlocked with hydrogen bonds (75). Moreover, BC possesses many unique structural and biochemical properties, including an ultrafine nanofibrous network structure (87), bioadaptability (88), chemical stability, and nontoxicity (89,90). Due to its uniform and ultrafine fibrous network structure, BC has excellent water-absorbance capacity. BC has also some interesting mechanical properties, including high tensile strength and elastic modulus (91,92).

Because of these unique properties, BC have been explored in several applications, but particularly in the biomedical field (73). In fact, plant-generated cellulose and its derived materials had been used for many years in medical applications, namely to stop bleeding. That is the case of cotton gauzes, consisting of an oxidized form of regenerated plant cellulose created during World War II (93,94). Cellulose hydrogels have also been applied in the skin, used to promote bone cell adhesion and proliferation with biocompatibility with the connective tissues.

First of all, a large number of studies have proven that bacterial cellulose can be used for various biomedical applications. For example, Kolodziejczyk and Pomorski (95) implanted pieces of bacterial cellulose (1 cm in diameter) into subcutaneous pockets on rabbits and periodically examined them after 1 and 3 weeks. The implants did not cause any macroscopic inflammatory responses, and histological observations showed only a small number of giant cells and a thin layer of fibroblasts at the interface between the cellulose and the tissue (95). In a systematic study by Helenius *et al.* (96), pieces of BC were also implanted into rats. Those implants were evaluated after 1, 4, and 12 weeks and showed no macroscopic or histologic signs of inflammation and no presence of giant cells. Also, no chronic inflammatory responses were observed throughout the course of these studies. Instead, they observed the formation of new blood vessels around and inside the implanted cellulose (96).

Therefore, BC is a good material for membranes that can be used for wound healing, substitutes of natural skin (75), among many other applications (97,98). Since it is a highly porous material, it allows the potential administration of antibiotics or other medicines required in the wound healing process, while at the same time it acts as a physical barrier against any external infection caused by bacteria (99). In addition, since it

is nontoxic and biocompatible, it allows a safe use in human skin or even in the human body (75).

Bacterial cellulose can absorb high volumes of liquids. This fact makes it a high-quality material for wound dressings (Table 1) since keeping the wound moist is one of the most important factors for a rapid healing process (100,101). For instance, BC has been used for the treatment of chronic ulcers and burns (99). Burns are very complex injuries, causing extensive damage to skin tissues. The healing process involves the regeneration of the epidermis and the repair of the dermis, both of which result in the formation of scar tissue (102). One of the major goals of burn therapy is to quickly accomplish effective wound closure so as to increase the rate of healing and to provide immediate pain relief (99). In Poland, a study was conducted on burned patients using BC (103). It was showed that the skin of patients whose burns were covered with never-dried BC membranes healed faster (faster re-epithelialization) than the wounds of patients who received a conventional wound dressing (such as wet gauze and ointments) (103), and even performing better when compared to conventional methods, such as multiple stages wherein the wound is debrided followed by chemotherapy and subsequent preparation of the wound bed for grafting (85). In studies conducted by Fontana *et al.* (104) and Mayall *et al*. (105), a bacterial cellulose product, called Biofill ®, proved also to be a very successful wound covering for damaged skin problems such as burns and chronic ulcers. In these studies, Biofill was shown to be more effective than other wound dressing materials, providing pain relief, protecting the wound against infection, accelerating the healing process, and reducing the cost of treatment (92). BC can also be combined with other materials, such has chitosan, which helps to conserve the moistness and hyaluronic acid that promotes the healing (106).

Table 1 - Properties of bacterial cellulose membranes and how they relate to the properties of an ideal wound dressing material (92)**.**

Properties of ideal wound care dressing	**Properties of Bacterial Cellulose**
To maintain a moist environment at the wound/dressing surface	High water holding capacity (typical membrane can hold up to 200 g of its dry mass in water); high water vapor transmission rate.
To provide physical barriers against bacterial infections	Nanoporous structure does not allow any external bacteria to penetrate the wound bed.
To be highly absorbable	Partially dehydrated membrane is able to absorb fluid up to its original capacity. Physical processing of the membrane (i.e., compressing), can remove part of the initial water to allow the membrane to be more absorbable.
To be sterile, easy to use and not expensive	Membranes are easy to sterilize (steam or y-radiation) and package. Estimated cost of 1 cm^2 is $0.02.
To be available in various shapes and sizes	Can be molded in situ.
To provide easy and close wound coverage but allow an easy and painless removal	High elasticity and conformability.
To reduce pain during treatment	Unique BC nanomorphology of never-dried membrane promotes specific interaction with the nerve endings.
Being of high porosity for gaseous and fluids exchange	Highly porous material with pores sizes ranging from several nanometers to micrometers.
To be nontoxic, non-pyrogenic and biocompatible	Biocompatible, non-pyrogenic and nontoxic.
To be mechanically stable	Young's modulus value of several GPa.
To be of high conformability and elasticity	High elasticity and conformability.

The differences between the various BC producing bacterial strains and the different types of growth are also important in a bioengineering point of view. Figure 9 depicts the morphology of BC produced by different bacteria. These different structures can be used to create different materials and adapted to different conditions (92). For example, cellulose for implanted skin should display high porosity, whereas temporary wound dressings should have a nanoporous structure and should keep the wound moist during the healing process (107). Figure 9 shows the 3-dimensional network of nanofibers which makes BC ideal for wound dressing.

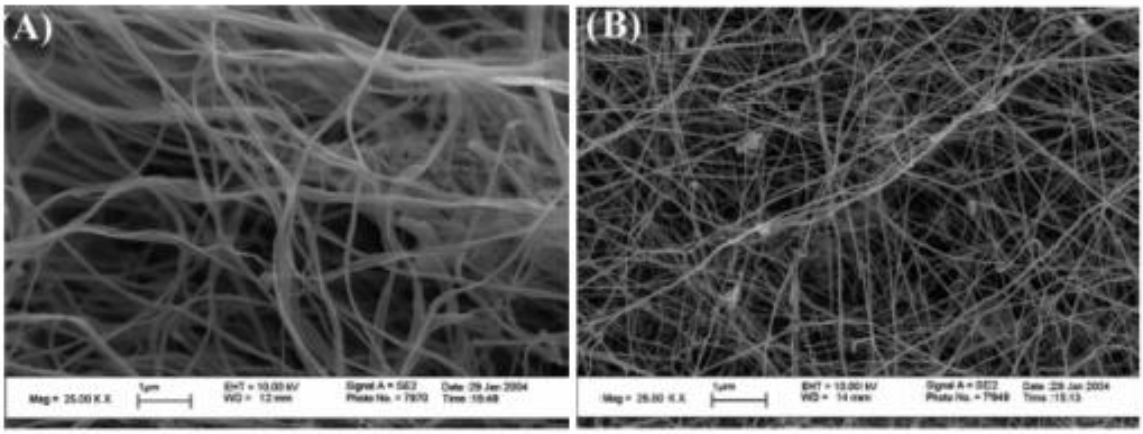

Figure 9 - Cellulose structure produced by two different *Gluconacetobacter* strains. (A) NQ5 (B) E5. NQ5 presents much larger ribbon structure which makes it a more compact and rigid membrane (92).

There are also reports in which BC has been used to mimic cardiovascular tissues (92). Yamanaka *et al.* (108) developed a process for the creation of long, hollow, bacterial cellulose tubes with an internal diameter f 2-6 mm. These BC tubes could be used as replacements of blood vessels or other tubular structures such as the ureter, the trachea, or the digestive tract. These vessels can be constructed using various different processes where the oxygen provided to the bacteria plays a major part (108).

In what regards bone replacement, the results are not as conclusive showing that some research is still needed (92). While there have been good results, assays showed that other existing membranes performed better than BC-derived ones that seemed to only promote cartilage growth instead of bone (109). However, other applications revealed promising results in the use of BC as scaffolds for *in vitro* tissue engineering (92),

involving the *in vitro* construction of a scaffold material which successfully mimics the extracellular matrix of normal tissues. Cells of the desired tissue are seeded onto the scaffold that helps in the development of a three dimensional structure. This scaffold can then be implanted into the affected area of the body, either as a replacement tissue or as a replacement organ (92).

4.2.2 **Incorporation of bioactive compounds in bacterial cellulose membranes**

The peculiar nanofibrillar structure of BC represents a perfect macromolecular support for inclusion of active compounds and therefore for the development of specific controlled drug release systems (for antibiotics, analgesics, anti-inflammatories, hormones, and anticancer drugs) (110,111). BC membranes are particularly useful for the design of topical drugs delivery since they have the ability to absorb exudates and adhere to irregular skin surfaces. In other words, transdermal delivery systems can work bilaterally, which means that they can both deliver the drug and adsorb exudates. This represents a good opportunity for the application of BC membranes.

The majority of patches that are already used are composed of superimposing different materials and BC-system can be composed of few materials or even a single layer (111,112). Moreover, *in vivo* compatibility studies have shown a good skin tolerance of BC until 24h (113). The inclusion of glycerin increased not only the malleability of the BC patch but also helped the moisturizing skin which in itself could help the treatment of skin diseases caused by dryness of the skin (113). BC membranes also represent a more appealing solution instead of oil-based formulations that can be easily lost due to contact (114). Due to all the properties mentioned above the pharmaceutical (and biomedical) industry has taken great interest in BC and several products and patents have already been released (115) as shown in Table 2.

For example, the diffusion potential of these membranes has been investigated by loading tetracycline in electron beam irradiated and non-irradiated BC (116). The results obtained showed that non-irradiated BC allows faster drug movement than with that afforded by the irradiated BC. This study revealed the potential of transport through the BC membrane but also proposed a model for the drug adsorption by this material (116).

Table 2 - Patents based on bacterial cellulose products (115).

Field of invention	Patent title	Patent number	Registration
Implantable device; soft tissue repair-drug delivery carriers	A method for producing implantable microbial cellulose materials for various medical applications	EP1795213 B1	European patent office (EPO)
Network meshed hydrogel. Drug delivery carrier, skin substitute	Novel network meshed hydrogel structure	TW M428771U1	Intellectual Property Office Taiwan (TIPO)
Calcium alginate capsule embedded and prepared *in situ* containing drugs, probiotics	Bacterial cellulose composite with capsules embedded therein and preparation thereof	US 2012308649A1	United states patent and trade mark office (USPTO)
Implantable bacterial cellulose; in-vivo application	Thermally modified microbial-derived cellulose for in-vivo implantation	EP1662976 A2 US20050042250 US8198261	USPTO, 2006 & EPO, 2005
Use of microbial (bacterial) cellulose in transdermal drug delivery	Microbial cellulose materials for use in transdermal drug delivery systems, method of manufacture and use	US 20060240084	USPTO, 2006
Medical implant; orthopaedic	Medical device including bacterial cellulose reinforced by resorbable or non-resorbable materials	US 20110262521A1	USPTO, 2011
Wide range of applications, dependent on density gradient dictated by thickness; number of drugs can be delivered	Bacterial cellulose films and uses thereof	EP 2390344 A1 US20110286948	EPO, 2011 USPTO, 2011
Cellulose hydrogels, making and applications; implant and ocular devices, release drug delivery systems	Cellulose-based hydrogels and methods of making thereof	US20130032059 A1	USPTO 2013

In a different study, Huang *et al.* (117) investigated the effects of BC membranes in the drug delivery of berberine hydrochloride and berberine sulphate when compared with commercial tablets. Their results showed that BC is a promising drug carrier that significantly extended the release duration of model drugs (117). Trovatti *et al.* (114,118) and Silva *et al.* (119,120) tested the drug delivery of lidocaine, ibuprofen, caffeine and diclofenac using BC membranes; in all studies, BC showed promising results due to the lower permeation rate observed when compared with commercial hydrogels or patches. It also has the advantages of being of easy application, simple preparation and being formed by a single layer structure (114,119,120). BC has also been used to keep the wounds from infecting by being imbedded with antimicrobial compounds (74,121,122). For example, antimicrobial BC dry films were obtained after immersion in benzalkonium chloride, an antimicrobial agent. The drug loading capacity *per* unit surface area was found to be 0.116 mg/cm^2 and its effect lasted for about 24h preventing contamination by *Staphylococcus aureus* and *Bacillus subtilis* (121). Other way of producing BC with antimicrobial properties is through incorporation of silver nanoparticles which produce up to 99.99% of antimicrobial activity against *Escherichia coli* and *S. aureus* (122).

Finally, BC can also be used for drug administration as a tablet excipient (123). *In-situ* fermentation of BC with hydroxypropyl methylcellulose (HPMC) produces HPMC-BC (HBC). This polymer can improve rehydration and small-molecule absorption, making it possible to deliver small drug molecules since HPMC is a well-established tablet excipient (123). Modified BC, in the form of microcrystalline cellulose has been synthetized using a method which employs *G. xylinus* (124). This form is similar to Avicel PH 101, which is a type of cellulose already commercialized (124). The use of plasticizers and additives can improve film properties and the coaslescence among the particles forming a film. The BC tablets, however, have moderate retardation drug release when compared to model paracetamol tablets (125).

In summary, and according to the literature and the information described above, BC has all properties required for the incorporation of bioactive materials, while ILs with antioxidant and anti-inflammatory activities are compounds that seem promising for therapeutic applications due to their low ecotoxicity and cytotoxicity values and high water-solubility. Therefore, these ILs can be incorporated in BC in order to develop biomaterials with both local and systemic applications.

5 Materials and methods

5.1 Materials

Bacterial Cellulose (~99 wt% water content), was produced using the bacterial strain *Gluconacetobacter sacchari*, as described below.

The PBS buffer at pH 7.4 (0.1 M) was prepared using the following compounds at the following concentrations: 8.01 g/L sodium chloride, NaCl, (extra pure, Acros); 1.78 g/L di-sodium hydrogen phosphate, Na_2HPO_4, (99 wt% of purity, Panreac); 0.20 g/L potassium phosphate monobasic, KH_2PO_4, (99 wt% of purity, Sigma-Aldrich) and 0.27 g/L potassium chloride, KCl, (99 wt% of purity, Sigma-Aldrich).

Choline hydroxide, [Chol]OH (in a methanol solution at 45 wt%, Sigma-Aldrich) and phenolic acids, namely gallic acid (99.5 wt% of purity, Merk), ellagic acid (97 wt% of purity, Alfa Aesar), caffeic acid (99 wt% of purity, ACROS), were used in the synthesis of cholinium-based ILs.

2,2-Diphenyl-2-picrylhydrazyl hydrate (DPPH) was acquired from Sigma-Aldrich. Methanol (HPLC grade), acetone (99.9 wt% of purity), and ethyl acetate (99 wt% of purity) were obtained from VWR. The water used in this study was double distilled, passed by a reverse osmosis system and further treated with a Milli-Q plus 185 water purification apparatus.

5.2 Methods

5.2.1 Cholinium-based ILs synthesis and characterization

Three cholinium-based ILs were synthesized by the neutralization of [Chol]OH with the respective acid, namely gallic, caffeic and ellagic acids, and according to literature protocols (6). [Chol]OH (1 eq., 45 wt % in a methanol solution) was added dropwise to the phenolic acid solution in methanol, with a molar excess of 1.1 equiv, at 0 °C, under nitrogen atmosphere. Regarding the $[Chol]_2[Ell]$ synthesis, the [Chol]OH was added to the ellagic acid solution in methanol, with a molar ratio of 2:1. The reaction mixture was stirred at room temperature, under nitrogen atmosphere, and protected from light overnight, producing the cholinium IL and water as the byproduct. The methanol and water

were then removed under reduced pressure. In the synthesis of [Chol][Caf], the unreacted acid was eliminated with acetone (3 × 20 mL), followed by filtration to remove the cholinium IL (which is in the solid state). The same procedure was adopted for [Chol][Gal], only replacing acetone by methanol. Finally, the residual solvent was removed under reduced pressure and the obtained compound was dried under high vacuum for at least 48 h.

As stated before, dicholinium ellagate ($[Chol]_2[Ell]$, di((2-hydroxyethyl)trimethylammonium) 3,8-dihydroxy- 5,10-dioxo-5,10-dihydrochromeno[5,4,3-*cde*]chromene-2,7-bis(olate)), cholinium gallate ([Chol][Gal], (2-hydroxyethyl)trimethylammonium 3,4,5-trihydroxybenzoate), and cholinium caffeate ([Chol][Caf], (2-hydroxyethyl)trimethylammonium (E)-3-(3,4- dihydroxyphenyl)acrylate) were synthesized, and their structures confirmed by ^{1}H and ^{13}C NMR spectroscopy showing a high purity level for all the ionic structures Annex 1. The ^{1}H NMR and ^{13}C NMR spectra were recorded using a Bruker Avance 300 at 300.13 MHz and 75.47 MHz, respectively, using deuterated water/dimethyl sulfoxide (D_2O/DMSO) as solvent and trimethylsilyl propanoic acid/tetramethylsilane (TSP/TMS) as internal reference.

Their full names, acronyms, and chemical structures are depicted in Table 3. Note that in the case of ellagic acid the reaction scheme should depict H_2A instead of HA and two [Chol]OH molecules.

Table 3 - Synthesis scheme and chemical structure of the cholinium-based ILs prepared.

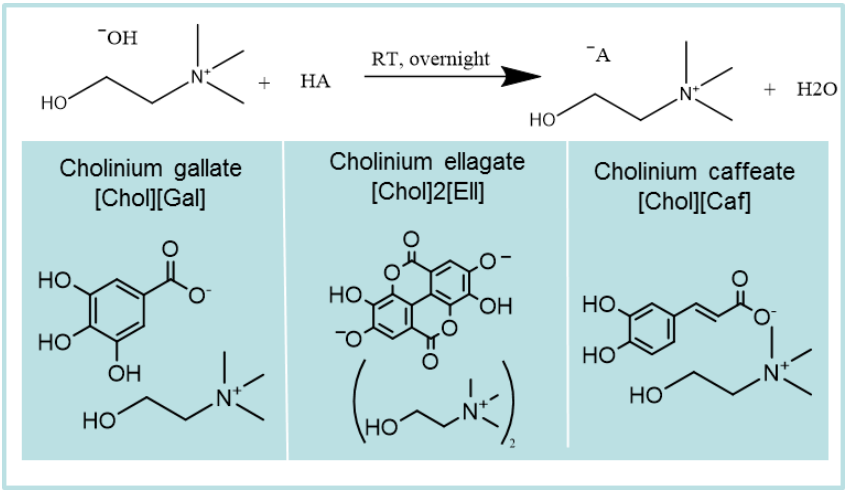

5.2.2 **BC production**

BC membranes (99 wt% water content) were produced in our laboratory using conventional Hestrin–Schramm culture medium (76). *G. sacchari* was the bacterium used as described elsewhere (80). After growing for 6 days, BC membranes were removed from culture media, washed three times with 0.5 M NaOH at 80 °C for 30 min, and then thoroughly washed and neutralized with distilled water. Pure BC membranes were kept in distilled water in a sterile environment at 4 °C until their use (114).

5.2.3 **Preparation and characterization of BC-IL membranes**

Wet BC membranes, with 2 cm diameter and about 0.8 cm thickness (around 23 mg of dry BC) were weighed and *circa* 50 % of their water content was drained by hand-pressing between two acrylic plates at room temperature. BC membranes were then soaked in 1 mL of a solution containing [Chol][Caf], $[Chol]_2[Ell]$ and [Chol][Gal] with a concentration of 10 mg/mL. After the complete absorption of the solution by the BC membranes, the BC-IL membranes were placed over Petri dishes and dried at room temperature under a nitrogen atmosphere. The dried BC-IL membranes were kept in a desiccator until use.

FTIR-ATR spectra of BC and BC-IL dried membranes (as well as of the individual components) were obtained on a Perkin Elmer spectrometer equipped with a single horizontal Golden Gate ATR cell. Thirty-two scans were acquired in the 4,000–600 cm^{-1} range, with a resolution of 4 cm^{-1}.

BC and BC-IL membranes were also analyzed by SEM by cutting an adequate size of membrane, while for cross-section images the membranes were broken after immersing them in liquid nitrogen. The samples were then covered with carbon and analyzed using a Hitachi SU-70 microscope at 4 and 10 kV.

^{13}C solid-state cross-polarized magic-angle spinning nuclear magnetic resonance (^{13}C CP-MAS NMR) spectra were recorded on a Bruker Avance 400 spectrometer. The samples (in this case, BC, BC-IL and pure ILs), were packed into a zirconia rotor sealed with Kel-F caps and spun at 7 kHz. The acquisition parameters were as follows: 4 μs 90° pulse width, 2 ms contact time, and 4 s dead time delay.

Tensile assays were performed using an Instron 5944 testing machine with Bluehill 3 software in tensile mode with a 1kN load cell. Samples were strips of 70mm×5mm and the gauge length 30 mm. At least 7 strips were tested for each sample. The corresponding stress (MPa)–strain (%) curves were plotted, and the Young's modulus values were determined from the slope of the low strain region in the vicinity of 0.05%.

The decomposition temperatures of the membranes were determined by TGA. TGA was conducted with a Shimadzu TGA 50 analyzer equipped with a platinum cell. Samples were heated at a constant rate of 10 °C min^{-1}, from room temperature to 800°C, under a nitrogen flow of 20 mL min^{-1}. The thermal decomposition temperatures were taken as the onset of significant (≥0.5%) weight loss, after the initial moisture loss.

X-ray diffraction patterns were measured using a Phillips X'pert MPD diffractometer using Cu Kα radiation. The XRD measurements were performed with a scan step size of 0.02° and a time per step of 2.5s from 4-40 2θ range.

Crystallinity index (C.I.) and percentage crystallinity (% Crystalline) of BC samples were calculated as follows (126):

$$C.I. = \frac{I_{200} - I_{am}}{I_{200}}, \quad (1)$$

$$\%\text{Crystalline} = \frac{I_{200}}{I_{200} + I_{am}} \times 100, \quad (2)$$

where I_{200} is the maximum intensity of diffraction of the (200) lattice peak (2θ of 22°–23°) and I_{am} is that of the amorphous part between 2θ of 18° and 19°, where the intensity is minimum.

5.2.4 **Quantification of cholinium-based ILs**

The quantification of cholinium-based salts in the solutions resulting from the dissolution assays, was carried out by UV spectroscopy, using a Thermo Scientific Evolution 600 spectrophotometer, at the wavelengths specified in Table 4. The calibration curves for each cholinium-based salt in PBS buffer are also presented in Table 4.

Table 4 - Calibration curves used to determine the concentration of the cholinium-based ILs in PBS buffer (absorbance *versus* concentration in mg/L).

	λ_{max}/ nm	Calibration curve	R^2
[Chol][Caf]	286	y = 0.0497x + 0.0123	0.9966
[Chol][Gal]	259	y = 0.0299x + 0.0048	0.9965
$[Chol]_2[Ell]$	253	y = 0.083x – 0.0063	0.9995

5.2.5 **Swelling rate assays**

Swelling rate assays were conducted using dried BC and BC-IL membranes. Membranes were weighted and then soaked in individual containers with distilled water at room temperature, during 24h. Samples were taken out of water, the excess of water was gently removed with absorbent paper and membranes were weighted and re-immersed again. The swelling of the membranes was calculated according to equation 3:

$$\frac{w_{wet} - w_{dry}}{w_{dry}} \times 100 \quad , \qquad (3)$$

where w_{dry} and w_{wet} are the weight of dried and wet BC samples, respectively.

5.2.6 **Dissolution assays**

BC-IL dried membranes were placed in a closed flask containing 180 mL of PBS solution at pH 7.4 to approach the blood pH. The cholinium-based ILs release was then evaluated under magnetic stirring and protected from light. At determined time intervals (during 24h), 1 mL of solution was withdrawn, and the same volume of fresh buffer was added to maintain a constant volume. The cholinium-based salt content in each aliquot was determined by UV spectroscopy, as described above. The IL content at each time was plotted as a cumulated percentage release, determined according to Equation 4:

$$\frac{1 \times C_{n-1}}{180} + C_n \quad , \qquad (4)$$

where C_{n-1} and C_n are the IL concentrations at time n - 1 and n. Two replicates were performed for each sample.

Dissolution assays of the ILs in methanol were also made using the same time intervals in order to relate the amount of IL dissolved in the media with its antioxidant

activity. The calibration curves used for the quantification of ILs in methanol are presented in Table 5.

Table 5 – Calibration curves used to determine the cholinium-based ILs concentration in methanol (absorbance *versus* concentration in mg/L).

	λ_{max}/ nm	Calibration curve	R^2
[Chol][Caf]	286	y = 0.0531x - 0.0299	0.9963
[Chol][Gal]	259	y = 0.0319x - 0.0005	0.9987
[Chol]$_2$[Ell]	253	y = 0.0632x + 0.0613	0.9786

5.2.7 **Computational approaches: COSMO-RS**

The molecular geometry of all molecular models (cellulose, water and ILs) were optimized at the B3LYP/6-31++G** computational level in the ideal gas-phase using the quantum chemical Gaussian03 package. Vibrational frequency calculations were performed for each case to confirm the presence of an energy minimum (127).

Then, the standard procedure was applied for COnductor like Screening MOdel for Real Solvents (COSMO-RS) calculations, which is comprised of two steps. In the first step, Gaussian03 was used to compute the COSMO files. The ideal screening charges on the molecular surface for each species were calculated by the continuum solvation COSMO model using BVP86/TZVP/DGA1 level of theory. Afterwards, COSMO files were used as an input in COSMOtherm code (128) to calculate the thermodynamic properties of the individual components and the ternary (water–IL–BC) system involved in the adsorption phenomena. The computational approach was de- scribed elsewhere (127,129). The ratio used was 90/10M cellulose-IL ratio.

The cellulose/buffer and cellulose/methanol partition coefficients (P) of IL at infinite dilution were calculated by COSMO-RS. According to the chosen quantum method, the functional and the basis set, we used the corresponding parameterization (BP_TZVP_ C30_01201) that is required for the calculation of physicochemical data and contains intrinsic parameters of COSMOtherm as well as element specific parameters (127).

5.2.8 **Antioxidant activity assays**

The antioxidant activities of the BC-ILs were determined using the 2,2-diphenyl-1-picrylhydrazyl (DPPH) radical scavenging assay. The principle of the assay is based on the color change of the DPPH solution from purple to yellow, as the radical is quenched by the antioxidant. When a solution of DPPH is mixed with a substance that can donate a hydrogen, the reduced form of DPPH is obtained, and the solution which started to be violet turns to be yellow. This change in color was monitored by visible spectroscopy at 517 nm (15).

Briefly, 3.34 mL of a DPPH solution (1 mM) in methanol was mixed with 50 mL of methanol with the BC-IL membrane in the medium. Samples were kept in the dark for 30 min, 1 h, 2 h, 4 h, 6 h and 24 h at room temperature and then the decrease in the absorbance at 517 nm was determined (130). A blank control was made with 250 µL of DPPH solution in methanol and then methanol was added until the volume of 4 mL was reached. The same process was applied to the precursor acids of each IL, using 10 mg/L of acid solution instead of methanol until the volume of 4 mL was reached. The readings were made at the same intervals in the ILs. DPPH radical scavenging activity, AA(%), was expressed using Eq. 5:

$$AA(\%) = \frac{(A_0 - A_1)}{A_0} \times 100 \quad (5)$$

where A_0 is the absorbance of the control and A_1 is the absorbance of the sample at 517 nm.

5.2.9 **Biological Assays**

5.2.9.1 **Cell Cultures**

Murine Raw 264.7 macrophages (ATCC number: TIB-71) were cultured in Dulbecco's Eagle Medium supplemented with 10% non-inactivated fetal bovine serum (FBS) and the human keratinocyte cell line HaCaT (DKFZ, Heidelberg, Germany) was cultured in Dulbecco's Modified Eagle Medium supplemented with 4 mM of glutamine, 4,5 g/L glucose and 10% heated inactivated FBS. Both media were supplemented with penicillin (100 $U.mL^{-1}$), and streptomycin (100 $\mu g.mL^{-1}$). Cells were incubated at 37 °C in

a humidified atmosphere of 95% of air and 5% of CO_2 and were used after reaching 70–80% confluence, which occurs approximately every 3 days after initial plating.

5.2.9.2 **Cell viability assays**

In order to investigate the biocompatibility of the BC matrices containing the different ILs we addressed their effect on macrophage and keratinocyte viability/metabolic activity by a resazurin assay (131). Briefly, 1.5x10^6 Raw 264.7 or 1.0x10^6 HaCaT cells were plated per well of a 6 well plate and let to stabilize overnight. Then, the BC membranes were put into contact with cell cultures during 24h by means of 24mm Trasnwell inserts with 0.4uM polycarbonate membranes (Corning, NY, USA). Resazurin was added to cells (final concentration of 50 mM) during the last 2 and 1 hour(s) of incubation for HaCat and Raw 264.7, respectively. Finally, 200 µl from each condition were transferred to a 96 wells plate and the absorbance of resorufin (the product of the resazurin reduction) measured at 570 and 600 nm in a standard spectrophotometer BioTek Synergy HT (Biotek Instruments, Winooski, VT, EUA). The data are the means of two biological independent experiments conducted in duplicate for each condition.

5.2.9.3 **Anti-inflammatory assays**

The anti-inflammatory activity of the cholinium-based ILs was tested using nitric oxide (NO) Measurement. The pro- or anti-inflammatory activity of BC-[Chol][Gal], BC-[Chol][Caf] and BC-$[Chol]_2$[Ell] was evaluated in the mouse macrophage cell line Raw 264.7. The production of NO was measured by the accumulation of nitrite in the culture supernatants, using a colorimetric reaction with the Griess reagent. The cells were plated at 3 × 105 cells/well in 48-well culture plates, allowed to stabilize for 12 h, and then incubated with the culture medium (control), in presence of three membranes with 0.167 mg of [Chol][Gal], [Chol][Caf], $[Chol]_2$[Ell] for 24 h in order to have the concentration of 56 mg/L in the media. Briefly, 100 µL of culture supernatants was collected and diluted with equal volume of the Griess reagent [0.1% (w/v) N-(1- naphthyl)ethylenediamine dihydrochloride and 1% (w/v) sulfanilamide containing 5% (w/v) H_3PO_4] during 30 min, in the dark. The absorbance at 550 nm was measured using a standard spectrophotometer MultiSkan Go (Thermo Fisher Scientific, Waltham, MA, USA)(6).

6 Results and Discussion

6.1 BC-IL membranes preparation and characterization

Bacterial cellulose (BC) was obtained in the form of 6–8 mm thick membranes after an incubation period of 6 days, at 30ºC, in static conditions. BC was then purified, as described in the experimental section, to remove all bacteria and culture medium imbedded in the membrane. After this step, 50 % (w/w) of the water in the membranes was drained by applying pressure, in order to facilitate the absorption of the 10 mg/mL aqueous solutions of the cholinium-based ILs. Since 1 mL of these solutions was added to 4 cm^2 membranes to be absorbed, the IL content in each of these membranes was of 10 mg, which results in a 2.5 mg load of compound *per* cm^2 of BC.

The visual aspect of the obtained membranes is depicted in Figure 10. It is possible to observe that the wet membranes appear as malleable hydrogels.

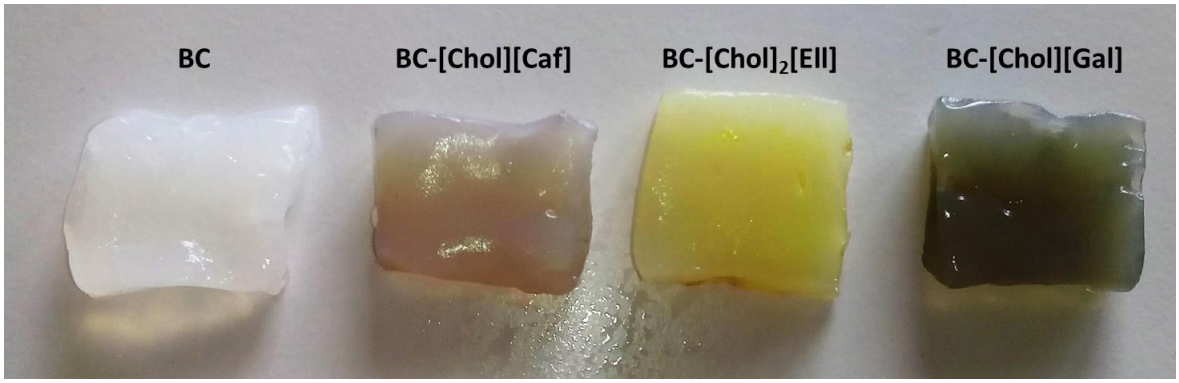

Figure 10 – Macroscopic appearance of the wet BC membranes incorporating different cholinium-based ILs.

The morphology of the BC and BC-IL dried membranes was assessed by SEM. Images of the surface and cross-section of the membranes with [Chol][Caf], $[Chol]_2[Ell]$ and [Chol][Gal] are presented in Figure 11. It is possible to observe that the typical BC surface tridimensional nanofibrillar network was unaltered with the incorporation of ILs. The same trend was observed for the lamellar cross-section morphology that was only filled with the ILs molecules. These results are according to previous works on drug-delivery systems using BC (114,119–121), in which it was also possible to observe the spaces between the BC strands were filled with the different bioactive compounds used.

Moreover, these SEM images suggest a uniform dispersion of the ILs in the membranes surface and bulk. Nevertheless, in the case of $[Chol]_2[Ell]$, there appears to be some IL crystallization on the surface of the membranes, showing that this IL does not disperse well in BC. In Trovatti *et al.* (114) work with incorporation of lidocaine in BC is suggested that compound crystallization might be due to some precipitation during the compound incorporation in BC or drying process.

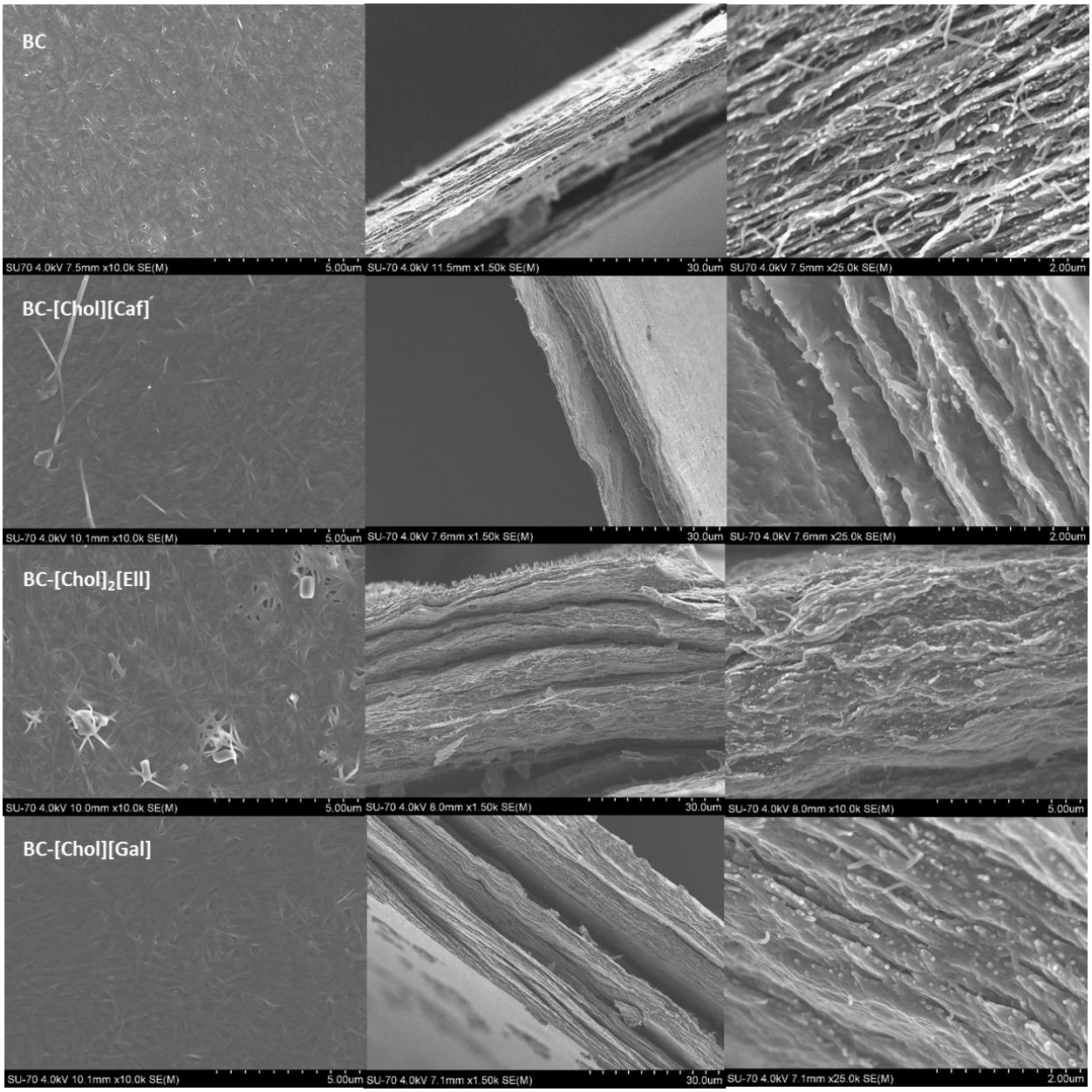

Figure 11 – Surface and transversal SEM images of BC and BC-IL. The first column corresponds to surface images while the second and third column correspond to transversal SEM images.

BC, pure ILs and BC-IL membranes were also analyzed by FTIR (Figure 12) in order to confirm the incorporation of the ILs into the BC matrix. The BC FTIR spectrum displays the typical peaks of a cellulosic substrate. The band at around 3300 cm^{-1} corresponds to the stretching vibration of the OH groups and the peaks between 2900 and 2800 cm^{-1} are associated with the axial deformation of CH and CH_2 groups (CHOH and CH_2OH). The absorption bands with lower wavelength values, around 1300–1400 cm^{-1} correspond to the angular bending of C–OH and CH groups, the peaks at 1150–900 cm^{-1} are associated with the C–H bonds of CH_2 groups and the stretching of C–O–C groups (119,120,132). These results are accordance with data in literature confirming the purity of the BC used (119,120,133,134).

The FTIR spectrum of [Chol][Caf] presents a band at 3024 cm^{-1} corresponding to the OH stretching vibration. It also presents a band at 1600 cm^{-1} corresponding to the C=O stretching vibration and the band at 1500 cm^{-1} which corresponds to the angular bending of CH. The peak at 1373 corresponds to C-OH stretching while the bands between 1300 and 1150 cm^{-1} correspond to the CN bond; finally, the peaks between 980 and 580 correspond to the C-H out-plane vibration from the aromatic ring (132,133).

The FTIR spectrum of $[Chol]_2[Ell]$ presents bands between 2893 representing the O-H stretching vibration and 1577 cm^{-1} present in the C=O functional group. The peak at 1400 cm^{-1} corresponds to the CH vibration. The peaks in the 1200-1300 cm^{-1} region, are associated with C-OH stretching bond vibrations typical of phenol functional groups. The peak at 1172 cm^{-1} corresponds to the CN vibration in the choline moiety and finally the peak at 825 cm^{-1} is due to the two neighboring aromatic rings (132,133).

The spectra obtained for [Chol][Gal] present a band at 3080 typical of O-H stretching vibrations and at 1600 cm^{-1} corresponding to C=O stretching vibration. The band in the 1200-1300 cm^{-1} region, is due to C-OH stretching bond vibrations typical of phenol functional groups. At 1185 cm^{-1} it is observed the peak corresponding to the CN vibration in choline moiety. Finally, between 1100 and 750 cm^{-1}, peaks corresponding to the CH out-of-plane bending vibration of the aromatic rings (132,133) are identified.

The spectra of the BC-ILs membranes are a sum of the BC and pure IL spectra which leads to the conclusion that the cholinium-based ILs were incorporated into the BC. However, the BC-IL spectra are much more similar to that of BC since the amount of the ILs is only about 20% of the total weight of the membranes.

These results are according with other works in literature related with the incorporation of bioactive compounds in BC such as the works of Silva *et al.* (119,120) in which there was incorporation of caffeine and diclofenac and the resulting FTIR spectra was a combination of BC, the compound and also glycerol.

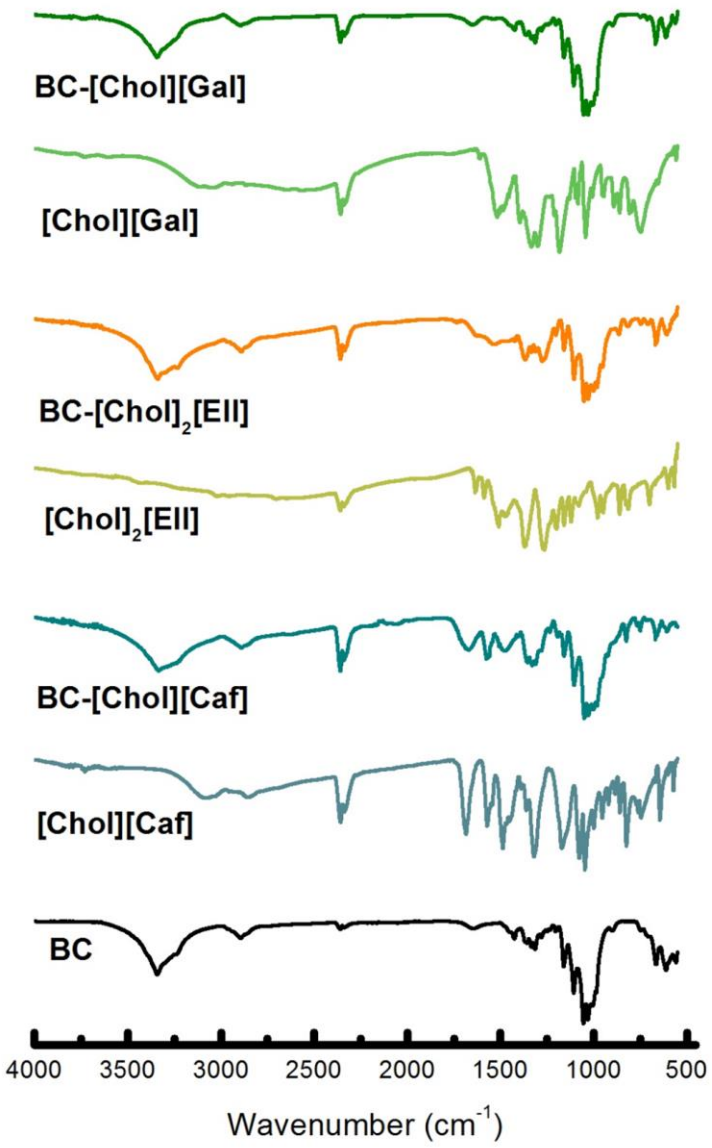

Figure 12 – FTIR spectra of BC, pure ILs and BC-ILs.

The incorporation of the ILs into the BC membranes was also confirmed by solid ^{13}C CPMAS NMR. In Figure 13 are depicted the spectra of BC, pure ILs and of BC-IL membranes.

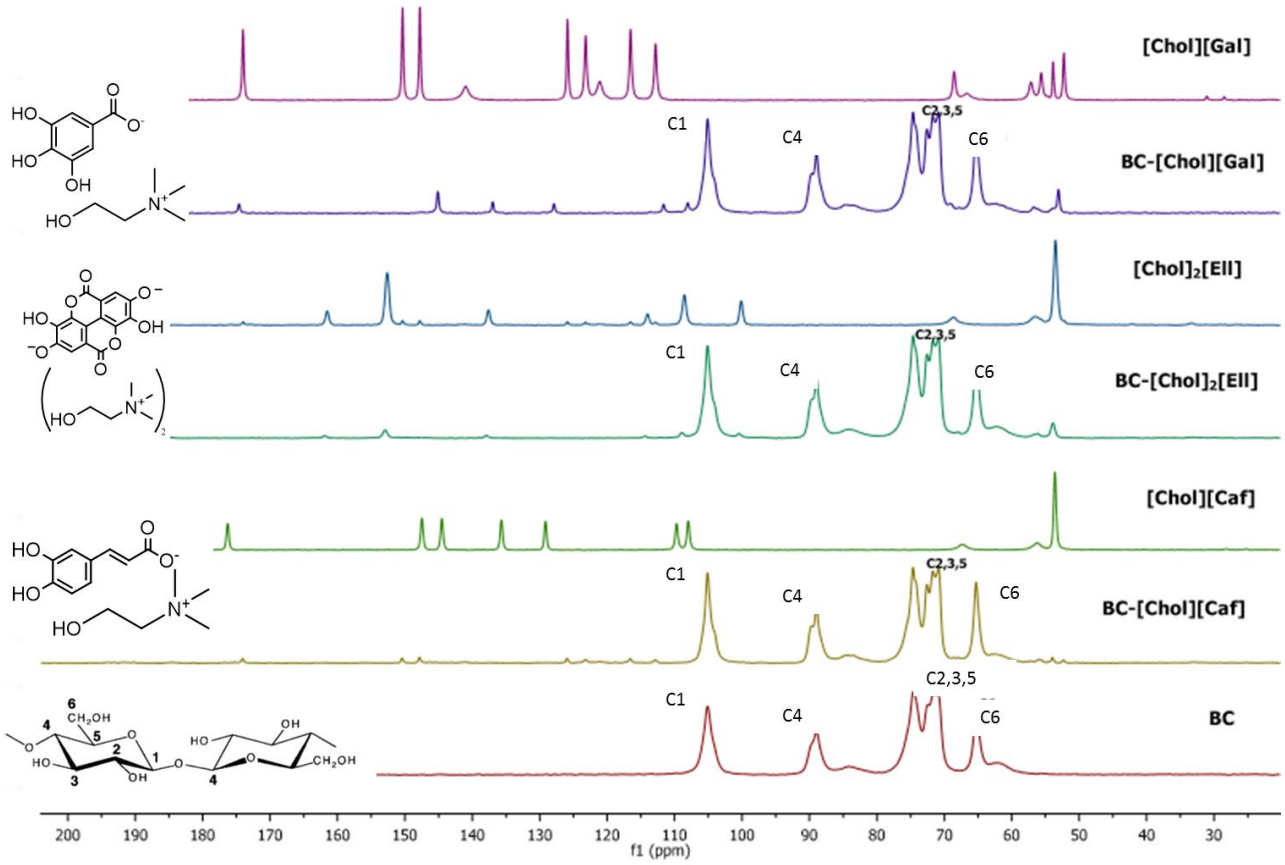

Figure 13 - Solid ^{13}C CPMAS NMR spectrum of BC, BC-ILs and pure ILs. NMR spectra of BC with the respective peaks identification.

The spectrum of BC is in close agreement with the literature (119,120,135,136). The peak corresponding to C1 appears at 105.11 ppm, C4 at 86.57 ppm, C2, 3 and 5 occur at around 72 ppm and finally C6 appears at 63.68 ppm.

In the case of BC-[Chol][Caf], in Figure 13, the peaks that are not from BC were identified as: δ 170.04 (COO), 150.41 (CHCHCOO), 147.93 (COH-4), 125.33 (COH-3), 123.22 (CHCHCOO), 116.60 (C-1), and 112.90 (C-6), and finally at 53.95 which seems to be for the three methyl groups of choline $N(CH_3)_3$ (6). In the same line, the peaks of the BC-$[Chol]_2$[Ell] spectra indentified in Figure 13 are as follows: δ 161.93 (2x (COO)), 142.46 (2x (CO)), 136.37 (2x (COCO)), 114.38 (2x (COCO)), 108.92 (2x (CCO)), 100.51 (2x $(C(C)_3)$), 56.18 (2x (NCH_2CH_2OH)), 53.88 (2x $(N(CH_3)_3)$). For BC-[Chol][Gal], in Figure 13 we have: δ 174.43 (COO), 145.12 (C-3 and C-5), 136.99 (C-4), 127.90 (C-1), 111.65 (C-2 and C-6), 56.474 (NCH_2CH_2OH), 53.09 $(N(CH_3)_3)$ (6). The peaks between

110 and 60 ppm of the IL do not appear since they correspond to the BC cellulose peaks and they sumperimpose over them.

Therefore, analyzing Figure 13 it is possible to see that the peaks corresponding to the pure ILs appear in the NMR spectra of the corresponding BC-IL membranes confirming that the ILs were incorporated in the BC network. Furthermore, the peaks in BC-[Chol][Caf] and BC-[Chol][Gal] spectrum slightly suffer some deviations in the chemical shifts when compared to the ones corresponding to the pure ILs. This indicates that these ILs interact with BC causing the resonances to be altered. However, $[Chol]_2[Ell]$ and BC-$[Chol]_2[Ell]$ spectra present the peaks at the same ppm value indicating that this compound does not interact strongly with BC.

Trovatti *et al.* (114) also used NMR to confirm the incorporation of lidocaine in BC, and like in this case the BC-lidocaine spectrum was a sum of the individual spectra of each component with the resonances for lidocaine shifting suggesting the interaction between the compound and BC.

The thermal stability of the BC and BC-IL membranes was assessed by TGA (Figure 14). BC presents a decomposition temperature close to 360 °C which is consistent with the literature (133,134). All ILs loaded BC membranes are less thermally stable than BC because of the lower thermal stability of the ILs (6). The initial decomposition temperatures of the BC-ILs increase in the following order: BC-[Chol][Caf] (187.1 °C) < BC-[Chol][Gal] (189.2 °C) < BC-$[Chol]_2[Ell]$ (189.6 °C). This order of thermal stability is in accordance with the stability of the pure ILs ([Chol][Caf] (155.0 °C) < [Chol][Gal] (185.3 °C) < $[Chol]_2[Ell]$ (265.0 °C) (6)) which leads to the conclusion that the second degradation step observed in the TGA thermogram (Figure 15) corresponds to the degradation of the IL-enriched fraction and the third one to the degradation of the BC enriched fraction. The first degradation step at 100 °C corresponds to the evaporation of water. Similar results were obtained with cholinium-based ILs incorporated in pullulan and chitosan films (137). In this work, there was also a decrease in the degradation temperature of the material, with a two-step degradation also corresponding to the degradation of the IL followed by the degradation of the polysaccharide.

For both [Chol][Caf] and [Chol][Gal] the Td_i are higher than those of pure ILs. However, in the case of $[Chol]_2[Ell]$ there is a high decrease of the Td_i which is in agreement with the ^{13}C NMR results. Since $[Chol]_2[Ell]$ does not interact with BC it starts

degrading earlier, while the other ILs, since they are interacting with BC, result in more stable membranes with higher Td_i values.

In summary, a decrease in the thermal stability of the BC membranes was observed after incorporation of the ILs; however, this decrease does not compromise the utilization of BC-IL for drug delivery and skin applications since the sterilization processes are typically carried out at temperatures bellow 135 °C, and therefore there is no risk of degradation of the material.

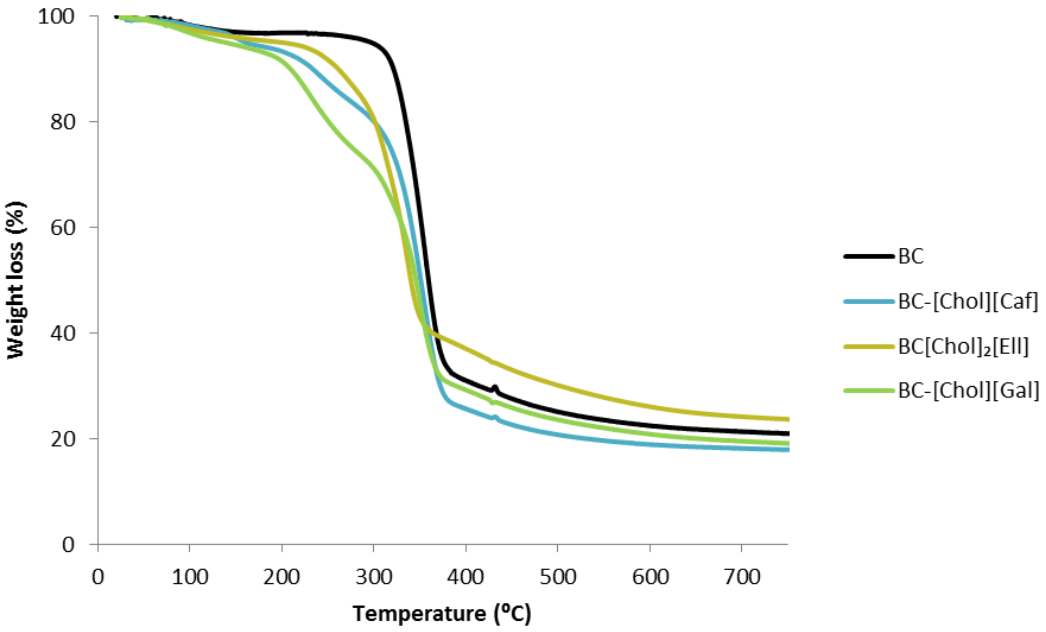

Figure 14 – TGA analysis results: weight fraction loss as function of temperature.

The last step on the BC and BC-IL membranes chemical characterization was the measurement of the XRD patterns in order to understand if there were any changes in the crystalline structure of BC with the incorporation of the ILs. As can be seen in Figure 15 the diffractogram of BC presents the typical cellulose I pattern. The XRD spectra of the pure cholinium-based ILs is also depicted in Figure 15. The main diffraction signals are at around 2θ = 14.5, 16.8, 22.6 and 34.9°, assigned to the 101, $10\overline{1}$, 200 and 040 diffraction planes, respectively (134,138). The BC-IL membranes preserved most of the of the XRD pattern of pure BC. Nevertheless, some additional peaks were observed in the BC-IL diffractograms, which correspond to the presence of ILs, as can be seen in the Figure 15.

Shahmohammadi *et al.* (139), obtained similar results, using ZnO nanoparticles loaded in BC. The diffractogram of BC-ZnO also displayed the typical cellulose I pattern with the addition of the typical peaks of zinc oxide. In this work, the BC-ZnO was also treated with US-radiation which caused a shift of the peaks to lower planes and decrease in intensity which suggests structural changes to BC.

Table 6 presents the crystallinity and crystallinity index values in which it is possible to observe that there are only very small decreases in both parameters after the incorporation of ILs were perceived.

Table 6 – Crystallinity and crystallinity index of BC and BC-IL.

Sample	At 2θ range		Crystallinity (%)	C.I.
	I_{am}	I_{200}		
BC	2692	26038	90.6	0.9
BC-[Chol][Caf]	2774	25462	90.2	0.9
BC-[Chol]$_2$[Ell]	2853	22118	88.6	0.9
BC-[Chol][Gal]	3146	19547	86.1	0.8

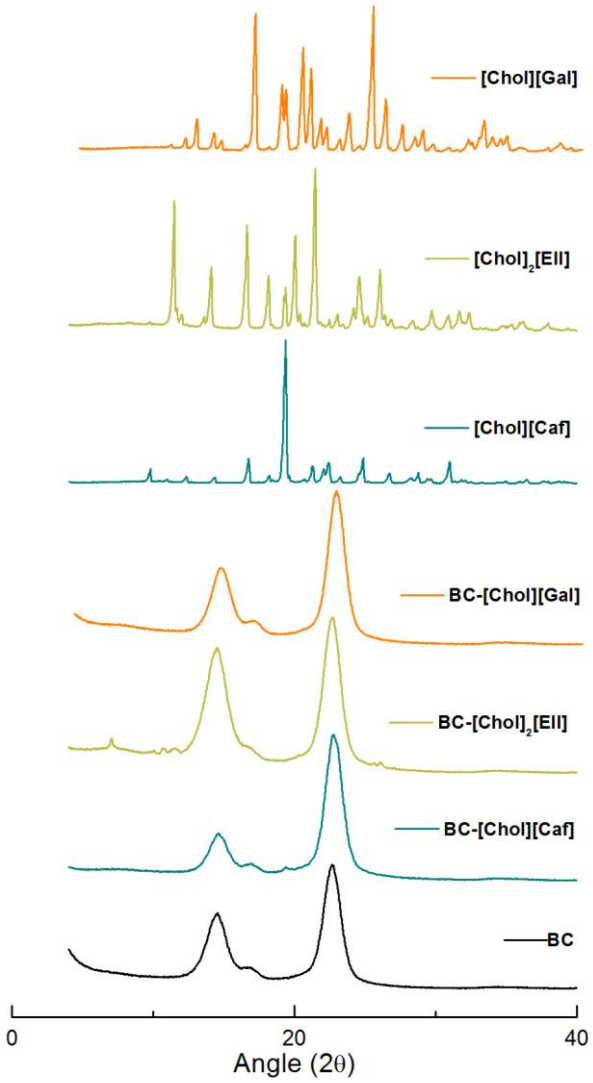

Figure 15 – XRD spectra for BC and BC-IL.

BC and BC-ILs were also characterized in regards to their mechanical properties (tensile tests). Three particular parameters were determined, namely elongation at break (%), Young Modulus (MPa) and tensile strength (MPa) (Figure 16). With these parameters it is possible to characterize the BC membranes according to their main mechanical characteristics and to understand how the incorporation of cholinium-based ILs influence or not the mechanical properties of the BC membranes.

The elongation at break, whose results are shown in Figure 16, is defined as the ratio between the initial length and final length after breakage of the test specimen. It expresses the capability of a material to resist to changes of shape without crack formation.

Analyzing Figure 16 it is possible to conclude that the elongations at break of BC-$[Chol]_2[Ell]$ (2.86%) membrane is slightly higher than that of BC (2.30%). The same was not verified for BC-[Chol][Caf] and BC-[Chol][Gal], that present lower elongation at break values than pure BC, with 1.93% and 0.93%, respectively.

The Young's modulus (Figure 16) is a mechanical property of linear elastic solid materials, and it defines the relationship between tensile stress (force *per* unit area) and tensile strain (proportional deformation) in a material. It characterizes the material regarding its stiffness (125). BC presents the highest modulus, namely 17835 ± 875 MPa, which is in accordance with the literature (140), followed by [Chol][Caf] (14273 ± 935 MPa) and [Chol][Gal] (14089 ± 404 MPa). On the other hand, $[Chol]_2[Ell]$ presents the lowest Young´s modulus value (11258 ± 636 MPa), which is in accordance with the its higher elongation discussed before which makes it less rigid. Therefore, in this case the IL acts as a plasticizer.

Finally, the tensile stress at tensile strength, the resistance of a material when a force is applied, was also measured (results shown in Figure 16). BC presents the highest tensile stress (376 ± 93 MPa) followed by BC-[Chol][Caf] and BC-$[Chol]_2[Ell]$, which presents tensile stress values approximately 30% lower than BC. BC-[Chol][Gal] presents the lowest tensile stress, (94 ± 35 MPa), which taking in account its lower elongation at break, can be considered the most brittle material among the membranes studied. Although some modifications to the main mechanical characteristics of BC were provoked by the ILs, the results obtained are still in the same direction with the scope of this project.

Tomé *et al.* (137), also obtained similar results for tensile strength and Young's Modulus using cholinium-based ILs incorporated in pullulan and chitosan films. There was also a decrease on those values when the ILs were incorporated. This behavior was attributed to the plasticizing role of the ILs, since they establish physical interactions with the polysaccharide chains separating them and thus giving them more flexibility.

In the inclusion of lidocaine into BC membranes (114), a decrease in elongation was also observed and, on the other hand, the Young's modulus and tensile strength increased showing that this compound made the material brittle and thus glycerol addition as plasticizer, necessary. In this case, although elongation diminished, so did the other parameters which is why the use of glycerol, that has been extensively used in other works (119,120), was foregone.

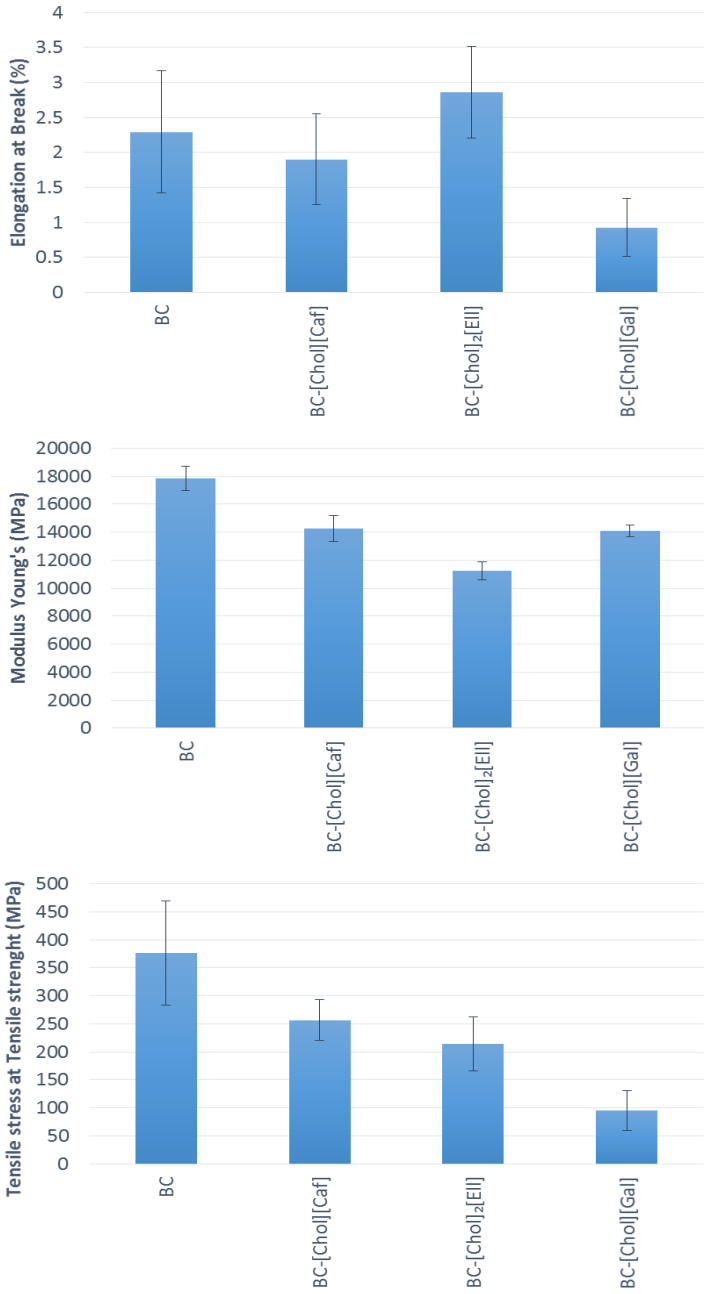

Figure 16 – Elongation at break (%), Young's modulus (MPa) and Tensile stress at tensile strength (MPa) of BC and BC-ILs.

6.2 **Swelling rate assays**

The swelling behavior of the BC-IL membranes was also investigated because it is an important parameter on topical drug delivery, since the ability of re-hydration in contact with skin influences the releasing rate of bioactive compounds. The results of this assay are

shown in Figure 17. For all BC-ILs membranes studied there was a quick absorption of water in the first 3 h of the assay; afterwards there was a tendency to stabilization with a small increase until 24 h. These results are in accordance with other studies carried out with BC-drug loaded membranes (119,120), in which there is a quick swelling rate of the membrane until 2 h of assay, and a much slower one afterwards. The maximum swelling rates observed for BC, BC-[Chol][Caf], BC-$[Chol]_2$[Ell] and BC-[Chol][Gal] were 175 ± 16%, 716 ± 95%, 676 ± 243%, and 377 ± 28%, respectively. These swelling rates are ordered according to the ILs solubility in water, also depicted in Figure 17. In conclusion, the swelling rate of BC-ILs is much higher than that of BC, which is related to the fact that the ILs are highly hydrophilic and hence provide cellulose with a higher ability to swell. This is a promising result since the swelling rate plays a major role on the release of ILs from the membrane to the skin.

In the previous referred works (119,120) drug loaded BC membranes also had a higher swelling ration but in this case it was due to the inclusion of glycerol which is an well-known humectant and hydrophilic compound.

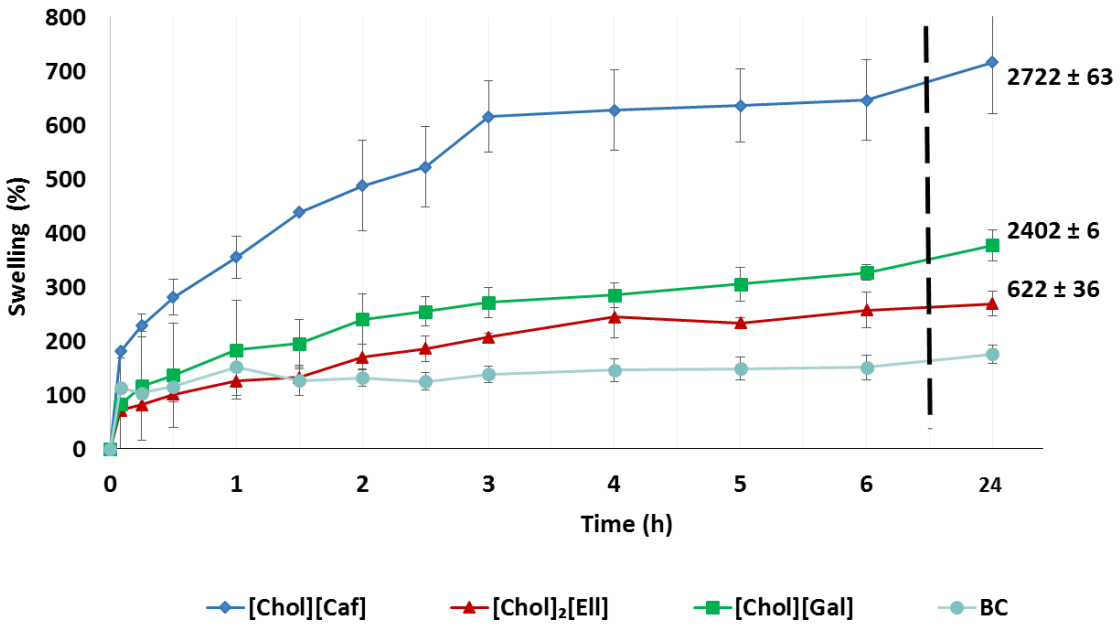

Figure 17 – Swelling rate assays results for BC and BC-IL membranes. The values represented are the solubility's in water for each of the ILs in mmol.L^{-1} (6)**.**

6.3 **Dissolution assays**

The dissolution assays (Figure 18) were carried out with 4 cm^2 membranes prepared as described in the Experimental section. The assays were performed during 24h, with solution aliquots taken at specific intervals until 24 h. PBS buffer solution (180 mL) at pH 7.4 was used in order to mimic the pH of the human blood. All aliquots volumes taken during the assay were replaced with fresh solution. The amount of accumulated IL in the solution was calculated as a cumulative percentage as described in the methods section. The calibration curves for each compound can be found in Annex III.

First of all it is possible to conclude that the dissolution of the ILs from the dried membranes is always faster than that from the wet counterparts, independently of the IL used. With wet membranes there is a diffusion process through the BC tridimensional network, while with the dried membranes there is an immediate dissolution of the ILs present in the membranes. Moreover, it was previously established that the tested ILs have a high solubility in water (6) which supports their quick dissolution (and diffusion) into the PBS buffer aqueous solution. Nevertheless, $[Chol]_2[Ell]$ precipitates in osmotic solutions due to the presence of salts; it was only possible to dissolve this compound until 46.53 mg/L (6) when used in solutions that contain salts. Although no precipitation was perceived during these assays it is still possible that some of the results can be influenced by this behavior, since the media used was PBS. The IL content for each membrane can be found in Annex III.

According to Figure 18, for both BC-[Chol][Caf] and BC-[Chol][Gal] wet membranes, about 70% dissolution of the ILs content in membranes was reached. The higher concentrations were observed at 8 h with an IL content of 73.91 ± 0.94 % and 65.95 ± 0.05 %, respectively. With BC-$[Chol]_2[Ell]$, the dissolution from the wet membranes was much lower reaching only 51.58 ± 0.97 % at 24h. This result might be explained by the low solubility of this compound in PBS buffer.

For dry membranes the dissolution is immediate for the cases of [Chol][Caf] and [Chol][Gal], and for the latter the IL content actually reaches 100%. In the case of $[Chol]_2[Ell]$ the dissolution rate was once again lower. The maximum dissolution observed for the dry membranes was 92.03 ± 0.85 % for BC-[Chol][Caf], 44.06 ± 0.99 % for $[Chol]_2[Ell]$ and 100.44 ± 1.58 % for BC-[Chol][Gal].

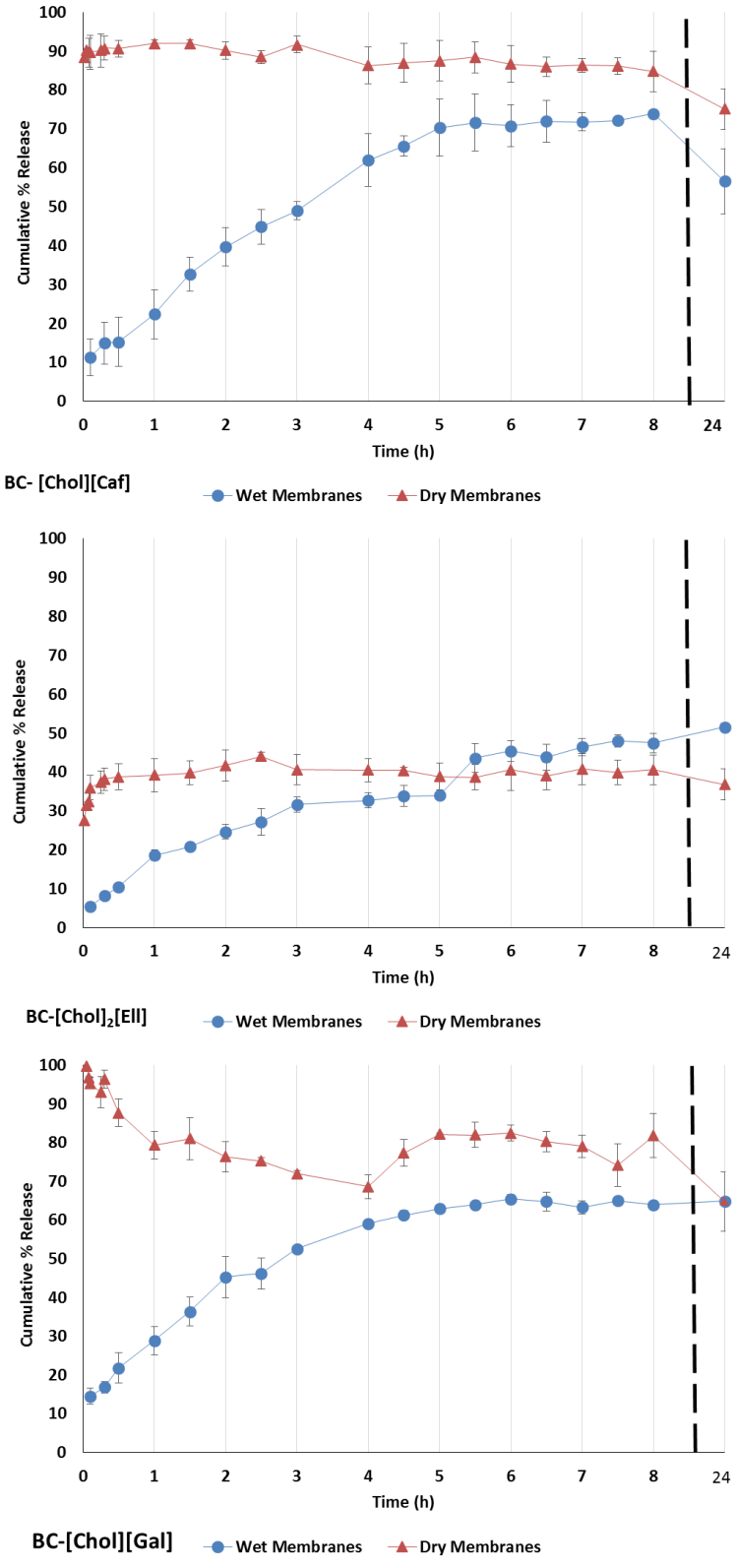

Figure 18 – Cumulative percentage of IL released from the BC to the PBS buffer solution during the 24h dissolution assay.

These results are according with similar assays conducted by Silva *et al.* (119,120) and Trovatti *et al*. (114) in which they used dry BC membranes with incorporation of different drugs, such as caffeine, diclofenac and lidocaine. For all these compounds there was a fast diffusion into the PBS buffer, usually in the first 20 minutes or less of the assay. Total compound diffusion was never achieved since a plateau was always reached. However, it was noted that the chemical nature of the compounds could influence the rate of dissolution according to its affinity for the buffer and BC.

Aiming to understand the dissolution results, COSMO-RS was used. COSMO-RS correctly predicts the affinities between the different ILs used, cellulose and in this case a 0.1M phosphate buffer, as can be seen in Figure 19. This method, has been used in various works as a reference quantitative parameter of the affinity of ILs for different materials and media (127,141).

According to COSMO-RS the lower the logP, the higher is the affinity of the compound to the buffer medium, as depicted in equation 6.

$$Log\ P = \log\left(\frac{[IL]cellulose}{[IL]medium}\right) \quad (6).$$

According to Figure 19, [Chol][Gal] has the highest affinity to the buffer medium followed by [Chol][Caf] and $[Chol]_2$[Ell], the latter with a very low affinity to the buffer aqueous solutions. The dots in the figure represent the highest percentage of IL released to the buffer medium during the assays, and the results are according to the COSMO-RS prediction.

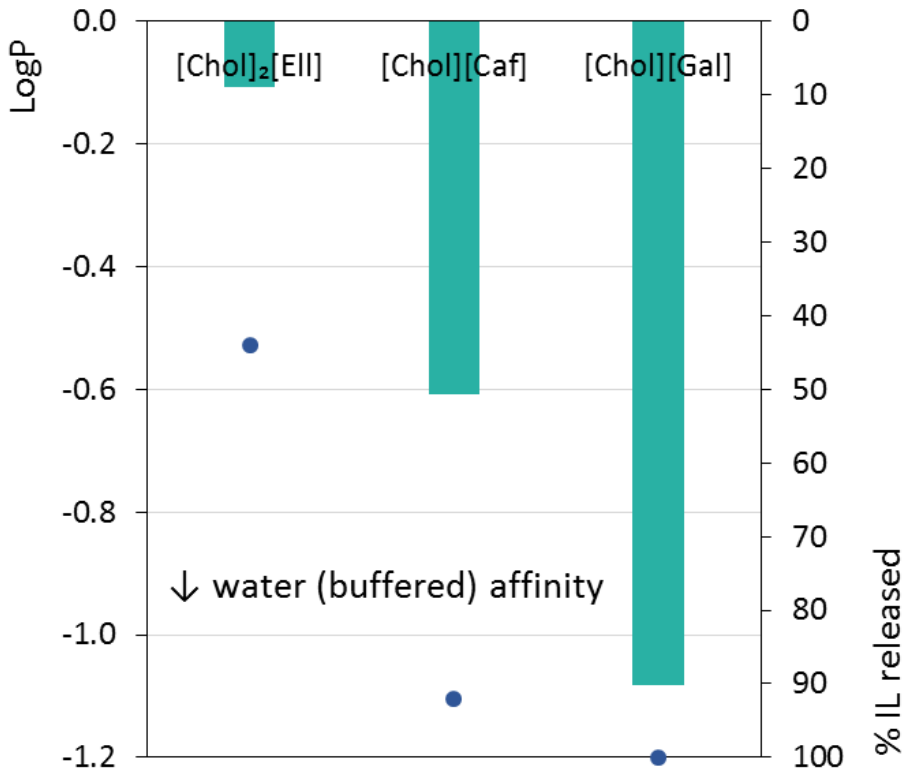

Figure 19 – COSMO-RS results for BC-ILs in a phosphate buffered media. • represents the maximum experimental values for the IL percentage released.

In Figure 20 are depicted the SEM images of the BC-IL membranes after the dissolution assays. The gaps between the fibbers are now hollow or collapsed. These results were expected since most of the cholinium-based ILs were dissolved into the buffer solution.

Also, in the case of BC-$[Chol]_2[Ell]$, IL crystals are still visible on the surface of the membrane. This result confirms the diffusion assays results using PBS buffer in which the cumulative percentage release of the IL was bellow 50%, and also portrayed in the COSMO simulation, thus confirming that the $[Chol]_2[Ell]$ was not totally diffused to the buffer staying in great extent incorporated in the BC network.

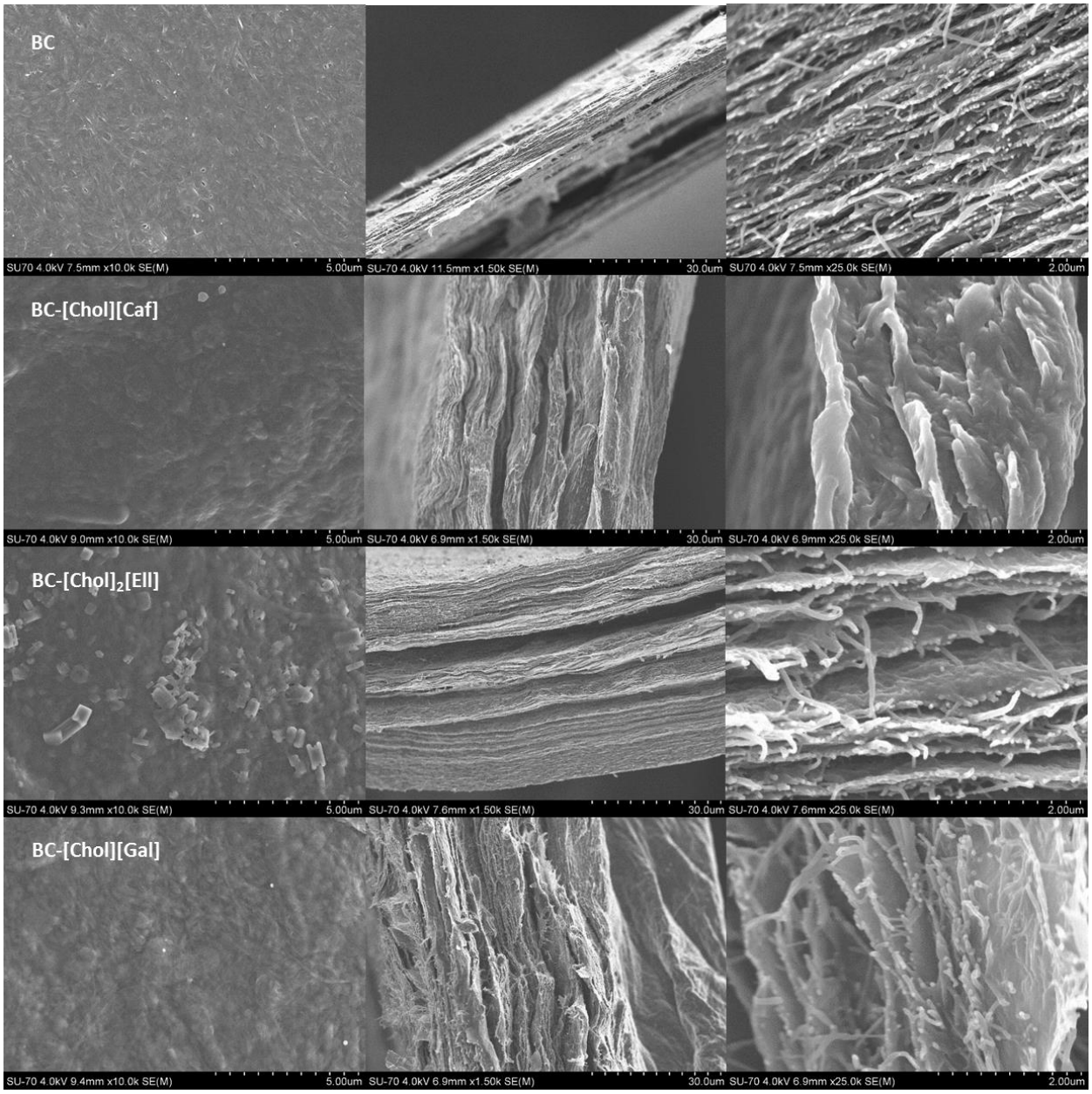

Figure 20 – Surface and transversal SEM images of BC and BC-IL after dissolution in PBS buffer. The first column corresponds to surface images while the second and third column correspond to transversal SEM images.

For most systems, there was a decrease in the ILs content in the buffer at 24h (Figure 21). In order to understand if it corresponds to a decomposition of the IL or if the IL is being absorbed again by the membrane, a test using only 10 mg of the pure IL (without BC) in the buffer was carried out (Figure 21). In fact, it was verified a decrease on the ILs content in the aqueous solution at 24h, leading to the conclusion that the ILs are unstable and suffer degradation after too much time in the buffer aqueous solution.

Moreover, $[Chol]_2[Ell]$ appears as a highly instable compound since after 2 h in a buffer aqueous solution it is observed a decrease of its amount. However, this needs to be further investigated with more assays using different concentrations.

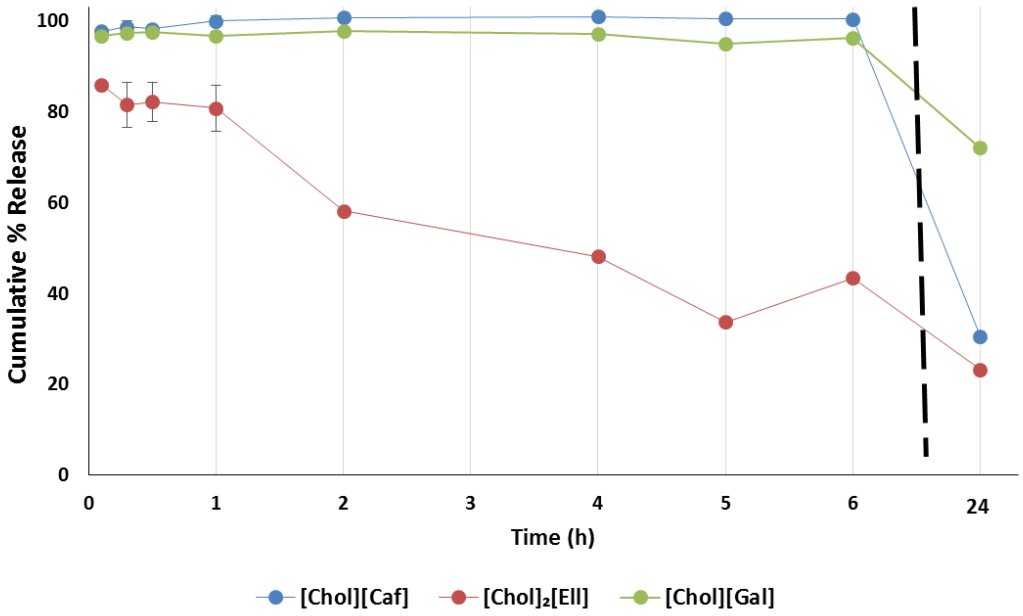

Figure 21 – Results for the test made to confirm the ILs stability in PBS buffer.

According to these results and having in mind the drug delivery application, the wet membranes seem to be the most promising systems since they allow a controlled drug diffusion through the membrane. These results are according to various studies that used wet BC membranes for drug-delivery (119,120,142,143).

6.4 Methanol dissolution assays and antioxidant activity tests

Methanol dissolution assays were also carried out in the same way as the dissolution assays using the PBS buffer aqueous solution. The calibration curves made for each compound using methanol and all related data can be found in Annex IV. These assays were made in order to correlate the amount of ILs dissolved during the dissolution assay and the results of the DPPH tests in methanol, in which samples were taken at the same intervals of time.

Concerning the dissolution of ILs in methanol the results also vary considerably depending on each IL and on the state of the membrane (wet or dry), as can be seen in

Figure 22. Similarly to the PBS assay, there is a faster dissolution of the ILs when using dry membranes, while wet membranes allow a more controlled release of the ILs. However, for both [Chol][Caf] and [Chol][Gal] there seems to be a faster dissolution rate in PBS rather than methanol when using dry membranes. In the case of wet membranes, the dissolution of [Chol][Caf] is faster and higher with methanol, while with [Chol][Gal] it is very similar.

It is also interesting to see that for the majority of the ILs, with the exception of $[Chol]_2[Ell]$, in the wet BC membranes the quantity of IL in methanol at 24 h is higher than in PBS aqueous solution, which means that ILs are more stable or more soluble in methanol than in PBS buffer/aqueous solution.

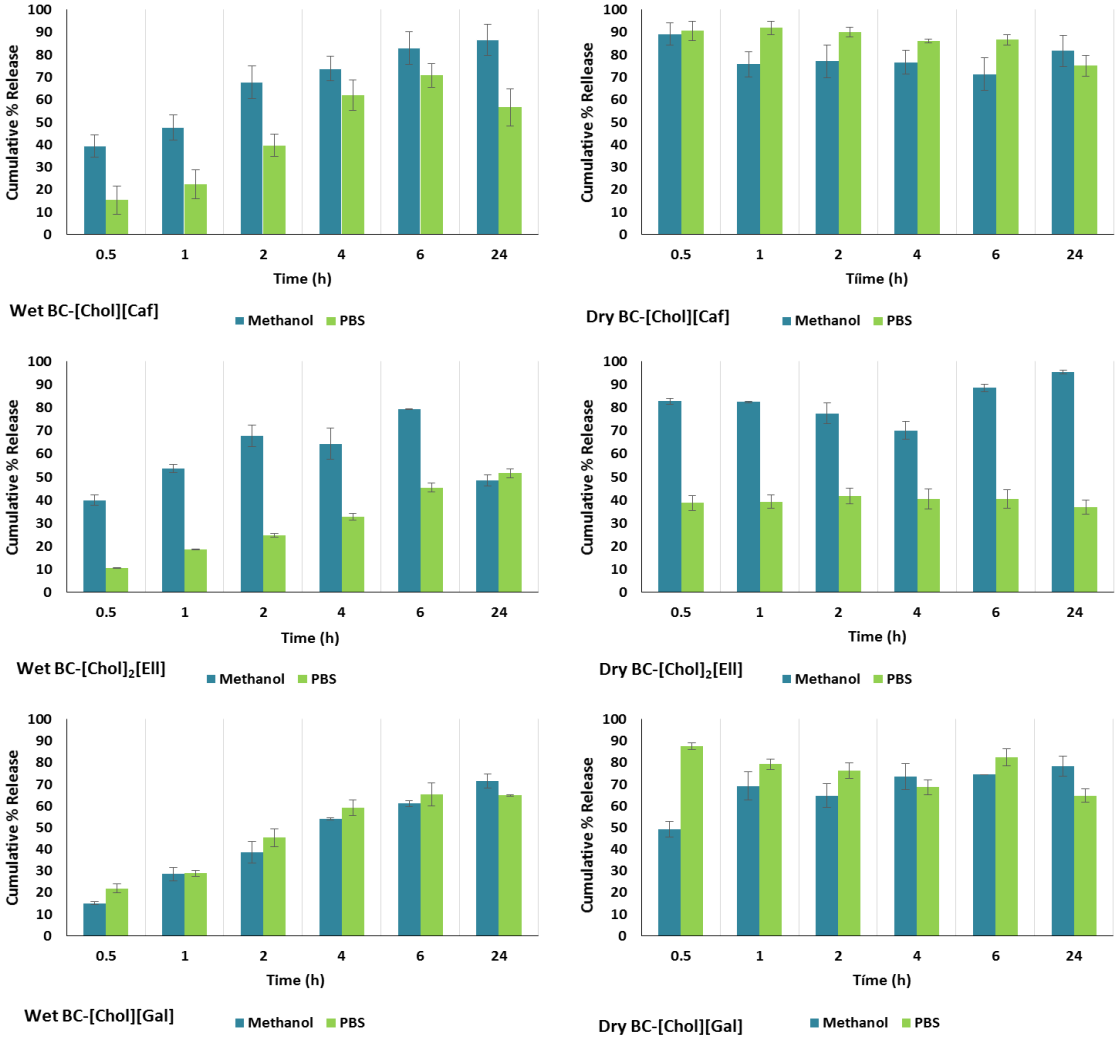

Figure 22 – Cumulative percentage released of IL into methanol and the PBS buffer solution.

COSMO-RS predictions were also carried out in order to understand the dissolution behaviors or controlled release of ILs in methanol - Figure 23. The experimental values are also included and correspond to dry membranes after 30 min of the assay. The 6h were chosen because of the possible IL degradation. However, the rank of ILs obtained from the experimental assays are slightly different to those predicted by COSMO-RS. In the case of [Chol][Caf] and [Chol][Gal] the results are according with COSMO-RS prediction. Neverthless, in the case of $[Chol]_2[Ell]$, its experimental release is higher than the predicted one.

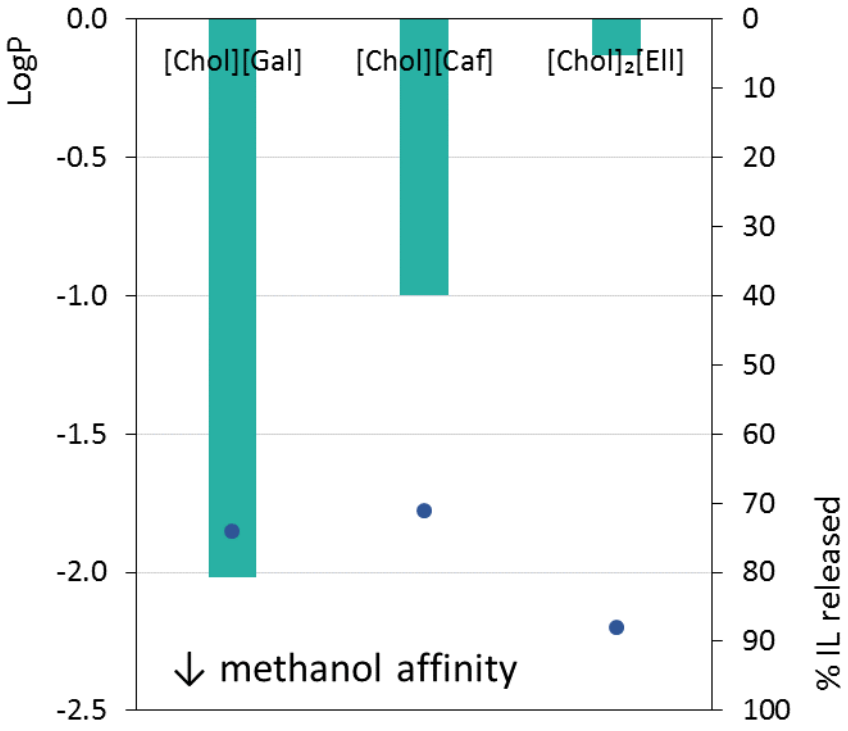

Figure 23 – COSMO-RS results for the affinity of the ILs in BC-ILs in methanol media. The • represent the experimental values for the IL percentage released until 6h of the assay.

In Figure 24 are depicted the results of the dissolution assays in methanol and the antioxidant activity of the membranes determined using the DPPH test. It is possible to conclude that the antioxidant activity is maintained over 80% for both BC-[Chol][Caf] and BC-[Chol][Gal], either with dry or wet membranes. On the other hand, BC-$[Chol]_2[Ell]$ seems to have less antioxidant activity than the other two studied BC-ILs membranes and suffers a decrease with time. In general, the wet BC-ILs membranes show antioxidant activity values higher than those displayed by the dry BC-ILs.

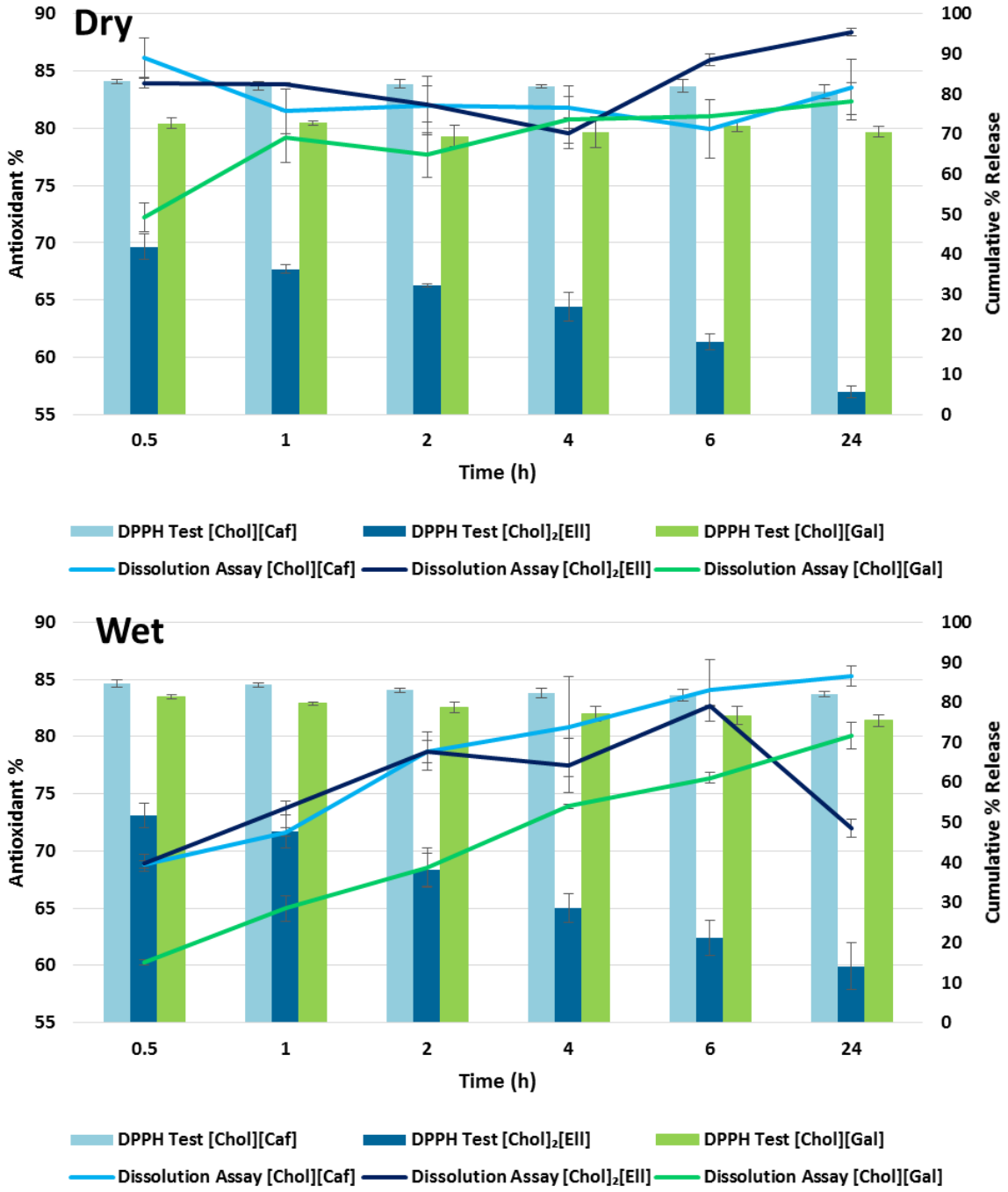

Figure 24 – Cumulative percentage release of the IL into the methanol dissolution and its antioxidant activity.

In Figure 25 are compared the values of antioxidant activity of the precursor acids and respective BC-ILs. The acid solutions used had a concentration of 10 g/L which corresponds to a total of 37.5 mg of acid in solution. In Annex 2 are presented the amounts of ILs that were assumed to be incorporated in each membrane

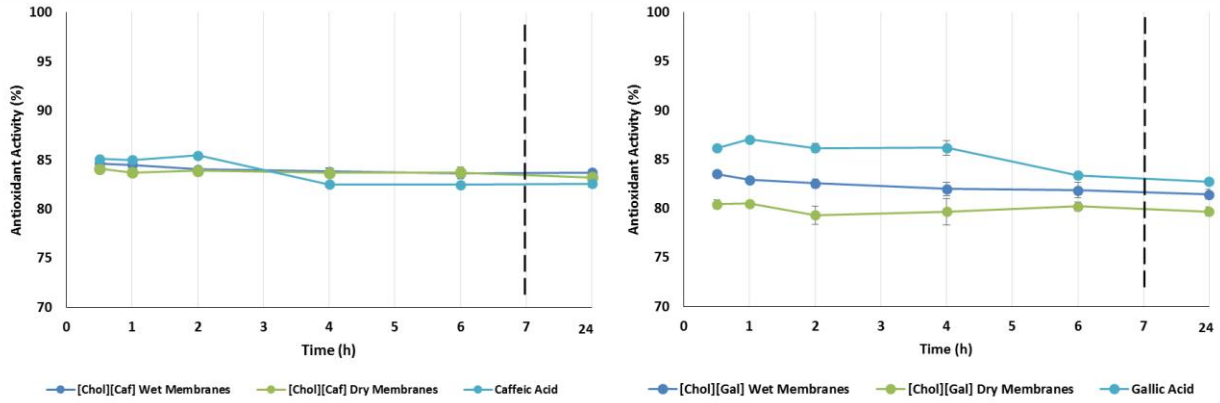

Figure 25 – Antioxidant activity percentage for BC-ILs and respective precursor acids.

The results obtained for all ILs are very similar, though for both gallic and caffeic acids the antioxidant activities are higher than for the corresponding BC-IL membranes. As stated before, the dissolution of ILs in the methanol is not total and these membrane dos not have exactly 10 mg of each IL, which means that with a smaller quantity of IL we can obtain the same antioxidant activity than with a higher amount of acid. These results are according with the previous work of Sintra *et al.* (6), in which the same was verified. In the case of ellagic acid, we could not measure the antioxidant activity due to dissolution problems as shown in Annex 3. The same issue was observed in previous works (6,144).

6.5 **Preliminary biological assays**

In order to evaluate if BC-IL membranes could be used as topical materials with no adverse effects, preliminary cytotoxicity assays were carried out. In these assays, it was evaluated the capacity of Raw 264.7 (macrophages) and HaCaT (keratinocytes) to metabolize the resazurin dye after being exposed to BC-IL membranes. Additionally, anti-inflammatory assays were also made using Raw 264.7 with the goal of confirming that the anti-inflammatory capacity of the ILs was not affected by their incorporation in the BC membranes (6).

The preliminary results for the cytotoxicity are depicted in Figure 26 and 27. It is clear that both BC-[Chol][Gal], BC-$[Chol]_2$[Ell] and also pure BC do not have any adverse effects since they maintain the cell viability at 100%. On the other hand, for [Chol][Caf] there seems to be a slight decrease of cell viability down to 92%. Still, this is not a very

significant decrease and all these results need to be further comproved by repeting these tests with more replicates.

BC has been subjected to numerous assays of bicompatibility and citotoxicity (96,145). Jeong *et al.* (145), in which a culture of vein endothelial cells (HUVEC) from the human umbilical cord were used in contact with BC, with no decrease of the cell viability.

Furthermore, in the work of Tomé *et al*. (137), using pullulan and chitosan films, the two cholinium-based ILs were also evaluated in regards of their citotoxicity using three different human cell lines having no significant citotoxicity. Due to this, it was expected that the combination of BC-ILs would not have an adverse effect on the cells.

It is also important to remark that BC is non cytotoxic and has already been used for many biomedical applications (73), including dermal applications (113) . Also the ILs used did not cause a significant decrease in cell viability, especially in the concentrations used in this work as previously depicted in the work of Sintra *et al.* (6).

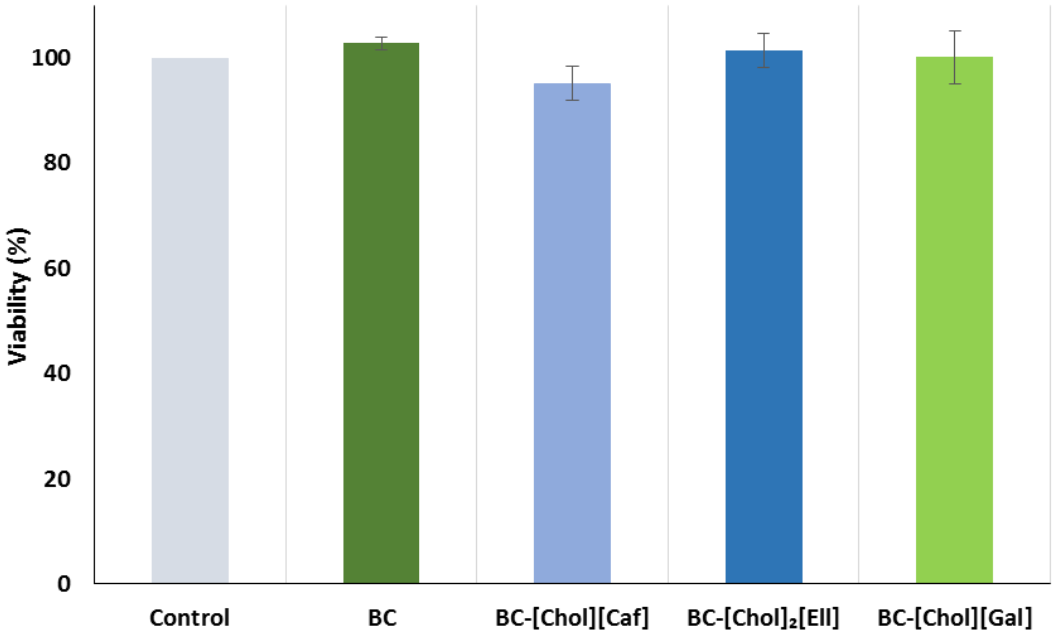

Figure 26 – Viability of Raw 264.7 accessed as the normalized response to cells exposed to BC, BC-ILs and untreated control.

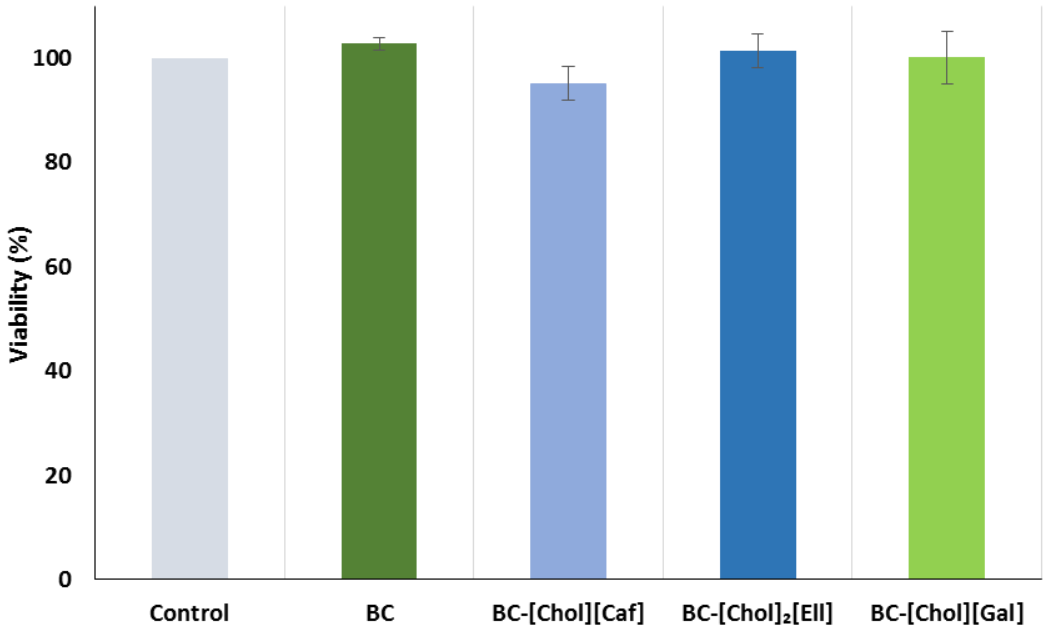

Figure 27 - Viability of HaCaT accessed as the normalized response to cells exposed to BC, BC-ILs and untreated control.

The results obtained for the anti-inflammatory assays are shown in Figure 28. These assays are usually performed by measuring the production of nitric oxide (NO) by the activation of macrophages and the consequent increased expression of NO synthase, which is a strong pro-inflammatory mediator closely associated with various inflammatory diseases.

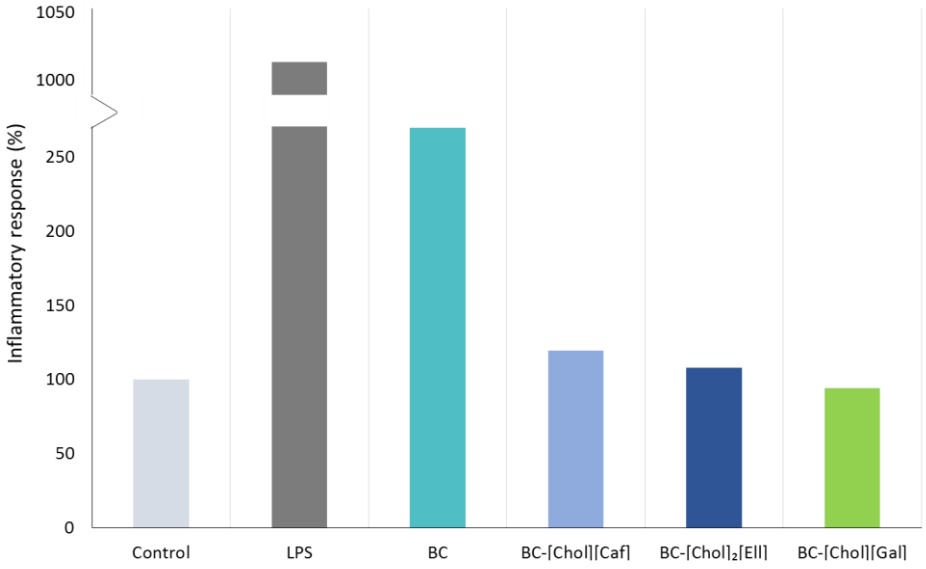

Figure 28 – Effect of BC and BC-ILs membranes on the inflammatory response by the macrophages.

Usually, cells are stimulated with LPS, which is a strong inflammation activator. However, during these assays, it was noticed that BC was activating the inflammatory response of macrophages which suggests that BC might has endotoxins that were not removed during the BC treatment process and that are therefore responsible for this reaction. Nevertheless, the BC-ILs were also tested and the results obtained reveal that ILs decrease the inflammation caused by BC showing that they do have anti-inflammatory properties, as previously reported using aqueous solutions (6) .

As can be seen in Figure 28, while BC has a 270% inflammatory response, the BC-ILs lead to values close to the reference value, in this case the control has the value of 100%. For [Chol][Caf] the inflammatory response was 120%, for $[Chol]_2[Ell]$ it was 108%, and in the case of [Chol][Gal] it was 94%. However, since BC was activating the inflammatory response of macrophages, it is required to carry further experiments by first eliminating the endotoxins from BC so that it can has the same value as the control. These assays will be repeated after the optimization and improvement of the BC purification process (146). However, and in general, from the preliminary results obtained, it can be concluded that BC-ILs membranes display anti-inflammatory characteristics.

7 Conclusions and Future Work

In this work, cholinium-based ILs with anti-oxidant and anti-inflammatory characteristics were incorporated in BC membranes to be used in topic applications. To this end, in this work, BC membranes were produced and all ILs synthesized. All BC-ILs membranes were characterized through Fourier transform infrared spectroscopy with attenuated total reflection (FTIR-ATR), solid nuclear magnetic resonance (NMR), X-ray diffraction, scanning electron microscopy (SEM), thermogravimetry and mechanical tests. All studies allowed to conclude that ILs were successfully incorporated in BC without changing significantly its crystallinity, mechanical properties and decomposition temperature.

Swelling assays were also conducted in order to determine the water holding capacity of BC and BC-ILs. For all BC-ILs it was observed an increase in the water holding capacity, and that was according to the water solubility of the tested ILs. The maximum swelling rate observed for BC, BC-[Chol][Caf], BC-$[Chol]_2$[Ell] and BC-[Chol][Gal] were 175, 716, 676 and 377 %, respectively.

Regarding the ILs dissolution, it was observed that for all BC-ILs membranes investigated, the IL dissolution was slower in wet membranes, while with dry membranes their release was immediate. In wet membranes the dissolution reached 73.91% for [Chol][Caf], 65.95% for [Chol][Gal] and 51.58% for $[Chol]_2$[Ell]. On the other hand, for dry membranes, the dissolution percentage values were 92.03% for BC-[Chol][Caf], 100.44% for BC-[Chol][Gal] and 44.06% for $[Chol]_2$[Ell] values reached within the first 10 minutes of the assays. Therefore, it is possible to conclude that wet membranes allow a more controlled dissolution of ILs.

Antioxidant tests were carried out with both BC-ILs and the respective precursor acids. The antioxidant activity was maintained at 80% for both [Chol][Caf] and [Chol][Gal], with either dry or wet membranes. On the other hand, $[Chol]_2$[Ell] antioxidant activity is lower but is always higher than 75% throughout the assays. In this case, ILs have similar antioxidant activities as the corresponding acids, but using a lower quantity, proving that BC-ILs are more effective in what concerns their antioxidant activity.

From preliminary biological assays it is possible to conclude that BC-ILs used display anti-inflammatory features since they inhibit the inflammatory. Also, BC-IL

membranes do not alter the cells viability, neither macrophages nor keratinocytes, pointing that they can be used in human skin. Nevertheless, an additional treatment of BC needs to be carried out and optimized in order to eliminate possible endotoxins that are causing an anti-inflammatory response.

In order to fully complete this work, while envisaging the use of BC-ILs membranes for topic drug delivery application, there is still need to carry out further investigations. In particular, the anti-inflammatory and cell viability assays need to be carried out again after the removal of BC's endotoxins. In addition to macrophages, keratinocytes should be also investigated.

Permeation assays are also an important step to complement this work in order to understand the IL permeation rate in human skin. Some preliminary tests were already carried out with human abdominal skin, using a 7 mL Franz cell using PBS as diffusion media at 32 °C, and will be finalized in the near future. To culminate the otimization of the produced materials, *in vivo* animal model tests need to be carried out aiming to fully understand determine the potential of these membranes.

8 REFERENCES

1. Podda M, Grundmann-Kollmann M. Low molecular weight antioxidants and their role in skin ageing. Clin dermatology. 2001;26:578–82.

2. Dai J, Mumper RJ. Plant phenolics: extraction, analysis and their antioxidant and anticancer properties. Molecules. 2010;15(10):7313–52.

3. Kusumawati I, Gunawan I, editors. Studies in Natural Products Chemistry. 1st ed. Amsterdam; 2013.

4. Kadam Vaishali , Chintale Ashwini G DKP. Cosmeceuticals an emerging concept: a comprehensive review. Int J Res Pharm Chem. 2013;3(2):308–16.

5. Marrucho IM, Branco LC, Rebelo LPN. Ionic liquids in pharmaceutical applications. Annu Rev Chem Biomol Eng. 2014;5:527–46.

6. Sintra T, Luís A, Rocha S, Ferreira Lobo A, Gonçalves F, Coutinho JAP. Enhancing the antioxidant characteristics of phenolic acids by their conversion into cholinium salts. ACS Sustainb. 2015;3(10):2558–65.

7. Yu T, Anderson D. Reactive oxygen species-induced DNA damage and its modification : A chemical investigation. Fundam Mol Mech Mutagen. 1997;379:1997.

8. Kovacic P, Somanathan R. Broad overview of oxidative stress and its complications in human health. Open J Prev Med. 2013;3(1):32–41.

9. Kinnula VL, Crapo JD. Superoxide dismutases in malignant cells and human tumors. Free Radic Biol Med. 2004;36(6):718–44.

10. Singh U, Jialal I. Oxidative stress and atherosclerosis. Pathophysiology. 2006;13(3):129–42.

11. Sas K, Robotka H, Toldi J, Vécsei L. Mitochondria, metabolic disturbances, oxidative stress and the kynurenine system, with focus on neurodegenerative disorders. J Neurol Sci. 2007;257(1-2):221–39.

12. Massaad CA. Neuronal and Vascular Oxidative Stress in Alzheimer's Disease. Curr Neuropharmacol. 2011;9:662–73.

13. Guidi I, Galimberti D, Lonati S, Novembrino C, Bamonti F, Bresolin N. Oxidative imbalance in patients with mild cognitive impairment and Alzheimer's disease. Neurobiol Aging. 2006;27(2):262–9.

14. Bolton JL, Trush MA, Penning TM, Dryhurst G, Monks TJ. Role of Quinones in Toxicology. Chem Res Toxicol. 2000;13(3).

15. Alam MN, Bristi NJ, Rafiquzzaman M. Review on in vivo and in vitro methods evaluation of antioxidant activity. Saudi Pharm J SPJ Off Publ Saudi Pharm Soc. 2013;21(2):143–52.

16. Poljšak B, Dahmane R. Free radicals and extrinsic skin aging. Dermatol Res Pract. 2012;2012:1-4.

17. Halliwell B. Antioxidant characterization. Methodology and mechanism. Biochem Pharmacol. 1995;49(10):1341–8.

18. Hamid, A A, Aiyelaagbe O, Usman, L A, Ameen M O. Antioxidants: Its medicinal and pharmacological applications. African J Pure Appl Chem. 2010;4(8):142–51.

19. Mandal S, Yadav S, Yadav S, Nema RK. Antioxidants: A Review. Jorunal Chem Pharm Res. 2009;1(1):102–4.

20. Zheng W, Wang SY. Antioxidant Activity and Phenolic Compounds in Selected Herbs. J Agric Food Chem. 2001;49(11):5165–70.

21. Manach C, Scalbert A, Morand C, Rémésy C, Jime L. Polyphenols: food sources and bioavailability. Am Soc Clin Nutr. 2004;79:727–47.

22. Archivio MD, Filesi C, Benedetto R Di, Gargiulo R, Giovannini C, Masella R. Polyphenols , dietary sources and bioavailability. Ann Ist Super Sanità. 2007;43:348–61.

23. Rice-Evans CA. MNJ. PG. Structure-antioxidant activity relationships of flavonoids and phenolic acids. Free Radic Biol Med. 1996;20(7):933–56.

24. Angeles L. Isolation and Identification of Strawberry Phenolics with Antioxidant and Human Cancer Cell Antiproliferative Properties. J Agric Food Chem. 2008;56(3):670–5.

25. Aniel DS, Cheuller HESS, Eber DAH. Blackberry , Black Raspberry , Blueberry , Cranberry , Red Raspberry , and Strawberry Extracts Inhibit Growth and Stimulate Apoptosis of Human Cancer Cells In Vitro. J Agric Food Chem. 2006;54(25):9329–9339.

26. Sudheer AR, Muthukumaran S, Devipriya N, Menon VP. Ellagic acid, a natural polyphenol protects rat peripheral blood lymphocytes against nicotine-induced cellular and DNA damage in vitro: with the comparison of N-acetylcysteine. Toxicology. 2007;230(1):11–21.

27. Schaefer S, Baum M, Eisenbrand G, Janzowski C. Modulation of oxidative cell damage by reconstituted mixtures of phenolic apple juice extracts in human colon cell lines. Mol Nutr Food Res. 2006;50(4-5):413–7.

28. Plechkova N V, Seddon KR. Applications of ionic liquids in the chemical industry. Chem Soc Rev. 2008;37(1):123–50.

29. Rogers RD, Seddon KR. Ionic Liquids — Solvents of the Future? Science. 2003;302:792 – 793.

30. Earle MJ, Esperanca JMSS, Gilea MA, Canongia Lopes JN, Rebelo LPN, Widegren JA. The distillation and volatility of ionic liquids. Nature. 2006;439(7078):831–4.

31. Meine N, Benedito F, Rinaldi R. Thermal stability of ionic liquids assessed by potentiometric titration. Green Chem. 2010;12(10):1711.

32. Welton T. Room-Temperature Ionic Liquids . Solvents for Synthesis and Catalysis. Chem Rev. 1999;99(1):2071–83.

33. Petkovic M, Ferguson JL, Gunaratne HQN, Ferreira R, Leitão MC, Pereira CS. Novel biocompatible cholinium-based ionic liquids—toxicity and biodegradability. Green Chem. 2010;12(4):643.

34. Malhotra , V S, editor. Ionic liquid applications: pharmaceuticals, therapeutics, and biotechnology. Washington DC; 2010.

35. Faridbod F, Ganjali MR, Norouzi P, Riahi S, Rashedi H. Application of Room Temperature Ionic Liquids in Electrochemical Sensors and Biosensors. In: Kokorin A, editor. Ionic Liquids: Applications and perspectives. 2009. p. 643 – 658.

36. Passos H, Freire MG, Coutinho JAP. Ionic liquid solutions as extractive solvents for value-added compounds from biomass. Green Chem. 2014;16:4786–815.

37. Pham TPT, Cho C-W, Yun Y-S. Environmental fate and toxicity of ionic liquids: a review. Water Res. 2010;44(2):352–72.

38. Freire MG, Cláudio AFM, Araújo JMM, Coutinho J a P, Marrucho IM, Rebelo LPN. Aqueous biphasic systems: a boost brought about by using ionic liquids. Chem Soc Rev. 2012;41(14):4966–95.

39. Rogers RD, Seddon KR. Ionic Liquids: industrial applications for green chemistry. Am Chem Soc. 2002;

40. Earle MJ. Ionic Liquids: Solvents for the Twenty-First Century. Am Chem Soc. 2002;818:90–105.

41. Wang X, Ohlin CA, Lu Q, Fei Z, Hu J, Paul J. Cytotoxicity of ionic liquids and precursor compounds towards human cell line HeLa. Green Chem. 2007;9:1191–97.

42. Stolte S. Effects of Different Head Groups and Functionalized Side Chains on the Cytotoxicity of Ionic Liquids. Green Chem. 2007;9:760–767.

43. Ventura SPM, Silva FA, Gonçalves AMM, Pereira JL, Gonçalves F, Coutinho JAP. Ecotoxicity analysis of cholinium-based ionic liquids to Vibrio fischeri marine bacteria. Ecotoxicol Environ Saf. 2014;102:48–54.

44. Vijayaraghavan R, Thompson BC, MacFarlane DR, Kumar R, Surianarayanan M, Sehgal PK. Biocompatibility of choline salts as crosslinking agents for collagen based biomaterials. Chem Commun (Camb). 2010;46(2):294–6.

45. Hou X-D, Liu Q-P, Smith TJ, Li N, Zong M-H. Evaluation of toxicity and biodegradability of cholinium amino acids ionic liquids. PLoS One. 2013;8(3):1–7.

46. Pernak J, Syguda A, Mirska I, Pernak A, Nawrot J, Rogers RD. Choline-derivative-based ionic liquids. Chemistry. 2007;13(24):6817–6827.

47. Petkovic M, Seddon KR, Rebelo LPN, Silva Pereira C. Ionic liquids: a pathway to environmental acceptability. Chem Soc Rev. 2011;40(3):1383–1403.

48. Goho A. The crystal form of a drug can be the secret to its sucess. Sci News. 2004;166:122–4.

49. Copp FC, Stephenson D. United States Patent 3038004. US; 1960. p. 1952–4.

50. Hunter MA, Stapler JH. Cetylpyridinium chloride and domiphen bromide in organic solvent. 1994.

51. Welton T, Wasserscheid P, editors. Chemical Synthesis Using Supercritical Fluids Organic Synthesis on Solid Phase Microwaves in Organic Synthesis Solvent-free Organic Synthesis. Germany; 2002.

52. Moniruzzaman M, Kamiya N, Goto M. Ionic liquid based microemulsion with pharmaceutically accepted components: Formulation and potential applications. J Colloid Interface Sci. 2010;352(1):136–42.

53. Stoimenovski J, MacFarlane DR, Bica K, Rogers RD. Crystalline vs. ionic liquid salt forms of active pharmaceutical ingredients: a position paper. Pharm Res. 2010;27(4):521–6.

54. Fujita K, Forsyth M, Macfarlane DR, Reid RW, Elliott GD, Carolina N. Unexpected Improvement in Stability and Utility of Cytochrome c by Solution in Biocompatible Ionic Liquids. Biotechnol Bioeng. 2006;94:1209 – 1213.

55. Weaver KD, Kim HJ, Sun J, MacFarlane DR, Elliott GD. Cyto-toxicity and biocompatibility of a family of choline phosphate ionic liquids designed for pharmaceutical applications. Green Chem. 2010;12(3):507.

56. Bonjela. A topical salicylate gel for control of pain and inflammation in dentistry and oral medicine. Lamp. 1972;29(1):24.

57. Hu S, Jiang T, Zhang Z, Zhu A, Han B, Li W. Functional ionic liquid from biorenewable materials: synthesis and application as a catalyst in direct aldol reactions. Tetrahedron Lett. 2007;48(32):5613–7.

58. Moriel P, García-Suárez EJ, Martínez M, García a. B, Montes-Morán M a., … Bañares M a. Synthesis, characterization, and catalytic activity of ionic liquids based on biosources. Tetrahedron Lett. 2010;51(37):4877–81.

59. Muhammad N, Hossain MI, Man Z, El-harbawi M, Bustam MA, Yin C. Synthesis and Physical Properties of Choline Carboxylate Ionic Liquids. J Chem Eng Data. 2012;57:2191–6.

60. Taha M, Almeida MR, Silva F a E, Domingues P, Ventura SPM, Freire MG. Novel biocompatible and self-buffering ionic liquids for biopharmaceutical applications. Chemistry. 2015;21(12):4781–8.

61. Sekar S, Surianarayanan M, Ranganathan V, Macfarlane DR, Mandal AB. Choline-Based Ionic Liquids-Enhanced Biodegradation of Azo Dyes. Environ Sci Technol. 2012;46:4902 – 4908.

62. Demberelnyamba D, Ariunaa M, Shim YK. Newly synthesized water soluble cholinium-purpurin photosensitizers and their stabilized gold nanoparticles as promising anticancer agents. Int J Mol Sci. 2008;9(5):864–71.

63. Garcia H, Ferreira R, Petkovic M, Ferguson JL, Leitão MC, Silva Pereira C. Dissolution of cork biopolymers in biocompatible ionic liquids. Green Chem. 2010;12(3):367.

64. Belgacem MN, Gandini A, editors. Monomers, Polymers and Composites. First edit. Amsterdam; 2008.

65. Tharanathan R. Biodegradable films and composite coatings: past, present and future. Trends Food Sci Technol. 2003;14(3):71–8.

66. Klemm D, Heublein B, Fink H-P, Bohn A. Cellulose: fascinating biopolymer and sustainable raw material. Angew Chem Int Ed Engl. 2005;44(22):3358–93.

67. Gilbert RD, Kadla JF. Biopolymers from Renewable Resources. In: Kaplan DL, editor. Berlin, Heidelberg; 1998. p. 47–95.

68. Isobe N, Lee D-S, Kwon Y-J, Kimura S, Kuga S, Kim U-J. Immobilization of protein on cellulose hydrogel. Cellulose. 2011;18(5):1251–6.

69. Credou J, Volland H, Dano J, Berthelot T. A one-step and biocompatible cellulose functionalization for covalent antibody immobilization on immunoassay membranes. J Mater Chem B. 2013;1(26):3277–86.

70. Ming Y, Zhao L, Zhang H, Shi Y, Li Y. Investigation of Enantiomer Separation by LC with a New Bonded Cellulose 3,5-Dimethylphenylcarbamate Chiral Stationary Phase. Chromatographia. 2006;64(5-6):273–80.

71. Sun Q, Mandalika A, Elder T, Nair SS, Meng X, Ragauskas AJ. Nanocomposite film prepared by depositing xylan on cellulose nanowhiskers matrix. Green Chem. 2014;16(7):3458.

72. Brown, J A. An acetic ferment which forms cellulose. J Chem Soc. 1886;49:432 – 439.

73. Czaja W, Krystynowicz A, Bielecki S, Brown RM. Microbial cellulose--the natural power to heal wounds. Biomaterials. 2006;27(2):145–51.

74. Esa F, Tasirin SM, Rahman NA. Overview of Bacterial Cellulose Production and Application. Agric Agric Sci Procedia. 2014;2:113–9.

75. Chawla PR, Bajaj IB, Survase SA, Singhal RS. Microbial Cellulose : Fermentative Production and Applications. Food Technol Biotechnol. 2009;47(2):107–24.

76. Hestrin S, Schramm M. Synthesis of Cellulose by Acetobacter xylinum. 1953;58:345–52.

77. Khan T, Khan S, Park JK. Simple fed-batch cultivation strategy for the enhanced production of a single-sugar glucuronic acid-based oligosaccharides by a cellulose-producing Gluconacetobacter hansenii strain. Biotechnol Bioprocess Eng. 2008;13(2):240–7.

78. Yoshino T, Asakura T, Toda K. Cellulose Production by Acetobacter pasteurianus on Silicone Membrane. J Ferment Bioeng. 1996;81(1):32–6.

79. Klemm D, Schumann D, Udhardt U, Marsch S. Bacterial synthesized cellulose - artificial blood vessels for microsurgery. Prog Polym Sci. 2001;26.

80. Trovatti E, Serafim LS, Freire CSR, Silvestre AJD, Neto CP. Gluconacetobacter sacchari: An efficient bacterial cellulose cell-factory. Carbohydr Polym. 2011;86(3):1417–20.

81. Rivas B, Moldes AB, Domínguez JM, Parajó JC. Development of culture media containing spent yeast cells of Debaryomyces hansenii and corn steep liquor for lactic acid production with Lactobacillus rhamnosus. Int J Food Microbiol. 2004;97(1):93–8.

82. Gomes FP, Silva NHCS, Trovatti E, Serafim LS, Duarte MF, Freire CSR. Production of bacterial cellulose by Gluconacetobacter sacchari using dry olive mill residue. Biomass and Bioenergy. 2013;55:205–11.

83. Wu J-M, Liu R-H. Thin stillage supplementation greatly enhances bacterial cellulose production by Gluconacetobacter xylinus. Carbohydr Polym. 2012;90(1):116–21.

84. Carreira P, Mendes J a. S, Trovatti E, Serafim LS, Freire CSR, Neto CP. Utilization of residues from agro-forest industries in the production of high value bacterial cellulose. Bioresour Technol. 2011;102(15):7354–60.

85. Czaja, W.; Krystynowicz, A.; Kawecki, M.; Wysota, K.; Sakiel, S.; Wroblewski, P.; Glik, J.; Nowak, P.; Bielecki S. Cellulose : Molecular and Structural Biology. Brown RM, editor. 2007.

86. Cakar F, Ozer I, Aytekin a Ö, Sahin F. Improvement production of bacterial cellulose by semi-continuous process in molasses medium. Carbohydr Polym. 2014;106:7–13.

87. Patel UD, Suresh S. Complete dechlorination of pentachlorophenol using palladized bacterial cellulose in a rotating catalyst contact reactor. J Colloid Interface Sci. 2008;319(2):462–9.

88. Hong F, Qiu K. An alternative carbon source from konjac powder for enhancing production of bacterial cellulose in static cultures by a model strain Acetobacter aceti subsp. xylinus ATCC 23770. Carbohydr Polym. 2008;72(3):545–9.

89. Moreira S, Silva NB, Almeida-Lima J, Rocha HAO, Medeiros SRB, Gama FM. BC nanofibres: in vitro study of genotoxicity and cell proliferation. Toxicol Lett. 2009;189(3):235–41.

90. Grzegorczyn S, Ślęzak A. Kinetics of concentration boundary layers buildup in the system consisted of microbial cellulose biomembrane and electrolyte solutions. J Memb Sci. 2007;304(1-2):148–55.

91. Hu W, Chen S, Li X, Shi S, Shen W, Wang H. In situ synthesis of silver chloride nanoparticles into bacterial cellulose membranes. Mater Sci Eng C. 2009;29(4):1216–9.

92. Czaja WK, Young DJ, Kawecki M, Brown RM. The Future Prospects of Microbial Cellulose in Biomedical Applications. Biomacromolecules. 2007;8(1):1–12.

93. Frantz VK. Absorbable cotton, paper and gauze. Ann Surg. 1943;118(1):116–26.

94. Kang BS, Na YC, Jin YW. Comparison of the Wound Healing Effect of Cellulose and Gelatin : An In Vivo Study. Arch Plast Surg. 2012;39(4):317–22.

95. Kolodziejcyk, M.; Pomorski L. Final Report on the Realization of the Grant No. 7 S20400407 from the Plish State Committee for Scientific Research (in Polish). 1999.

96. Helenius G, Bäckdahl H, Bodin A, Nannmark U, Gatenholm P, Risberg B. In vivo biocompatibility of bacterial cellulose. J Biomed Mater Res Part A. 2006;76A(2):431–8.

97. Shah J, Brown RM. Towards electronic paper displays made from microbial cellulose. Appl Microbiol Biotechnol. 2005;66(4):352–5.

98. J.A. Westland JA, Penny GS, Stephens RS, Winslow AR. Method of supporting fractures in geologic formations and hydraulic fluid composition for same. US patent 5350528. 1994.

99. Jones I, Currie L, Martin R. A guide to biological skin substitutes. Br J Plast Surg. 2002;55:185–93.

100. Barthe N, Baquey C. Cellulose phosphates as biomaterials . In vivo biocompatibility studies. Biomaterials. 2002;23:971–80.

101. Granja L, Granja PL, Bareille R, Rouais F, Baquey C, Engenharia F De. Mineralization of regenerated cellulose hydrogels induced by human bane marrow stromal cells. Eur Cells Mater. 2005;10:31–9.

102. Balasubramani M, Kumar TR, Babu M. Skin substitutes: a review. Burns. 2001;27:534–44.

103. Cazja, W., Krystynowicz, A., Kawacki, M., Wysota, K., Sakiel, S., Wróblewski, P., Glik, J.; Nowak, P., Bielecki S. Cellulose: Molecular and Structural Biology. Brown, E. M., Saxena IM, editor. Netherlands; 2007.

104. Fontana JD, de Souza AM, Fontana CK, Torriani IL, Moreschi JC, Galloti B. J. Acetobacter cellulose pellicle as a temporary skin substitute. Appl Biochem Biotechnol. 1990;24(25):253–4.

105. Mayall RC, Mayall AC, Mayall LC, Rocha HC, Marques LC. Tratamento das ulceras troficas dos membros com um novo substitute da pele. ReV Bras Cir. 1990;80(4):120–4.

106. Drury JL, Mooney DJ. Hydrogels for tissue engineering: scaffold design variables and applications. Biomaterials. 2003;24(24):4337–51.

107. Bencherif SA, Braschler TM, Renaud P. Advances in the design of macroporous polymer scaffolds for potential applications in dentistry. 2013;251–61.

108. Yamanaka, S., Ono, E., Watanabe, K., Kusakabe, M., Suzuki Y. Hollow microbial cellulose, process for preparation thereof, and artificial blood vessel formed of said cellulose. European Patent; No. 0396344, 1990.

109. Hatton P V, Devlin AJ, Craig GT, Brook IM. In vitro and in vivo evaluation of e-PTFE and alkali-cellulose membranes for guided bone regeneration. Clin Oral Implants Res. 2001;12:62–8.

110. Nguyen VT, Gidley MJ, Dykes GA. Potential of a nisin-containing bacterial cellulose film to inhibit Listeria monocytogenes on processed meats. Food Microbiol. 2008;25(3):471–8.

111. Schirhagl R. Bioapplications for Molecularly Imprinted Polymers. Anal Chem. 2014;86(1):250–61.

112. Mudry B., Carrupt PA, Guy H.R. D-CBM. Quantitative structure-permeation relationship for iontophoretic transport across the skin. Natl Institutes Heal. 2008;122(2):165–72.

113. Almeida IF, Pereira T, Silva NHCS, Gomes FP, Silvestre a JD, Costa PC. Bacterial cellulose membranes as drug delivery systems: an in vivo skin compatibility study. Eur J Pharm Biopharm. 2014;86(3):332–6.

114. Trovatti E, Silva NHCS, Duarte IF, Rosado CF, Almeida IF, Neto CP. Biocellulose Membranes as Supports for Dermal Release of Lidocaine. Biomacromolecules. 2011;12:4162–8.

115. Abeer MM, Mohd Amin MCI, Martin C. A review of bacterial cellulose-based drug delivery systems: their biochemistry, current approaches and future prospects. J Pharm Pharmacol. 2014;66:1047 – 1061.

116. Stoica-Guzun A, Stroescu M, Tache F, Zaharescu T, Grosu E. Effect of electron beam irradiation on bacterial cellulose membranes used as transdermal drug delivery systems. Beam Interact with Mater Atoms. 2007;265(1):434–8.

117. Huang L, Chen X, Nguyen TX, Tang H, Zhang L, Yang G. Nano-cellulose 3D-networks as controlled-release drug carriers. J Mater Chem B. 2013;1(23):2976.

118. Trovatti E, Freire CSR, Pinto PC, Almeida IF, Costa P, Rosado C. Bacterial cellulose membranes applied in topical and transdermal delivery of lidocaine hydrochloride and ibuprofen: In vitro diffusion studies. Int J Pharm. 2012;435(1):83–7.

119. Silva NHCS, Rodrigues AF, Almeida IF, Costa PC, Rosado C, Freire CSR. Bacterial cellulose membranes as transdermal delivery systems for diclofenac: in vitro dissolution and permeation studies. Carbohydr Polym. 2014;106:264–9.

120. Silva NHCS, Drumond I, Almeida IF, Costa P, Rosado CF, Silvestre AJD. Topical caffeine delivery using biocellulose membranes: a potential innovative system for cellulite treatment. Cellulose. 2013;21(1):665–74.

121. Wei B, Yang G, Hong F. Preparation and evaluation of a kind of bacterial cellulose dry films with antibacterial properties. Carbohydr Polym. 2011;84(1):533–8.

122. Lam E, Male KB, Chong JH, Leung ACW, Luong JHT. Applications of functionalized and nanoparticle-modified nanocrystalline cellulose. Trends Biotechnol. 2012;30(5):283–90.

123. Guimard NK, Gomez N, Schmidt CE. Conducting polymers in biomedical engineering. Prog Polym Sci. 2007;32(8-9):876–921.

124. Keshk SM a. S, Haija MA. A new method for producing microcrystalline cellulose from Gluconacetobacter xylinus and kenaf. Carbohydr Polym. 2011;84(4):1301–5.

125. Airul MOHDC, Ohd IQM, Badi ABGUA. Bacterial Cellulose Film Coating as Drug Delivery System : Physicochemical , Thermal and Drug Release Properties. Sains Malays. 2012;41(5):561–8.

126. Erbas Kiziltas E, Kiziltas A, Blumentritt M, Gardner DJ. Biosynthesis of bacterial cellulose in the presence of different nanoparticles to create novel hybrid materials. Carbohydr Polym. 2015;129:148–55.

127. Lemus J, Palomar J, Heras F, Gilarranz MA, Rodriguez JJ. Developing criteria for the recovery of ionic liquids from aqueous phase by adsorption with activated carbon. Sep Purif Technol. 2012;97:11–9.

128. COSMOtherm C2.1, release 01.06. Germany; 2003.

129. Palomar J, Lemus J, Gilarranz M a., Rodriguez JJ. Adsorption of ionic liquids from aqueous effluents by activated carbon. Carbon N Y. 2009;47(7):1846–56.

130. Huang D, Ou B, Prior, L. R. The Chemistry behind Antioxidant Capacity Assays. J Agric Food Chem. 2005;53:1841 – 1856.

131. Brien JO, Wilson I, Orton T, Pognan Ë. Investigation of the Alamar Blue (resazurin) fluorescent dye for the assessment of mammalian cell cytotoxicity. J Biochem. 2000;5426:5421–6.

132. Hesse M, Meier H, Zeeh B. Spectroscopic Methods in Organic Chemistry. 1997.

133. Mohd Amin MCI, Ahmad N, Halib N, Ahmad I. Synthesis and characterization of thermo- and pH-responsive bacterial cellulose/acrylic acid hydrogels for drug delivery. Carbohydr Polym. 2012;88(2):465–73.

134. Cunha AG, Freire CSR, Silvestre AJD, Neto CP, Gandini A, Fardim P. Bi-phobic Cellulose Fibers Derivatives via Surface Trifluoropropanoylation. Am Chem Soc. 2007;9(12):10801–6.

135. Tokoh C, Takabe K, Sugiyama J, Fujita M. CP/MAS 13C NMR and electron diffraction study of bacterial cellulose structure affected by cell wall polysaccharides. Cellulse. 2002;9:351–60.

136. Kono H, Yunoki S, Shikano T, Fujiwara M. CP/MAS 13 C NMR Study of Cellulose and Cellulose Derivatives . 1 . Complete Assignment of the CP/MAS 13C NMR Spectrum of the Native Cellulose. J Am Chem Soc. 2002;(9):7506–11.

137. Tomé LC, Silva NHCS, Soares HR, Coroadinha AS, Sadocco P, Freire CSR. Bioactive transparent films based on polysaccharides and choliniumcarboxylate ionic liquids. Green C. 2015;17:4291–9.

138. Meshitsuka G, Isogai A. Chemical Structures of Cellulose, Hemicelluloses, and Lignin. In: Chemical Modification of Lignocellulosic Materials. New York; 1995. p. 11–34.

139. Shahmohammadi Jebel F, Almasi H. Morphological, physical, antimicrobial and release properties of ZnO nanoparticles-loaded bacterial cellulose films. Carbohydr Polym. 2016;149:8–19.

140. Yamanaka S, Watanabe K, Kitamura N, Igushi M, Mitsuhashi S, Uryu M. The structure and mechanical properties of sheets prepared from bacterial cellulose. J Mater Sci. 1989;24:1–5.

141. Neves CMSS, Lemus J, Freire MG, Palomar J, Coutinho J a P. Enhancing the adsorption of ionic liquids onto activated carbon by the addition of inorganic salts. Chem Eng J. 2014;252:305–10.

142. Huang L, Chen X, Nguyen TX, Tang H, Zhang L, Yang G. Nano-cellulose 3D-networks as controlled-release drug carriers. J Mater Chem B. 2013;1(23):2976.

143. Müller A, Ni Z, Hessler N. The biopolymer bacterial nanocellulose as drug delivery system: investigation of drug loading and release using the model protein albumin. J Pharm Sci. 2013;102(2):6–8.

144. Queimada JA, Mota LF, Pinho PS, Macedo AE. Solubilities of Biologically Active Phenolic Compounds : Measurements and Modeling. J Phys Chem. 2009;113:3469–76.

145. Jeong S Il, Lee SE, Yang H, Jin Y-H, Park C-S, Park YS. Toxicologic evaluation of bacterial synthesized cellulose in endothelial cells and animals. Mol & Cell Toxicol. 2010;6(4):370–7.

146. Cacicedo ML, León IE, Gonzalez JS, Porto LM, Alvarez VA, Castro GR. Modified bacterial cellulose scaffolds for localized doxorubicin release in human colorectal HT-29 cells. Colloids Surf B Biointerfaces. 2016;140:421–9.

9 Annex

9.1 Annex 1 – Synthesis and characterization of cholinium-based ILs

Cholinium based-ILs were synthetized and their purities confirmed through ^{1}H and ^{13}C NMR.

In Figures 29, 30 and 31 are depicted the ^{1}H and ^{13}C NMR spectra of [Chol][Caf], $[Chol]_2[Ell]$ and [Chol][Gal], which are according to the literature (6).

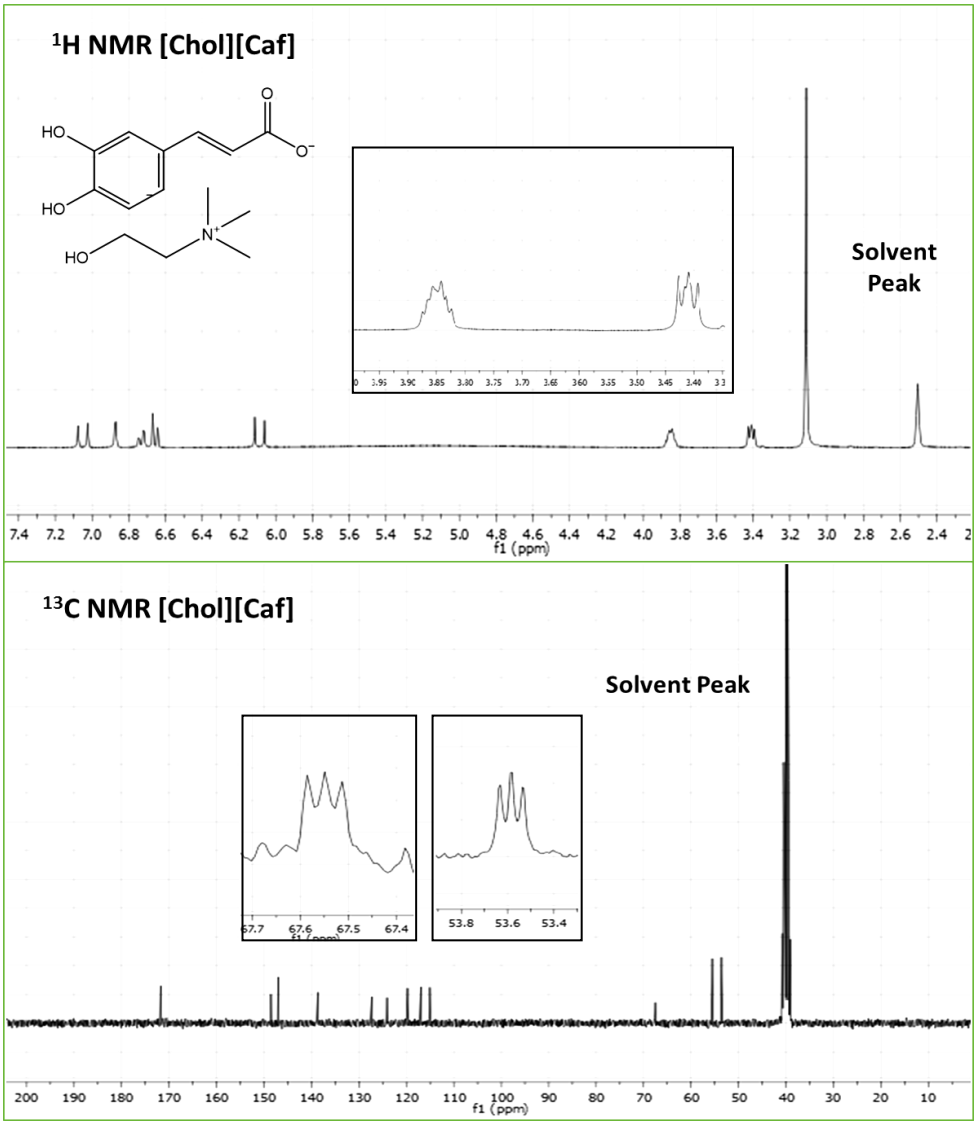

Figure 29 - ^{1}H and ^{13}C NMR spectra of [Chol][Caf] in DMSO with TMS as internal reference.

[Chol][Caf] was obtained as a white solid (98% yield). ^{1}H NMR (d_6-DMSO, 300 MHz, [ppm]): δ 7.08 (d, 1H, J_{HH} = 15.7 Hz, C<u>H</u>CHCOO), 6.88 (d, 1H, J_{HH} = 1.9 Hz, <u>H</u>-2), 6.74 (dd, 1H, J_{HH} = 8.2 Hz and J_{HH} = 1.9 Hz, <u>H</u>-6), 6.67 (d, 1H, J_{HH} = 8.1 Hz, <u>H</u>-5), 6.11 (d, 1H, J_{HH} = 15.8 Hz, CH<u>C</u>HCOO), 3.94-3.79 (m, 2H, NCH$_2$C<u>H</u>$_2$OH), 3.49-3.34 (m, 2H, NC<u>H</u>$_2$CH$_2$OH), 3.11 (s, 9H, (N(C<u>H</u>$_3$)$_3$). ^{13}C NMR (d_6-DMSO, 75.47 MHz, [ppm]): δ 171.99 (<u>C</u>OO), 148.66 (<u>C</u>HCHCOO), 147.07 (<u>C</u>OH-4), 138.93 (<u>C</u>OH-3), 127.22 (CH<u>C</u>HCOO), 123.76 (<u>C</u>-1), 119.76 (<u>C</u>-6), 117.06 (<u>C</u>-5), 115.25 (<u>C</u>-2), 67.54 (t, J_{CN} = 2.8 Hz, N<u>C</u>H$_2$CH$_2$OH), 55.55 (NCH$_2$<u>C</u>H$_2$OH), 53.57 (t, J_{CN} = 3.8 Hz, N(<u>C</u>H$_3$)$_3$ (6).

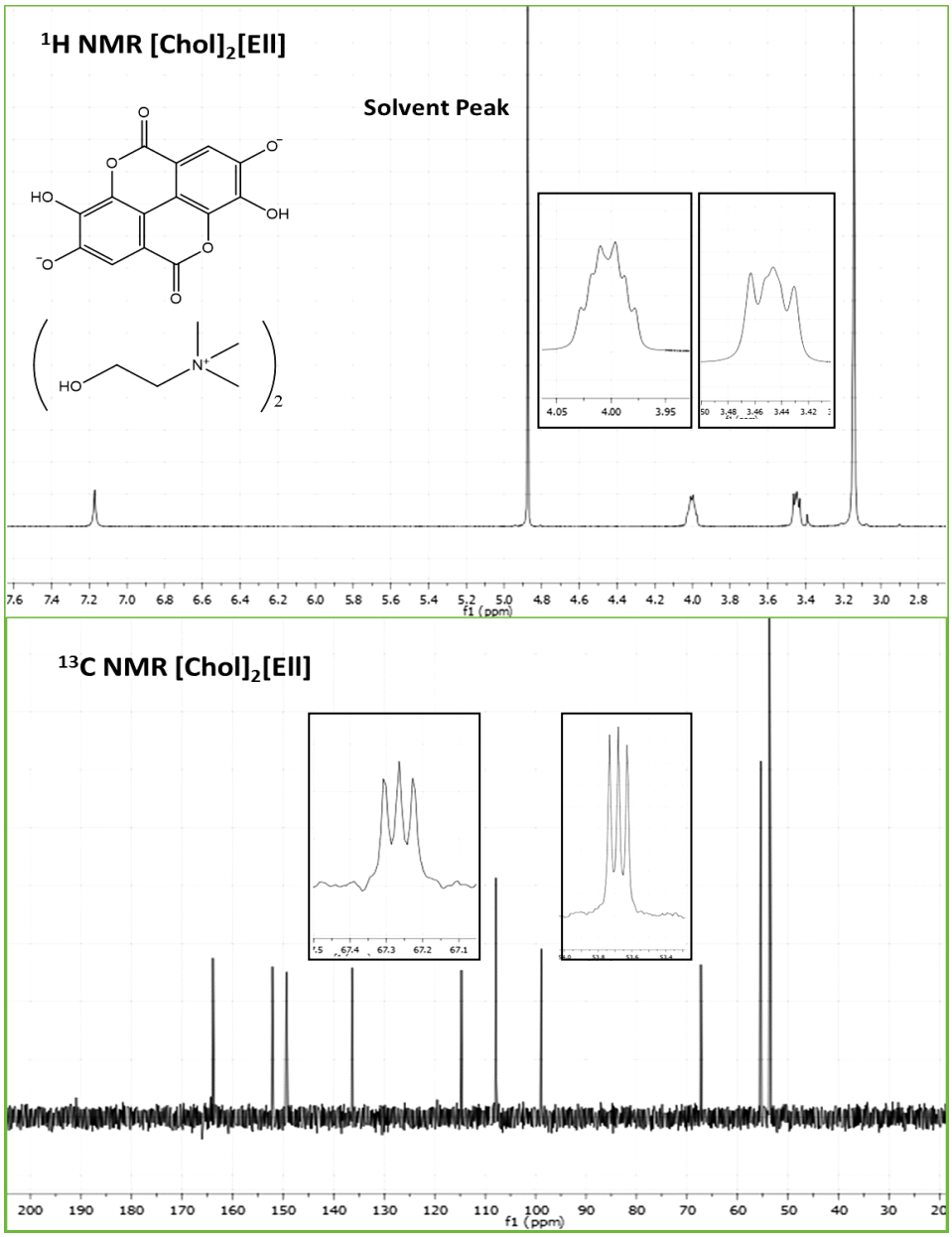

Figure 30 - ^{1}H and ^{13}C NMR spectra of [Chol]$_2$[Ell] in D$_2$O with TSP as internal reference.

[Chol]$_2$[Ell] was obtained as a light brown solid (87% yield). ^{1}H NMR (D_2O, 300 MHz, [ppm]): δ 7.16 (s, 2H, (2x C<u>H</u>CO)), 4.10-3.95 (m, 4H, (2x (NC<u>H</u>$_2$CH$_2$OH)), 3.54-3.37 (m, 4H, (2x (NCH$_2$C<u>H</u>$_2$OH)), 3.15 (s, 18H, (2x (N(C<u>H</u>$_3$)$_3$)). ^{13}C NMR (D_2O, 75.47 MHz, [ppm]): δ 163.85 (2x (<u>C</u>OO)), 152.13 (2x (<u>C</u>O)), 149.13 (2x (<u>C</u>OH)), 136.32 (2x (<u>C</u>OCO)), 114.66 (2x (<u>C</u>OCO)), 107.78 (2x (<u>C</u>CO)), 98.81 (2x (<u>C</u>(C)$_3$)), 67.24 (t, J_{CN} = 3.0 Hz, 2x (N<u>C</u>H$_2$CH$_2$OH)), 55.43 (2x (NCH$_2$<u>C</u>H$_2$OH)), 53.68 (t, J_{CN} = 4.0 Hz, 2x (N(<u>C</u>H$_3$)$_3$))(6).

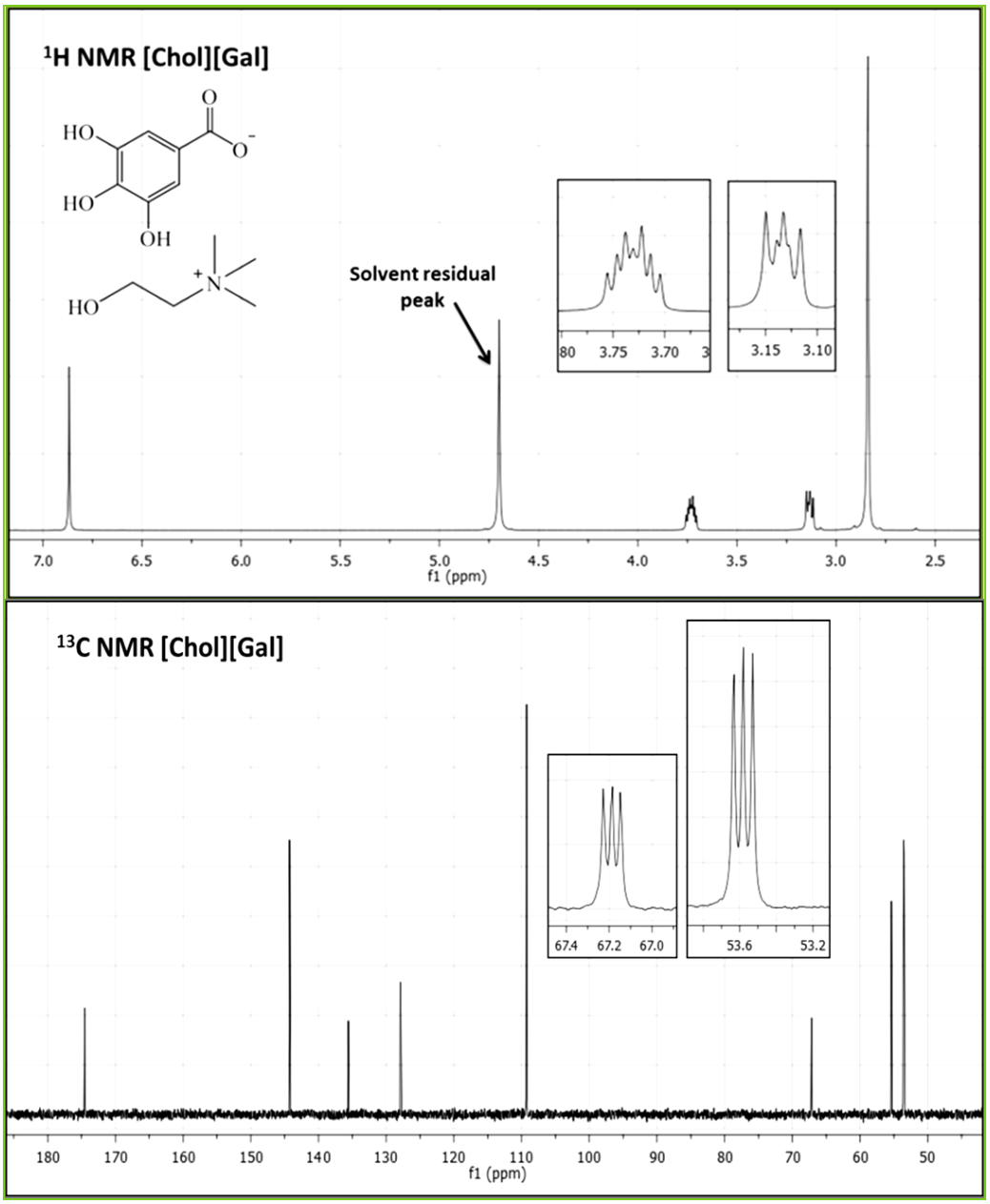

Figure 31 - ^{1}H and ^{13}C NMR spectra of [Chol][Gal] in D_2O with TSP as internal reference.

[Chol][Gal] was obtained as a white solid (87% yield). ^{1}H NMR (D_2O, 300 MHz, [ppm]): δ 6.87 (s, 2H, H-2 and H-6), 3.79-3.67 (m, 2H, NCH_2CH_2OH), 3.18-309 (m, 2H, NCH_2CH_2OH), 2.84 (s, 9H, $N(CH_3)_3$). ^{13}C NMR (D_2O, 75.47 MHz, [ppm]): δ 174.73 (COO), 144.28 (C-3 and C-5), 135.62 (C-4), 128.01 (C-1), 109.33 (C-2 and C-6), 67.30 (t, J_{CN} = 2.9 Hz, NCH_2CH_2OH), 55.49 (NCH_2CH_2OH), 53.72 (t, J_{CN} = 3.9 Hz, $N(CH_3)_3$) (6).

9.2 Annex 2 – Calibration curves and auxiliary tables

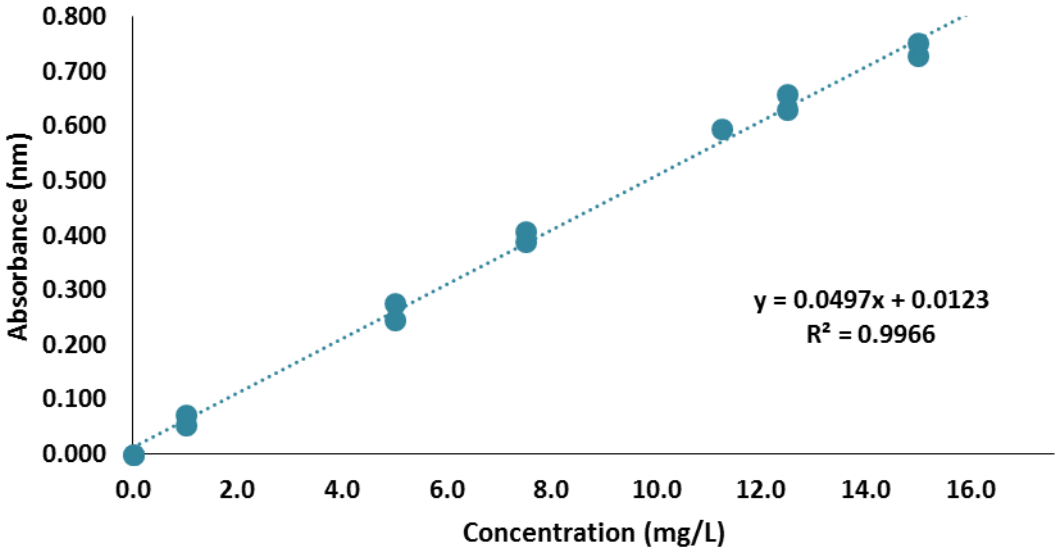

Figure 32 – Calibration curve for [Chol][Caf] in a PBS buffer aqueous solution at 286 nm.

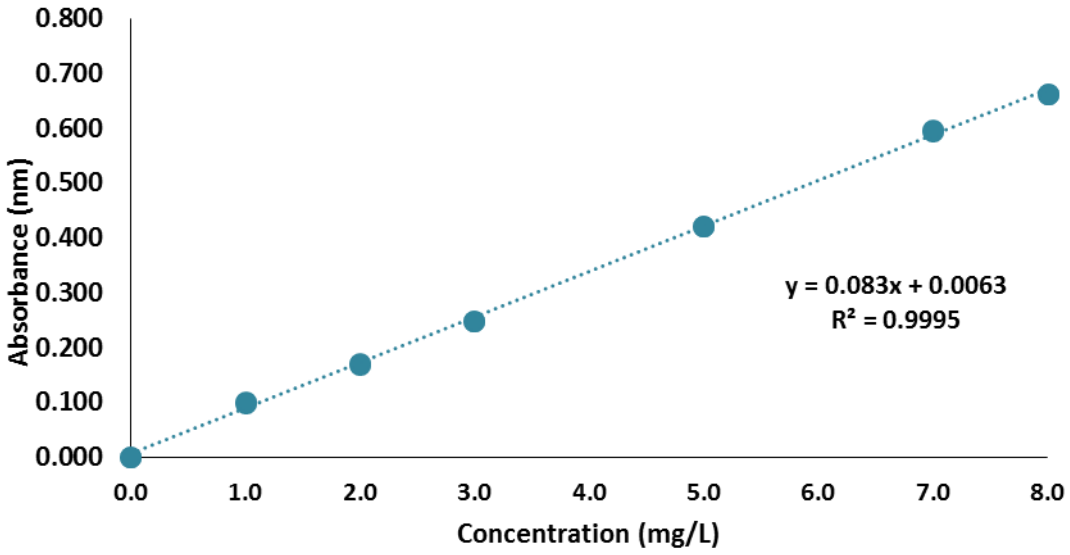

Figure 33 – Calibration curve for $[Chol]_2[Ell]$ in a PBS buffer aqueous solution at 253 nm.

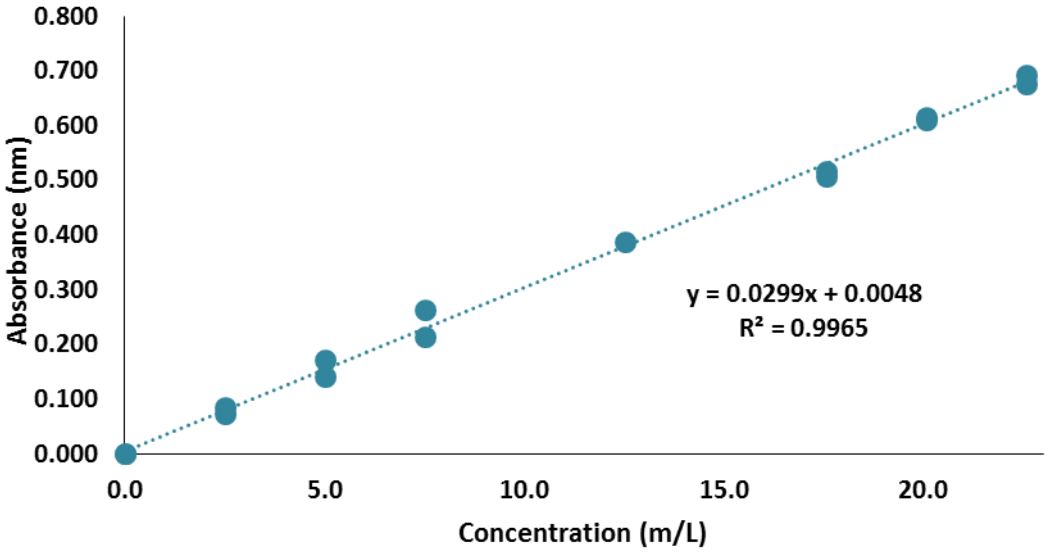

Figure 34 - Calibration curve for [Chol][Gal] in a PBS buffer aqueous solution at 259 nm.

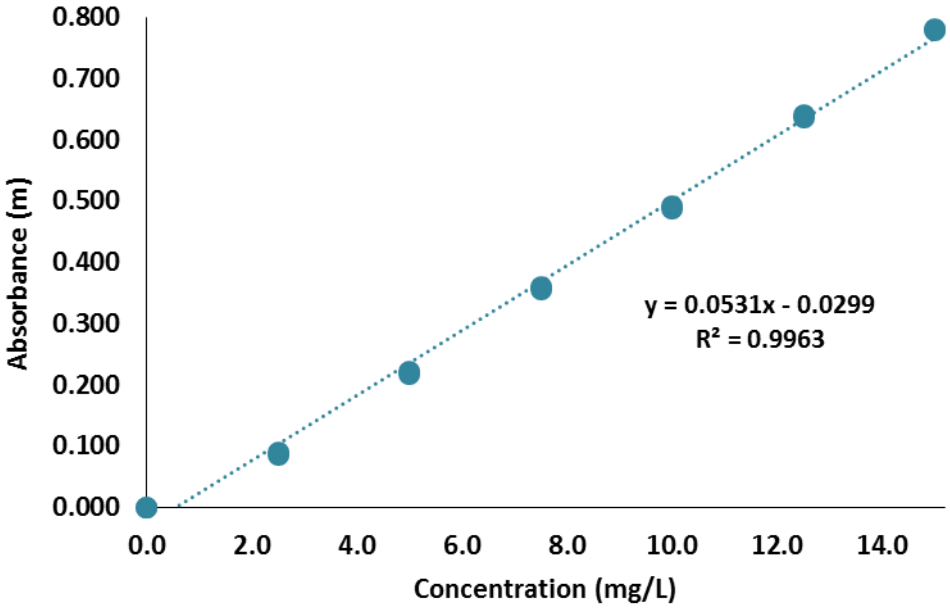

Figure 35 - Calibration curve for [Chol][Caf] in methanol at 286 nm.

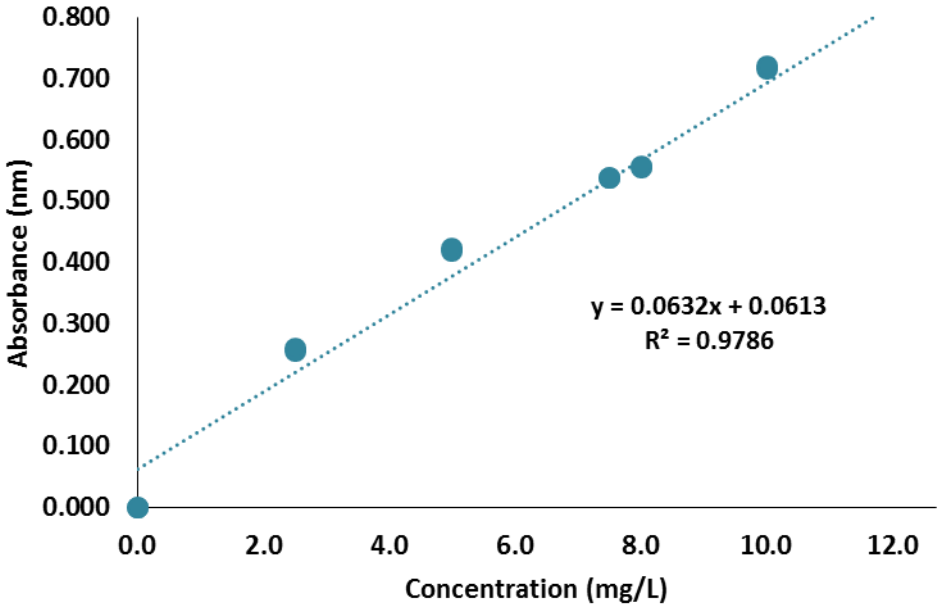

Figure 36 - Calibration curve for $[Chol]_2[Ell]$ in methanol at 253 nm.

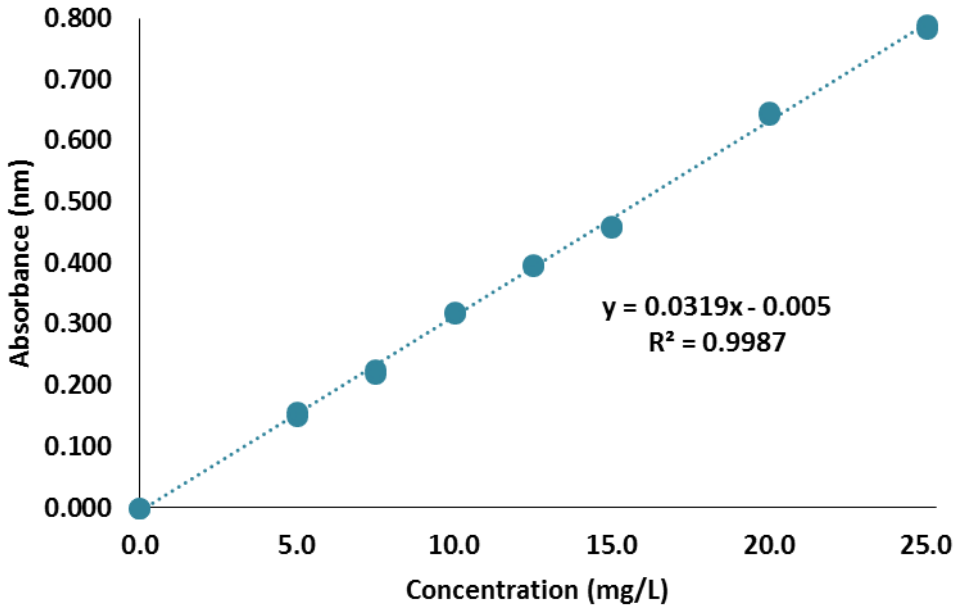

Figure 37 - Calibration curve for [Chol][Gal] in methanol at 259 nm.

Table 7 – Calculations made to determine the amount of IL present in each BC-IL for the TGA assays.

Compound	Nº-Wet or Dry (W or D)	Weight of BC / g	Weight after absorption / g	Absorbed IL %	Weight of IL in solution / mg	Weight of IL in BC / mg
[Chol][Caf]	1-D	5.2109	2.3953	19.8	1.37	8.63
	2-D	5.4019	2.5498	25.0	0.81	9.19
$[Chol]_2[Ell]$	1-D	5.5582	3.0116	13.9	0.15	9.85
	2-D	5.6511	3.0933	28.6	0.16	9.84
[Chol][Gal]	1-D	2.7606	1.3561	48.3	0.53	9.47
	2-D	3.3805	1.8453	28.2	1.24	8.76

Table 8– Calculations made to determine the amount of IL present in the BC-IL for the TGA assays.

Compound	Nº-Wet or Dry (W or D)	Weight of BC / g	Weight after absorption / g	Absorbed IL %	Weight of IL in solution / mg	Weight of IL in BC / mg
[Chol][Caf]	1-D	5.2109	2.3953	19.8	1.37	8.63
	2-D	5.4019	2.5498	25.0	0.81	9.19
$[Chol]_2[Ell]$	1-D	5.5582	3.0116	13.9	0.15	9.85
	2-D	5.6511	3.0933	28.6	0.16	9.84
[Chol][Gal]	1-D	2.7606	1.3561	48.3	0.53	9.47
	2-D	3.3805	1.8453	28.2	1.24	8.76

Table 9 – Calculations made to determine the amount of IL present in the BC-IL for the dissolution assays in PBS buffer.

Compound	Nº-Wet or Dry (W or D)	Weight of BC / g	Weight after absorption / g	Absorbed IL %	Weight of IL in solution / mg	Weight of IL in BC / mg
[Chol][Caf]	1-W	6.2707	2.7604	9.2	1.49	8.51
	2-W	5.2448	2.6384	14.7	1.81	8.19
	3-D	3.1595	2.0487	23.6	0.77	9.23
	4-D	3.5417	1.5162	31.4	0.69	9.31
$[Chol]_2[Ell]$	1-W	5.146	2.8654	12.4	1.28	8.72
	2-W	4.939	1.4575	22.4	1.34	8.66
	3-D	2.998	1.4918	23.6	1.37	8.63
	4-D	5.2095	2.2022	21.4	0.38	9.62
[Chol][Gal]	1-W	4.0816	1.9686	27.5	0.57	9.43
	2-W	3.2838	1.217	26.8	0.75	9.25
	3-D	2.8104	1.6485	20.4	0.69	9.31
	4-D	2.8375	1.372	30.3	0.45	9.55

Table 10 – Calculations made to determine the amount of IL present in the BC-IL for the dissolution assays in PBS methanol.

Compound	Nº-Wet or Dry (W or D)	Weight of BC / g	Weight after absorption / g	Absorbed IL %	Weight of IL in solution / mg	Weight of IL in BC / mg
[Chol][Caf]	1-W	4.707	2.056	31.0	3.18	6.82
	2-W	4.7361	2.8482	16.0	3.60	6.40
	3-D	5.2422	2.9197	18.4	4.40	5.60
	4--D	5.0625	3.2098	24.9	1.12	8.88
$[Chol]_2[Ell]$	1-W	4.1975	3.3372	27.2	0.46	9.54
	2-W	5.0762	2.9807	17.4	1.01	8.99
	3-D	5.0081	3.9807	41.0	0.58	9.42
	4-D	5.715	4.1604	42.2	0.25	9.75
[Chol][Gal]	1-W	4.1975	2.588	29.9	0.46	9.54
	2-W	5.0762	2.6397	25.2	1.01	8.99
	3-D	5.0081	2.6765	22.5	0.58	9.42
	4-D	5.715	3.3206	24.3	0.25	9.75

Table 11 – Calculations made to determine the amount of IL present in the BC-IL for the antioxidant assays.

Compound	Nº-Wet or Dry (W or D)	Weight of BC / g	Weight after absorption / g	Absorbed IL %	Weight of IL in solution / mg	Weight of IL in BC / mg
[Chol][Caf]	1-W	4.707	2.056	31.0	3.18	6.82
	2-W	4.7361	2.8482	16.0	3.60	6.40
	3-D	5.2422	2.9197	18.4	4.40	5.60
	4-D	5.0625	3.2098	24.9	1.12	8.88
$[Chol]_2[Ell]$	1-W	5.3459	3.3372	27.2	0.14	9.86
	2-W	5.1144	2.9807	17.4	0.08	9.92
	3-D	5.3566	3.9807	41.0	0.09	9.91
	4-D	5.45	4.1604	42.2	0.09	9.91
[Chol][Gal]	1-W	4.1975	2.588	29.9	0.46	9.54
	2-W	5.0762	2.6397	25.2	1.01	8.99
	3-D	5.0081	2.6765	22.5	0.58	9.42
	4-D	5.715	3.3206	24.3	0.25	9.75

9.3 Annex 3 – Auxiliary photos

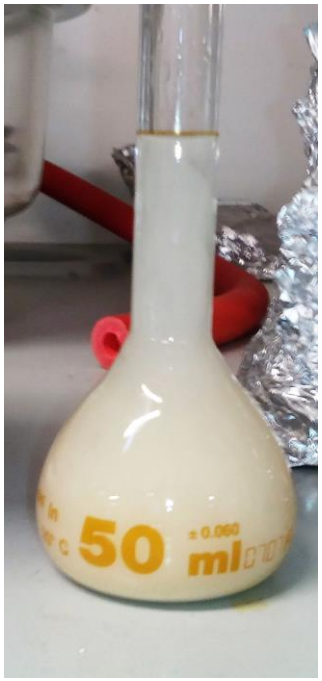

Figure 39 – Photo of the ellagic acid solution attempted to use for the precursor acids antioxidant assay.